UNIVERSITA' DEGLI STUDI DI MESSINA

Department of Chemical, Biological, Pharmaceutical and Environmental Sciences

PhD in: APPLIED BIOLOGY AND EXPERIMENTAL MEDICINE

XXXV Cycle

SSD: BIO/13

Coordinator: Prof. Nunziacarla Spanò

NEW INSIGHTS ON TMAU MECHANISMS: UNVEILING A NEW ROLE OF *FMO3* HAPLOTYPES AND A POSSIBLE MICROBIOTA CROSSTALK WITH NERVOUS SYSTEM

PhD Student:

Dr. Simona Alibrandi

Tutor:

Illustrious Professor:

Antonina Sidoti

ACADEMIC YEAR 2021/2022

Summary

ABSTRACT

Trimethylaminuria is a rare metabolic syndrome characterized by excessive excretion of trimethylamine (TMA) from body fluids. The latter is a malodorous amine, synthesized by specific gut bacterial families, that causes the typical rotten fish odor in affected patients. The primary form (TMAU1) is determined by causative mutations in *FMO3* gene inherited in an autosomal recessive pattern. It encodes for the enzyme Flavin monooxygenase 3 that converts TMA to odorless TMA-*N*-oxide (TMAO). The secondary form is linked to environmental factors, especially gut dysbiosis. To date, several aspects of both forms are unclear, so the diagnosis is often uncertain, and it is difficult to advise the correct therapeutic approach to the patient. One of the objectives of the present work was to investigate the role of some haplotypes on the FMO3 enzyme catalytic activity. To do this, a TMAO/TMA urine quantification by ^{1}H-NMR spectroscopy was performed in 38 suspected TMAU patients. Subsequently, a mutational analysis was realized by Sanger sequencing. Detected variants were in silico characterized by a docking prediction for TMA/FMO3 and an unbinding pathway study were performed. Furthermore, the gut microbiota 16s rRNA sequencing of 12 patients, negative to *FMO3* screening, was performed to verify a possible dysbiosis condition. In addition, a metabolic pathways analysis was performed to clarify the possible network between bacterial metabolites and behavioral disturbances, phenotype common to many TMAU patients. The results obtained showed that the *FMO3* haplotypes could modify the enzyme catalytic activity probably by reducing the interaction time between the FMO3 catalytic site and the TMA or by compromising the TMA N-oxidation process. Analysis of bacterial metabolite pathways has shown that there is a connection between TMA production, metabolites (short-chain fatty acids and neurotransmitters) and psychiatric disorders. The mental disturbs affecting TMAU patients are probably not only related to social consequence of their metabolic disease but also to a physiopathological effect determined by TMA

accumulation. These studies, if confirmed with in vitro and in vivo experiments, could improve the TMAU diagnosis.

1. INTRODUCTION

Trimethylaminuria (TMAU), known as fish odor syndrome, is a rare metabolic disorder characterized by the accumulation and subsequent trimethylamine (TMA) excretion through the urine, breath, and biological fluids such as sweat, saliva and vaginal secretions resulting in an unpleasant smell of rotten fish in affected patients. TMA is a volatile tertiary amine synthesized by the gut microbiota following TMA precursors fermentation process such as choline, L-carnitine, betaine, ergothioneine introduced with diet. Afterwards, TMA passively diffuses through the enterocyte membranes, and it is transported via portal circulation to the liver where, in healthy subjects, it is converted in its oxidized odorless form (TMAO) by FMO3 enzyme. TMAO then enters the systemic circulation, reaching fasting plasma concentrations of between 2 and 40 μM, prior to excretion[1]. Today, different forms of TMAU are known. The first is a genetic form (TMAU 1) caused by the total or partial deficiency of the hepatic microsomal enzyme Flavin monooxygenase 3 (FMO3). This enzyme is responsible for the TMA conversion in Trimethylamine N-oxide (TMAO). The secondary form (TMAU 2) is mainly determined by gut dysbiosis, which favours the bacterial species producing TMA and, consequently, its overproduction and accumulation. Lastly, the transient form can manifest itself intermittently depending on the patient's physiological conditions. Most patients do not feel the bad smell they produce, but they discover that are suffering from this syndrome due to friends or work colleagues' rejection reactions or simply because it is communicated by relatives. No physical symptoms are associated with the syndrome. Affected individuals appear normal and healthy. However, the unpleasant odor, characteristic of the disorder, often results in social and psychological disturbs such as depression, anxiety, isolation, schizophrenia states and, in extreme cases, even attempted suicide. The first TMAU clinical case has been described in 1970 on the medical journal Lancet. It was a 6-year-old girl with Noonan syndrome and splenomegaly, phenotype then confirmed by the high

urinary TMA concentration. From literary citations dating back to A.D. 400 it is clear that this syndrome has much more remote origins. In *Mahabharata*, the ancient India epic poem, the words in the epiphrasis "she grew to be beautiful and beautiful, but a fishy smell always clung to her" refer to a young woman, Satyavati, condemned to endure a lonely life as a ferryman, expelled from society because she smelled like a rotting fish. Even William Shakespeare, in the play "The Tempest", denigrates Caliban, a savage and deformed slave, with these words: "What have we here? a man or a fish? dead or alive? A fish: he smells like a fish; a very ancient and fish-like smell; a kind of, not of the newest, Poor John" [2,3].

1.1.Primary Trimethylaminuria (TMAU1)

Primary Trimethylaminuria (TMAU1) is caused by *FMO3* gene mutations that determine the FMO3 enzyme misfolding or the truncation. The FMO3 enzyme catalytic activity results, then, compromised, causing TMA accumulation and its subsequent excretion through biological fluids. The disease-related first symptoms appear in childhood together with weaning and with the TMA precursors administration[4]. Although TMAU incidence remains still uncertain, it is classified as a rare monogenic condition linked to *FMO3* gene mutations inherited in an autosomal recessive pattern. However, a compound heterozygosity was reported in few patients[5, 6].

1.1.1. The Flavin-containing Monooxygenase genes cluster: tissue-specific expression

Human genome is made up of 11 FMO genes, organized in two clusters on the long arm of chromosome 1, of which only 5 (*FMO1* to *FMO5*) encode a functional protein. In detail, the first cluster contains *FMO1* to *FMO4* genes and a pseudogene *FMO6P* in the region q24.3. *FMO5* is located ~26 Mb closer to the centromere at 1q21.1. The second cluster contains only *FMO7P* to *FMO11P* pseudogenes at 1q24.2[7]

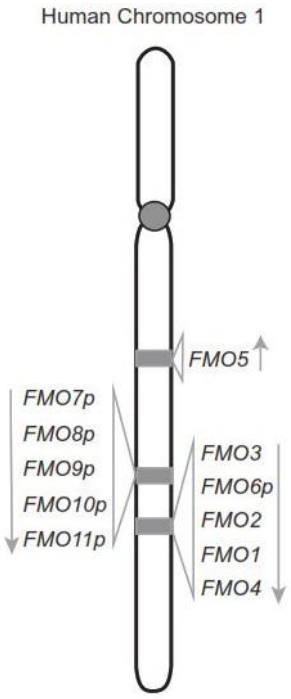

Figure 1. FMO gene cluster representation on chromosome 1.

FMO members show distinct developmental- and tissue-specific expression patterns.

- *FMO1*

The *FMO1* gene consists of 9 exons. It encodes the enzyme Flavin monooxygenase 1, mainly located in the kidney and small intestine. This enzyme is involved in the oxidative metabolism of different xenobiotics such as drugs and pesticides, catalyzing the N-oxidation of secondary and tertiary amines (https://www.uniprot.org/). Moreover, it is expressed in fetal liver, even if it is switched off in adult liver. This could be caused due to the presence, upstream of the hepatic promoter P0, of a LINE-1 element that acts as a powerful transcriptional repressor[8].

- *FMO2*

The *FMO2* gene consists of 9 exons and encodes the Flavin monooxygenase 2, a protein of 60,907 Da containing 535 amino acids. It is mainly expressed in lung but

also in kidney. FMO2 participates in the oxidative metabolism of numerous xenobiotics such as therapeutic drugs, insecticides that contain a soft nucleophile, most commonly nitrogen and sulfur, and participates to their bioactivation (https://www.uniprot.org/). In some regions of sub-Saharan Africa almost 50% of individuals have a homozygous nonsense mutation, c.1414C>T (p. Gln472*), which causes the inactive truncated protein synthesis. This determines a different response to drugs, especially those whose target organ is the lung, such as the antitubercular prodrugs ethionamide and thioacetazone[7].

- *FMO3*

The *FMO3* gene is 27 kb long and has 9 exons, of which the first is non-coding. It encodes the Flavin-containing Monooxigenase 3 containing 532 amino acids and mass of 60,033 Da. (https://www.uniprot.org/). Further details of this gene will be discussed in the paragraph 1.2.

- *FMO4*

The *FMO4* gene consists of 10 exons and encodes the Flavin monooxygenase 4, a protein of 63,343 Da, containing 558 amino acids, mainly expressed in pancreas. The enzyme catalyzes the heteroatomic nucleophilic centers oxidation in drugs, pesticides, and xenobiotics (https://www.uniprot.org/).

- *FMO5*

The *FMO5* gene has 9 exons. It encodes the Flavin monooxygenase 5 whose catalytic activity is different from other FMO enzymes. In details, it is non- or poorly active on 'classical' substrates such as drugs, pesticides, and dietary components containing soft nucleophilic heteroatoms. Instead, FMO5 acts as Baeyer-Villiger monooxygenase on a wide range of substrates. It catalyzes the insertion of an oxygen atom into a carbon-carbon bond adjacent to a carbonyl, which converts ketones to esters (https://www.uniprot.org/).

1.1.2. The Flavin-containing monooxygenase protein family (FMO): structure and function

The Flavin-containing monooxygenase (FMO) is a family of microsomal, oxidoreductase, NADPH-dependent enzymes found in various organisms such as bacteria, fungi, plants, invertebrates, and vertebrates (monkey, rabbit, rat, and human)[9,10]. They are responsible for about 2.5% of all metabolic reactions and therefore about 6% of all the phase I metabolic reactions. In fact, as well as cytochrome P450, FMOs are involved in phase 1 detoxification reactions of various xenobiotics such as phosphines, hydrazines, sulfides, selenides, iodides, primary, secondary, and tertiary amines, dietary compounds, environmental toxins and endogenous substrates such as trimethylamine, catecholamines, methionine and cysteamine[11]. The oxidation process carried out by these enzymes is essential to transform lipophilic substances into polar ones and easier to excrete from the body. The FMO family was first studied in 1970 in pig liver microsomes by Doctor Daniel Ziegler at the University of Texas[9]. Later in 1984, the FMO enzyme was purified from rabbit lung microsomes demonstrating that FMO multiple forms exist[12]. Despite their discovery over 30 years ago, the mammalian FMO structure and function enzymes have not yet been well described because they are insoluble membrane-bound proteins and their crystallization by X-ray diffraction is difficult. Although the primary structure of these enzymes is not highly conserved, it has been shown that the tertiary structures are very similar and that all members are dimers composed of identical subunits. The FMOs dimeric tertiary structure has been studied in yeasts and bacteria, but a percentage of homology has been seen with Human FMOs. In detail, the FMOs present in yeast share 22% of sequence identity with the human FMOs; while, bacterial FMOs have a sequence homology of 31%[13, 14]. Moreover, it has recently been possible to reconstruct the ancestral gene sequences for three *FMO* genes, AncFMO2, AncFMO3-6 and AncFMO5,

respectively. The AncFMOs exhibited catalysis like human FMOs and, with sequence and functional identities between 82% and 92%[15].

To date it is known that FMOs consist of two structural domains:

- a small domain that binds NADPH
- an extended domain that binds FAD
- the active site

Moreover, the two domains are connected to each other by a double linker (Fig. 2).

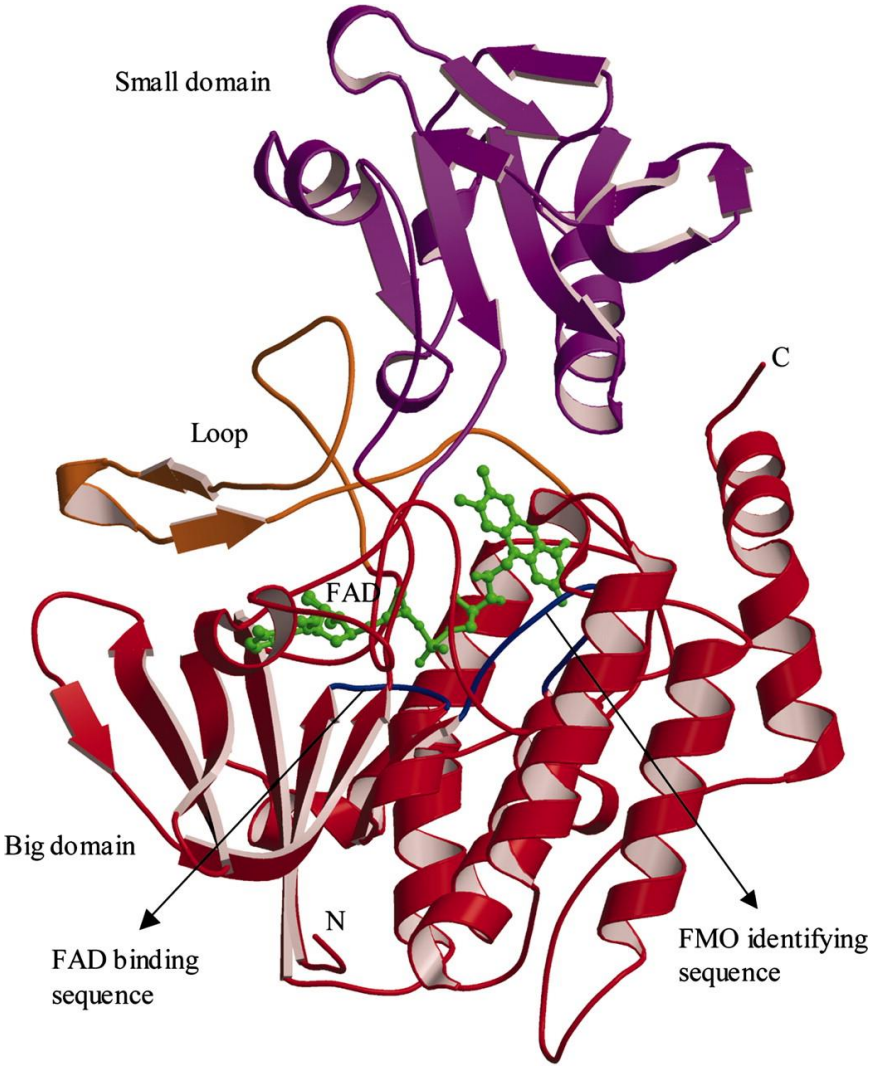

Figure 2 FMO three-dimensional structure of Schizosaccharomyces Pombe.

1.1.3. The FMO family catalytic cycle

The catalytic mechanism of the substrate oxidation occurs in the same way in all FMOs enzyme families. Flavin adenine dinucleotide (FAD), as a prosthetic group, Nicotinamide adenine dinucleotide phosphate (NADPH) as a cofactor, and molecular oxygen as a co-substrate are essential for catalysis. Water, $NADP^+$ and the oxidized substrate represent the final products of this cycle. Moreover, the substrate oxidation process takes place in two phases, one of which is faster than the other. In detail, the reaction begins when the NADPH binds the FAD, reducing it to $FADH_2$. Then molecular oxygen binds to the $NADP^+$ - $FADH_2$ - enzyme complex, forming the 4a-hydroperoxyflavin compound that is stabilized by $NADP^+$ in the enzyme catalytic site and is ready to oxidize the substrate within the active site. In the slower following steps, the substrate is oxidized thanks to the oxygen nucleophilic attack released by the 4a-hydroperoxyflavin intermediate which becomes C4a-hydroxyflavin. In the final step water and $NADP^+$ are released (Fig.3). The FMO enzymes do not follow the classic Michaelis Menten kinetic, and several factors can influence the substrate access to the enzyme active site, such as substrate size, shape, and charge. The best substrates are neutral or have only one positive charge, instead zwitterions and substrates with multiple positive charges or with one negative charge showing an enzyme lower affinity [7,10,13] .

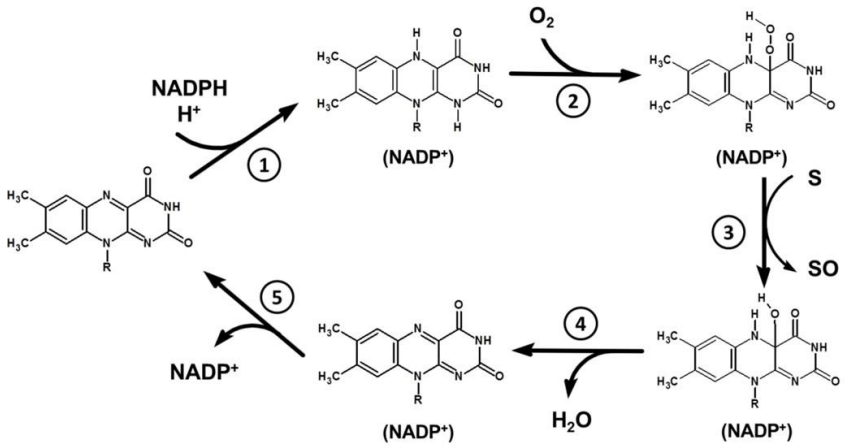

Figure 3. Catalytic cycle of FMO enzymes.

1.1.4. FMO and Cytochrome P450: similarities and differences

To date it is known that most drugs are metabolized by the cytochrome enzyme family. The main involved enzyme is the Cyp450, and only 2.5% of all metabolic reactions, with about 6% of all the phase I metabolic reactions, are catalyzed by FMO enzymes, although their drug metabolism contribution could be underestimated[10]. Despite this, the two enzyme families have some common features. They have similar molecular weights and are highly concentrated within the endoplasmic reticulum of liver cells, but also present within other organs such as lungs, skin, intestines, and kidneys, responsible for xenobiotics excretion. The FMOs are more active than cytochromes in the brain and work in tandem with CYP3A4 in the liver. Despite these similarities, CYPs and FMOs have many differences regarding both their chemical-physical characteristics and the ways in which they oxidize the substrate. The FMO enzymes are more susceptible to heat and are active a higher pH than CYPs. Moreover, FMOs have nucleophilic substrates affinity unlike CYPs which catalyze electrophilic reactions. The catalytic process is also different because the FMOs do not bind the substrate, and this is oxidized directly by NADPH, which releases two electrons and stabilizes the hydroperoxyflavin intermediate. The products of these reactions are polar, non-toxic, and easily excreted. Conversely, CYP enzymes binds the substrate and oxidize it by a mechanism involving only one electron, released from NADPH via an accessory protein called NADPH-CYP reductase. The products deriving from the CYPs catalytic process are often toxic. In addition, there is a specific inhibitor for almost each FMO enzyme, but there are no identified mechanism-based inhibitors for FMOs[7, 9, 10].

1.2. *FMO3* gene: structural organization

FMO3 gene belongs to the FMO gene cluster. It maps on chromosome 1 at 1q24.3, is 27 kb long and has 9 exons, of which the first is non-coding. It codes for the Flavin Monooxygenase 3 enzyme. *FMO3* is expressed in the human liver between birth and 2 years of age, increasing during childhood and adolescence and, finally, reaching its

maximum level in adults. *FMO3* mutations determine a Flavin Monooxygenase 3 enzyme malfunction and, consequently, the trimethylamine accumulation, determining the TMAU phenotype. To date, 94 mutations within the *FMO3* are known, classified as follows:

- 81 missense/nonsense mutations
- 1 splicing mutation
- 1 regulatory mutation
- 7 small deletions
- 2 small insertions
- 1 gross deletion

Regarding the functional consequences on disease phenotype, it is possible further classify them in (https://www.hgmd.cf.ac.uk/ac/index.php) :

- 59 disease-causing mutations (DM) (tab.1)
- 18 mutations highly related to the TMAU etiopathogenesis but not yet been confirmed (DM?)
- 13 functional polymorphisms with no reported disease association (FP)
- 2 Disease-associated polymorphisms (DP)
- 2 disease-associated polymorphisms with supporting functional evidence e.g., by an in vitro luciferase assay (DFP)

HGMD ACCESSION	NUCLEOTIDE CHANGE	AMINO ACID CHANGE
CM1512333	c.20T>C	Ile7Thr
CM035641	c.94G>A	Glu32Lys
CM061774	c.110T>C	Ile37Thr
CM136982	c.112G>T	Gly38Trp
CM1512334	c.122G>A	Trp41Term
CM1512335	c.127T>A	Phe43Ile
CM032234	c.151A>G	Arg51Gly
CM992883	c.154G>A	Ala52Thr
CM085438	c.172G>A	Val58Ile
CM004472	c.182A>G	Asn61Ser
CM980769	c.198G>C	Met66Ile
CM990602	c.198G>T	Met66Ile
CM129719	c.209C>T	Pro70Leu
CM004473	c.245T>C	Met82Thr
CM073070	c.341A>G	Asn114Ser
CM970532	c.458C>T	Pro153Leu
CM1512336	c.488T>C	Leu163Pro

CM093466	c.560T>C	Val187Ala
CM068526	c.578G>A	Gly193Glu
CM129718	c.584C>T	Ser195Leu
CM002018	c.596T>C	Ile199Thr
CM078327	c.668G>A	Arg223Gln
CM197296	c.682G>A	Gly228Ser
CM197297	c.694G>T	Asp232Tyr
CM136983	c.695A>T	Asp232Val
CM094688	c.713G>A	Arg238Gln
CM061775	c.713G>C	Arg238Pro
CM1816157	c.845C>T	Pro282Leu
CM980770	c.913G>T	Glu305Term
CM136984	c.919A>C	Thr307Pro
CM136985	c.929C>T	Ser310Leu
CM992886	c.940G>T	Glu314Term
CM1816158	c.985A>G	Thr329Ala
CM197299	c.989G>A	Gly330Glu
CM176549	c.1091C>A	Ser364Term
CM1512338	c.1127G>A	Gly376Glu
CM1724057	c.1160G>A	Arg387His
CM992887	c.1160G>T	Arg387Leu
CM073072	c.1164G>A	Trp388Term
CM129720	c.1262G>T	Gly421Val
CM1816159	c.1286A>G	Asp429Gly
CM004474	c.1302G>A	Met434Ile
CM073071	c.1408C>T	Gln470Term
CM1816160	c.1418T>C	Leu473Pro
CM002019	c.1424G>A	Gly475Asp
CM068527	c.1448G>C	Arg483Thr
CM990603	c.1474C>T	Arg492Trp
CM070133	c.1498C>T	Arg500Term
CD035666	c.192delA	p. (Glu65Argfs*2)
CD1912931	c.458_459delCC	p. (Pro153Glnfs*14)
CD070468	c.591_592delTG	p. (Cys197*)
CD1912938	c.632delT	p. (Met211Argfs*10)
CD141264	c.993_994delTA	p. (Tyr331*)
CD085185	c.1215delG	p. (Met405Ilefs*2)
CI1512337	c.850_860dup11	p. (Glu287Aspfs*17)
CI138618	c.1118dupA	p. (Ser374Valfs*10)
CX093467	c.1247_1248delAGinsT	p. (Lys416Ilefs*72)

Table 1. FMO3 causative mutations in Human genome mutation database.

1.3. Genotype-phenotype correlation

Since TMAU is a very rare syndrome, little is known about the disease incidence in the world population. *FMO3* gene causative variants in homozygous or compound heterozygous conditions could cause a greater reduction in the ability to metabolize trimethylamine. An epidemiological study performed on the British population showed that the heterozygous carriers' incidence is 0.5%-1%, giving an estimated frequency of the disorder in this population of about one in 40,000. Nevertheless, carrier incidence may be higher in other populations such as in New Guinea, with an incidence rate of 11%, 1.7% in Jordan, 3.8% in Ecuador[16]. The first mutation that has been identified in a trimethylaminuria patient was the c.458C>T (p. Pro153Leu), which is one of the most common identified to date[17]. Moreover, the allele frequency of 9 variants, 2 synonymous and 7 non-synonymous, was evaluated in African, Asian, and European ethnic groups. This frequency was found to be greater than 1% in at least one group of the population. The polymorphic variant with the highest frequency in all considered groups was Glu158Lys. The Glu308Gly variant resulted also frequent in European and Asian populations but less common in Africa. In vitro studies have shown that these two polymorphisms individually have little or no effect on the enzyme catalytic activity. However, in Europeans and Asians these two variants are found in *cis* on the same chromosome with a high frequency (20%). These variants association has a greater effect than the single one, reducing the catalytic activity of the enzyme. A third polymorphism, Val257Met, was more frequent in Asians but less frequent in Europeans and Africans and its enzyme activity influence is substrate dependent[18]. This variant has different effect on the enzyme catalytic activity in both anticancer aurora kinase inhibitors, Danusertib and Tozasertib. In details, it showed a reduction in the Danusertib oxygenation process, but no effect on the Tozasertib. Moreover, it has been demonstrated that this polymorphism does not even alter the TMA N-oxidation process. The Asp132His variant has a higher frequency in Africans, but it is very

rare in Asians and Europeans. It showed a catalytic activity reduction towards Methimazole and TMA, but not towards 10-(N, N-dimethylaminopentyl)-2-(trifluoromethyl) phenothiazine. In addition, the Val277Ala and Glu362Gln variants are frequent only in the African population, but their consequences on enzyme activity have not yet been determined. The Gly180Val variant, found only in Europeans, has no effect on enzyme activity but a combination of this variant in *cis* configuration with p. Glu158Lys severely affects enzyme activity and contributes to severe trimethylaminuria[19]. Lastly, another non-synonymous variant, Asn61Lys, with a frequency of 3.5% in African Americans and 5% in non-Latino white populations, causes a severe enzyme catalytic activity reduction. All other non-synonymous variants are almost rare, with a frequency lower than 1% and often limited to a single ethnic group. Furthermore, for most of these, the effect on enzyme catalytic activity is still unknown. *FMO3* genetic variants have been associated not only to Trimethylaminuria but also to other diseases such as the sudden infant death syndrome. From a recent study, it emerged that the c.472G>A [p. (Glu158Lys)] homozygous variant was more common in infants born to mothers who smoke. Provided that nicotine is a substrate of various enzymes of which the major ones are FMO3 and CYP2A6, considering that the latter is not expressed in the brain, the Glu158Lys variant could be one of the major risk factors. Moreover, the rs1795240 polymorphism, located upstream of the *FMO3* gene, it was highly associated with differences in lentiform volume nucleus. This results in several neurodegenerative and psychiatric disorders such as Parkinson, Huntingdon, Wilson diseases, and Tourette attention deficit hyperactivity disorder. In addition, the Gly158Lys/Glu308Gly compound variants showed positive effects in patients affected by adenomatous polyposis, even if associated with the TMAU phenotype as consequence of a reduced enzyme catalytic activity. These patients were treated with the Sulindac drug, a FMO3 enzyme substrate. Because of the lower enzyme catalytic activity, it was less metabolized and would have greater persistence and effectiveness in the body[18].

1.4. fmo3 enzyme: structure and function.

Flavin-containing Monooxygenase 3 contains 532 amino acid residues and has a molecular mass of 60,047 Da. It is a transmembrane protein located mainly in the adult human liver endoplasmic reticulum, but it is also expressed in skin, pancreas, cortex, and adrenal medulla. To date, the three-dimensional structure of the FMO3 human enzyme is not known as it is very difficult to perform x-ray liver microsomes crystallography. This is caused by the FMO3 protein insolubility which is anchored to the endoplasmic reticulum membrane via the c-terminal domain consisting of seventeen amino acids. However, since FMO yeast and bacterial enzymes are soluble, high-resolution FMOs crystal structures have been obtained. Based on high sequence homology of the latter with human FMOs, it was possible to determine the active site volume of the FMO3 enzyme which varies from a minimum of 1000 A^0 to a maximum of 1200A^0. Regarding function, as already described for the other FMO enzymes, it acts oxidizing specific substrates such as drugs and endogenous substances. While in the past most drug detoxification reactions were attributed to CYP3A4, today it is known that the FMO3 enzyme also plays a significant role. In fact, many drugs are substrates of both enzymes which together contribute to phase 1 functionalization reactions such as Arbidol, an antiviral agent, that first undergoes a S-oxidation and then a N-demethylation by FMO3 and CYP3A4 enzyme, respectively. In addition, Trimethylamine, a gut microbiota fermentation product deriving from precursors introduced with the diet is exclusively oxidized by FMO3 enzyme. Moreover, information on the enzyme-substrate interaction mode is known thanks to a recent *in silico* simulation model (Metasite) that considers both enzyme-substrate recognition, and the chemical transformations induced by the enzyme[20]. This software has been used to study the potential interactions between FMO3 and candidate drugs, already known to be substrates of the enzyme or not. This study showed that the enzyme-substrate interaction mechanism is very complex and may depend on various factors. Among them, the most important are

the substrate reactivity and its three-dimensional structure. The substrate reactivity is directly proportional to its nucleophilicity. Potential N-oxidation sites contain nitrogen and sulfur atoms. Furthermore, the enzyme-substrate interaction is very specific and sensitive to small changes in the substrate three-dimensional structure. The different enzyme-substrate reactivity depends on the substrate spatial orientation. So, different oxidation sites will be more exposed than others. For this reason, chemically favorable molecules for enzyme interaction may not be reactive due to their oxidation sites which are probably poorly exposed to the enzyme active site[21]. fmo3 protein abundance is age-, hormone, and gender-dependent. Age was positively associated with enzyme abundance. This was significantly lower in neonatal liver than that observed in childhood (6-12 years) and adolescents (12-18 years), and it is 1.9-fold lower than in adult[22]. A recent study also found FMO3 abundance differences between men and women. In the latter it was higher than in men. Interindividual variations in the FMO3 enzyme levels, probably due to physiological factors, have also been found within the same gender. The FMO3 enzyme abundance decreases in women during menstruation as a response to the female sex hormones variation which would cause a decrease in the FMO3 gene expression. Furthermore, it has also been demonstrated that the dietary indoles present in brassicas and nitric oxide mediated S-nitrosylation can inhibit the FMO3 enzyme catalytic activity both *in vitro* and *in vivo*[18]. The mechanism of action of FMOs is distinctly different from that of other monooxygenases. FMOs do not require substrate for dioxygen reduction of the prosthetic group FAD by NADPH. Instead, the protein plus the prosthetic group and the cofactor in its 4α-hydroperoxyflavin form stand ready to perform chemistry on available nucleophiles.

1.5. Trimethylaminuria primary form: Diagnosis

Receiving a diagnosis is very important for the patient. Having the certainty that it is a medical condition and not a psychological belief is helpful for the patient to live with the disease. The characteristic symptom described by TMAU patients is the pungent and unpleasant smell emanation similar to rotten fish. One of the patients' concerns is that this odor is occasional and may not be perceived by the doctor. Furthermore, the TMA olfactory sensitivity is different in each individual and some people are not able even smell it. This condition is known as TMA anosmia and about 7% of people suffer from it[17,23]. In addition, the odor could also be very similar to TMA but caused by other compounds. All these factors could cause a diagnosis delay and consequently it cannot be based on the examiner's sense of smell. Therefore, the initial diagnosis is usually biochemical which consists in TMA and TMAO levels urine determination. The genetic screening will help confirm the diagnosis and distinguish between primary and secondary forms of the disorder.

1.5.1. Trimethylamine and Trimethylamine N-oxide dosage in urine

This analysis is performed with and without choline loading. The patient is asked to do not eat foods that contain choline and to perform an initial urine collection (24h urine). The second urine collection (8h urine) will be carried out the following day after choline loading. The latter consists in taking 5 g of choline dissolved in orange juice or alternatively by administering a meal rich in choline such as fish (300 gr) or two eggs with haricot (400 gr)[19]. In healthy individuals, about 1 mg of TMA and 40 mg of TMAO are excreted in the urine. The TMA levels determination is based on the TMAO/TMA ratio according to the formula TMAO/TMAO+ TMA X 100. The lower this ratio, the more severe the phenotype shown:

- Ratios of 70%- 80% are classified as mild phenotype
- Ratios lower than 70% are classified ad severe phenotype

Thus, a correct diagnosis is based on this ratio and not only on the TMA levels. Furthermore, urinary tract infections, bacterial vaginosis, advanced liver or kidney disease, cervical cancer could determine an increase in urine TMA concentration. This analysis is also not recommended for women during menstruation because in this condition they may have a transient TMAU form. The analytical techniques used to carry out this analysis are proton nuclear magnetic resonance (H-NMR) spectroscopy, gas chromatography, electrospray ionization tandem mass spectrometry, direct infusion electrospray quadrupole time-offlight mass spectrometry, and matrix-assisted laser desorption/ionization time-of-flight mass spectrometry. Mass spectrometry and H-NMR are more advantageous because can detect TMA and TMAO simultaneously with great sensitivity. Moreover, by H-NMR no metabolites extraction or separation are required, and measurement can be performed directly on urine samples[24]. In addition to determining the TMA and TMAO urine levels, the diagnostic procedure includes the genetic test execution to verify if the subject could be affected by the TMAU primary form.

1.5.2. *FMO3* genetic test

To date, only the *FMO3* gene is known to cause the TMAU primary form. Missense mutations, deletions, insertions, and nonsense variants could determine a partial or total deficiency of FMO3 enzyme activity. Thus, genetic screening is useful to verify the presence of such variants. It is usually performed by direct Sanger sequencing. Considering that this pathology is transmitted in an autosomal recessive manner and referring to the diagnostic guidelines, the genetic test gives a positive result when the causative homozygous mutations in the *FMO3* are identified[4].

1.6. Secondary Trimethylaminuria (TMAU2)

The TMAU secondary form or TMAU2 is characterized by the TMA body accumulation but unlike TMAU1, this condition is not caused by the FMO3 enzyme malfunctioning, but by environmental factors that can be grouped into:

1.6.1. Liver dysfunction

Individuals affected by viral hepatitis, hepatic insufficiency or cirrhosis, and portosystemic shunt may present the TMAU phenotype due to the reduced FMO3 enzyme catalytic activity. However, the portosystemic shunt condition can be resolved by endovascular closure[19].

1.6.2. Hormone therapy

It is known that subjects subjected to hormonal therapy, especially based on androgens, manifest the characteristic smell of rotten fish, due to still unknown molecular mechanisms that induce the FMO3 enzyme down regulation[16].

1.6.3. Treatment with TMA precursors

Choline-based therapies for Alzheimer and Huntington diseases could contribute to the TMAU phenotype onset. Elevated daily choline intake could cause the TMA levels increase and its consequent accumulation as a consequence of FMO3 enzyme saturation.

1.6.4. Kidney diseases

Trimethylaminuria can be accompanied by chronic kidney disease or urinary tract infections that cause TMA to be produced directly in the urine, causing a false positive result.

1.6.5. Gut Dysbiosis

In most cases, the TMA secondary form is determined by the gut microbiota alteration in favor of the bacterial species that produce TMA. In fact, specific bacterial species can convert some compounds introduced with the diet such as TMAO, choline, betaine, carnitine, ergothioneine into TMA. This bacteria overproduction could cause the TMA accumulation which, due to the FMO3 enzyme saturation, will be excreted through the biological fluids causing the characteristic and unpleasant rotten fish smell. The alteration of the gut microbiota

composition, both qualitatively and quantitatively, can occur as a consequence of the prolonged intake of antibiotics. In addition, diet has an important role. In fact, it has been demonstrated that even the diet determines the inter-individual variability known as "bacterial fingerprint".

1.6.5.1.Gut microbiota: composition and physiological functions

The composition of the gut microbiota has been the subject of intense metagenomic investigations which have allowed the qualitative and quantitative characterization of the microbial community residing in the gastrointestinal tract. The latter is colonized by a large variety of microorganisms such as bacteria, viruses, fungi, and yeasts that perform different but fundamental and vital functions for the human body. Considering the relationship between bacterial cells residing in the intestine and the individual's own cells, it is easy to understand the important role played by these microorganisms. In fact, a 10 times greater number of bacterial cells has been estimated, comprising about 1000 species. The gut microbiota and host have a symbiotic relationship. Microbiota receives complex nutrients from the host, that the latter is unable to digest, and converts them into metabolic intermediates that can thus be absorbed and metabolized. The qualitative and quantitative gut microbiota composition along the gastrointestinal tract is different. This variability may depend on the chemical-physical environment which is different along the intestinal tract. In fact, the pH, the composition and the mucous layer thickness, the speed of nutrients transit are all factors that determine different habitats favoring the growth of some bacterial species rather than others. Furthermore, each individual has a specific and characteristic gut microbiota. This interindividual variability depends on external factors such as the gut exposure by microorganisms, in the early stages of life, from both the mother and the environment. Colonization of the human gut with microbes begins immediately at birth. Upon passage through the birth canal, infants are exposed to a complex microbial population. Evidence that the immediate contact with microbes during birth can affect the development

of the gut microbiota comes from the fact that the intestinal microbiota of infants and the vaginal microbiota of their mothers show similarities. Other factors that influence the gut microbiota variability are the different lifestyles, antibiotic intake, diet, and geographical origin[25]. However, there are 57 species common to all individuals. The dominant microbial phila are *Firmicutes* and *Bacteroidetes* which represent 90% of the entire microbiota and the remaining part is occupied by *Actinobacteria*, *Proteobacteria* and *Verrucomicobria* (Fig.4).

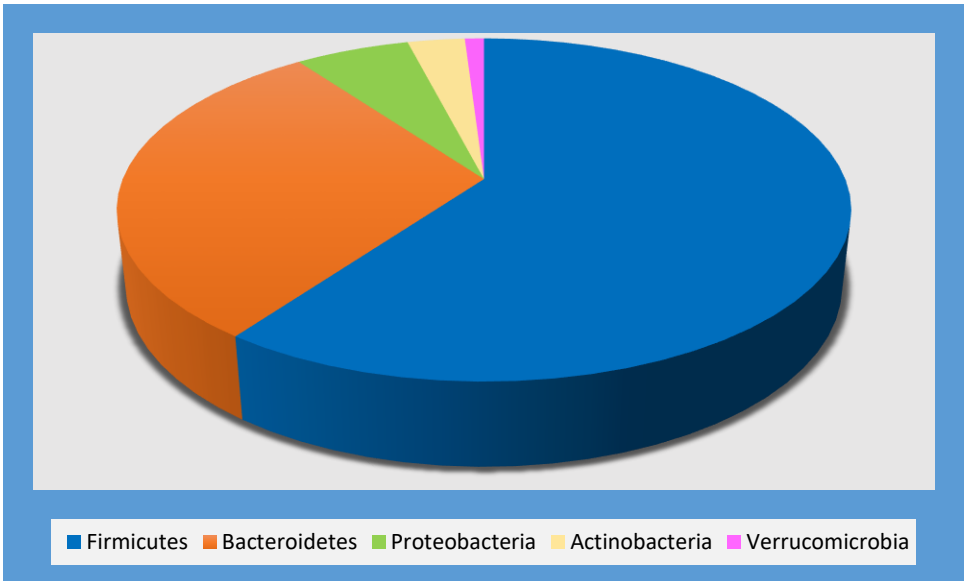

Figure 4. Estimation of bacteria phyla relative abundance in Human gut.

The main bacterial families belonging to the firmicutes phylum are *Lachnospiraceae* e *Ruminococcaceae*. On the other hand, *Bifidobacterium* is one of the most represented species of the *Actinobacteria* phylum. The beneficial effects of these bacteria are known and for this reason are used as probiotics. Their abundance varies during life, they are more represented in breastfed infants but gradually decrease in adults. *Bacteroides*, *Parabacteroides*, *Alistipes* and *Prevotella* are the most represented genera in *Bacteroidetes* phylum. Unlike *Bifidobacterium*, their abundance is not related to age. *Proteobacteria* is the least represented phylum of the gut microbiota. Some species,

belonging to this phylum, such as *Escherichia*, *Klebsiella*, and *Enterobacter* are responsible for the infections and inflammations onset as they are opportunistic pathogens. Finally, the *Verrucomicrobia* phylum, even if it is poorly represented, has an important role in the intestinal ecosystem. The *Akkermansia* species, belonging to this phylum, guarantees intestinal homeostasis[26]. In eubiosis conditions, therefore when the different bacterial taxa are distributed in the various portions of the intestine according to a correct balance, the microbiota performs important and several functions which guarantee the maintenance of host health good state. The main functions are metabolic, structural, immune or defense function, and influence on the psychic sphere.

1.6.5.2. Metabolic function

The metabolic function consists in the complex and very often unassimilable macromolecules digestion, introduced with diet, into simpler metabolites. The degradation process of these compounds is called fermentation. This occurs mainly in the proximal colon, which is the gut district where most of the microbiota is located. The gut microbiota metabolic function is influenced by several factors. One of them is the intestinal pH gradients regulation. the pH is more acidic in the proximal colon and close to neutral in the distal portion. Firmicutes are more tolerant of acidic pH while *Bacteroidetes* grow better at higher pH. One of the main microbiota functions is the complex polysaccharides degradation, known as "saccharolytic fermentation". The gut microbiota contribution to carbohydrate metabolism is greater the human host. The latter produces only 17 carbohydrate-active enzymes, whereas some gut bacterial species have more than 200 carbohydrate-active enzymes. Insoluble dietary fibers such as dietary oligosaccharides, undigested (resistant) starch and plant cell wall components such as cellulose, hemicellulose (xylan) and pectin are fermented by some gut microbiota classes such as *Bifidobacteria* and *Clostridia*. The main saccharolytic fermentation products are short-chain fatty acids or SCFAs such as butyrate, propionate, and

acetate. These have different tissue destinations and functions and the approximate molar ratio acetate:propionate:butyrate is 60:25:15 and remains constant in different colon regions. After being produced, acetate reaches the liver and can enter in the cholesterol synthesis metabolic pathway as a precursor. However, a large fraction reaches peripheral tissues providing energy. Instead, propionate is mainly involved in the gluconeogenesis process. The *Bacteroidetes* phylum is known as the major propionate producer. Butyrate represents the main energy source used by colonocytes. Proteins, on the other hand, are degraded through "proteolytic" fermentation and occurs mainly in the distal colon. The main bacterial species responsible for this process are *Bacilli*, *Streptococchi*, *Propionibacterium*, *Clostridium* e *Bacteroides*. The latter, being highly expressed in the distal colon, are the species most involved in the protein degradation process[26]. The products of this proteolytic fermentation process are mainly branched-chain fatty acids and, in limited quantities, also short-chain fatty acids. The main metabolites produced by these bacterial species are summarized in tab.2. Moreover, neurotransmitters such as serotonin, dopamine, tryptamine, and γ-aminobutyric acid (GABA) are produced from some amino acids catabolism. Serotonin is a neurotransmitter involved in many processes including mood, appetite, hemostasis, immunity, and bone development. Its dysregulation is thus reported in many disorders, including inflammatory bowel disease (IBD), irritable bowel syndrome (IBS), cardiovascular disease, and osteoporosis. Tryptamine is produced by the tryptofane catabolism. This reaction is catalyzed by the decarboxylase enzyme produced by the Clostridium sporogens species. Tryptamine is important because regulates intestinal motility, has an immune function, and induces the serotonin release by cells of the enteroendocrine and enteric nervous systems. Gamma-aminobutyrate (GABA) is the major inhibitory neurotransmitter of the central nervous system. Its production is induced by *Lactobacillus* and *Bifidobacterium* species. Its decrease has been associated with the depression and anxiety onset.

Phylum	Family	Metabolites produced
Actinobacteria	Bifidobacteriaceae	Acetate, Formate, Lactate
Bacteroidetes	Bacteroidaceae	Acetate, Propionate, Succinate, Carbon dioxide, Formate
	Prevotellaceae	Acetate, Propionate, Succinate,
	Rikenellaceae	Acetate, Propionate, Succinate, Carbon dioxide, Formate,
Firmicutes	Clostridiaceae	Acetate, Propionate, Succinate, Carbon dioxide, Formate, Lactate, Butyrate
	Erisypelotrichaceae	Acetate, Formate, Lactate, Carbon dioxid
	Lachnospiraceae	Acetate, Formate, Lactate, Propionate
	Lactobacillaceae	Acetate, Formate, Lactate, Propionate
	Ruminococcaceae	Acetate, Formate, Lactate, Succinate
	Streptococcaceae	Acetate, Formate, Lactate, Ethanol
	Veilonellaceae	Acetate, Propionate, Succinate, Carbon dioxide, Formate, Lactate
Proteobacteria	Enterobacteriaceae	Acetate, Succinate, Carbon dioxide, Formate, Lactate, Butyrate

Table 2. Metabolites produced by the main bacteria families in Human gut.

The fats, contained in diet, consist of 95% triglycerides and phospholipids, the latter in the phosphatidylcholine form. They are degraded and transformed into simpler molecules by the action of bacterial lipases. *Lactobacilli*, *Enterococci*, *Clostridia*, and *Proteobacteria* are responsible for this process. Trimethylamine is produced by choline bacterial metabolism[27].

1.6.5.3. Structural function

An important structural function performed by the microbiota is the modulation of mucus glycosylation. *Bacteroides Thetaiotaomicron* species produces a signal molecule, inositol, which contributes to this mechanism by providing adhesion sites for the beneficial microbes colonization. Another function is to maintain the tight junctions integrity among the intestinal epithelium cells. The fulfillment of this

function occurs thanks to a signal mediated by the type 2 toll-like receptor following the glycan peptide recognition of the microbial wall. In addition, gut microbiota contributes to the intestinal microvasculature development by inducing the angiogenin factor 3 transcription. Moreover, *Lactobacillus rhamnosus* produces two soluble proteins, p40 and p75, which can prevent epithelial cell apoptosis. Lastly, Akkermansia species grows in the mucus layer, degrading host-derived mucins and producing propionate and acetate, which can be further utilized by other bacteria. It adheres to enterocytes and stimulates the gut barrier mechanism[26].

1.6.5.4. Immune or defense function

Another important function performed by the gut microbiota is the immune role. It prevents the pathogenic bacteria growth in different ways. It alters the intestinal pH, competes with them for growth substrates and ensuring the intestinal barrier integrity, produces antimicrobial substances inactivating them. *Lactobacillus Plantarum* and *Bifidobacterium Lactis* species induce proteins gene expression, such as occludin, involved in the epithelial cells tight junctions. This prevents the pathogens, toxins, food allergens and other metabolites passage into the bloodstream which could cause inflammation and the other disturbs onset.

1.6.5.5. Influence on the psychic sphere

In recent years, the interest in the possible gut microbiota influence on the individual psychic sphere has grown with advances in high throughput omics-based technologies. Recent studies suggest It could be involved in behavior disorders such as depression, anxiety, obsessive-compulsive behavior but also may contribute to the development or progression of neurodegenerative diseases and dementia such as Alzheimer's disease (AD), vascular dementia, frontotemporal dementia, Parkinson's disease (PD), and dementia with Lewy bodies. This connection is justified considering the microbiota role has on the gut-brain axis[28]. The latter is a bidirectional communication network includes the central nervous

system (CNS), both brain and spinal cord, the autonomic nervous system (ANS), the enteric nervous system (ENS) and the hypothalamic pituitary adrenal (HPA) axis[29] (fig.5).

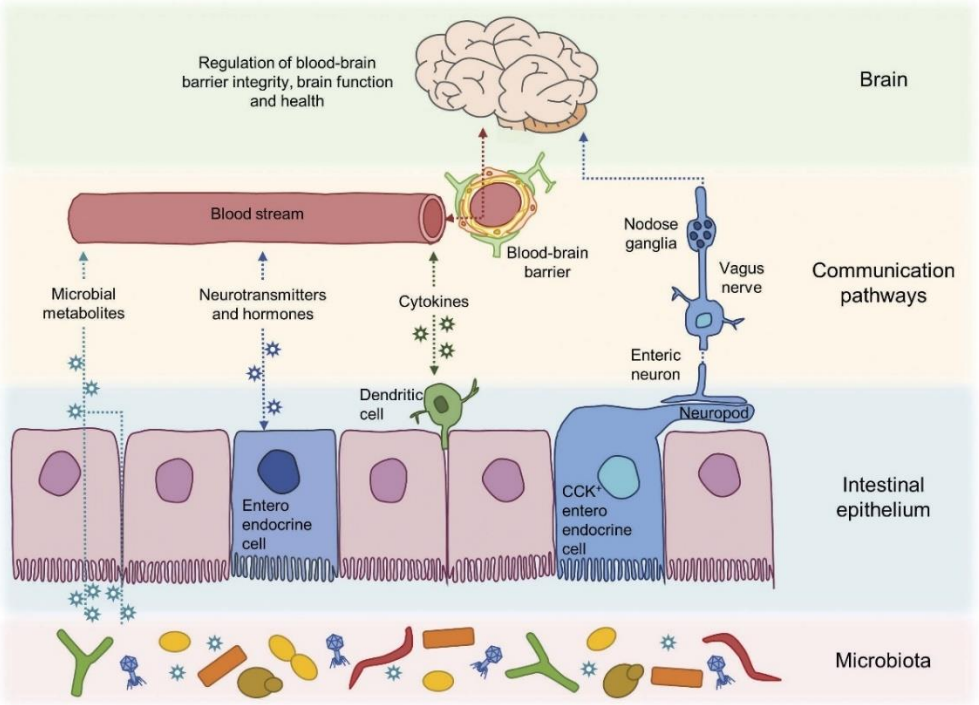

Figure 5. Pathways of communication along the gut-microbiota axis. A complex interplay of epithelial, immune, and neural cell signalling networks is involved in communicating changes in microbial metabolites in the gut and the brain involving both circulatory and neural routes.

The autonomic nervous system, with the sympathetic and parasympathetic limbs, drives both afferent signals, arising from the lumen and transmitted though enteric, spinal and vagal pathways to central nervous system, and efferent signals from CNS to the intestinal wall. The enteric nervous system is considered the second brain. Intestine and brain have a structural homology because the intestinal loops resemble the cerebral convolutions. The intestine nerve cells number (about 100 million) is similar to those present in the spinal cord. Enteric neurons are organized into ganglionated networks encircling the intestinal tube and spatially categorized into two layers: the myenteric plexus, between the circular and longitudinal muscle layer, and the submucosal plexus in the submucosa. These two portions are closely interconnected by interneurons, motor neurons, and enteric glial cells[30]. The gut and the brain interaction is called neuromodulation and occurs through the direct

production of both neurotransmitters and active metabolites, the SCFAs. More than 30 classes of neurotransmitters, also identified in the central nervous system, are produced in the enteric nervous system. Most of these are produced by the gut microbiota such as serotonin, dopamine, norepinephrine, acetylcholine, histamine, and γ-aminobutyric acid. These can turn on or off the vagus nerve stimulation which in turn transmits the electrical impulse to the central nervous system. Furthermore, neurotransmitters can be produced indirectly by enterochromaffin cells of the gastrointestinal mucosa. These cells have receptors to which bacterial metabolites such as SCFA, carbohydrates, and peptides bind, inducing the peptide hormones release. The latter can act directly on enteric neurons or reach the central nervous system through the bloodstream. Furthermore, the bacterial metabolites can activate the immune response through the cytokines production. This process can occur through three mechanisms. Conditions of dysbiosis, infections cause the epithelial barrier alteration allowing the bacteria, toxins, and lipopolysaccharides (LPS) access. This results in the inflammatory cytokines secretion into the bloodstream which reach the blood brain barrier. Furthermore, cytokine secretion can act locally on enteric neurons inducing their apoptosis. This causes both the intestinal functions alteration and the loss of communication between gut and brain. Finally, cytokines induced by bacterial metabolites can release soluble factors to the blood-brain barrier, altering its permeability and increasing the brain cells inflammatory state[28].

1.6.6. Trimethylamine Chemical-physical properties and its precursors

Trimethylamine is a tertiary amine with a characteristic pungent odor similar to that of rotten fish. Being both water and fat soluble, it is able to struggle throughout the body and easily volatilizes at room temperature[31]. In various living organisms, both animals and plants, it acts as a repellent or attractive chemical compound, performing various functions. In fish, TMA is produced post-mortem by TMAO degradation by their own microbiota. TMA levels gradually increase during

product storage time and gradually decrease during putrefaction stage along with TMAO levels[11]. The TMA and TMAO ratio is one of the parameters monitored by the fishing industry to evaluate the fish freshness. Additionally, TMA is also found in the reproductive organs of plants, fungi, and animals. In the latter, it has a role in the courtship phases, especially in amphibians[31]. It also induces mating in cattle by being present in the cow's vaginal fluid. Some plants use it as a deterrent to herbivores. Furthermore, while for rats it is a chemical repellent, for mosquitoes and mice it is a chemical attractant. The latter, in fact, use it for territorial reporting. In humans, TMA is a repellent compound that is sensed by the olfactory system at levels as low as 0.12 ppb[17]. The perceived pungent odor is thought to be a protective reflex evolved during evolution to avoid consuming spoiled food. In fact, TMA is not present directly in foods but is synthesized by the gut microbiota starting from its precursors[32]. To date, the main known TMA precursors, available in diet, are choline, carnitine, betaine, ergothioneine and trimethylamine N-oxide. The table 3 summarizes the main foods containing these precursors.

TMA precursors	Food
Choline	Beef liver, egg yolk, fish, seafood, chicken, cauliflower, peanuts, and soy milk
Carnitine	Red meat, and dairy, low concentration in vegetables, cereals, and fruit
Betaine	cereali, spinaci, farina integrale e pane, farina di orzo, barbabietola, crusca di frumento
Ergothioneine	porcini mushrooms, oysters, liver and kidneys, black and red beans, oat bran
Trimethilamine N-Oxide	shellfish, saltwater fish, swordfish, salmon, and cod, tuna, mackerel, sardines, oily fish.

Table 3. Main food containing Trimethylamine precursors.

1.6.6.1. Choline

Choline is a quaternary ammonium salt containing a trimethylammonium residue that serves as the TMA source. It is found in many foods. Beef liver, egg yolk, fish, seafood, chicken, cauliflower, peanuts, and soy milk are foods high in choline. It is introduced into the body usually in the form of lecithin or phosphatidylcholine. For example, meat contains 0.5% of lecithin, which is one of the most important cell membranes components ensuring its fluidity. In the liver, choline has the function of packing and exporting triglycerides into low-density lipoprotein (VLDL). Furthermore, it has a role in lipid metabolism, in the signaling mechanism mediated by lipid second messengers, in the cholesterol and bile enterohepatic circulation process, in nuclear receptors activation and finally it is the neurotransmitter acetylcholine precursor contributing to the nerve signals transmission[33].After being introduced with the diet, part of choline is absorbed in the small intestine, while the excess is metabolized into TMA in the large intestine by the gut microbiota. The major pathway of TMA formation from choline is catalyzed by the bacterial enzyme TMA lyase. In this reaction, acetaldehyde is also produced. The TMA synthesis can also take place indirectly from phosphatidylcholine which is converted into choline by the Phospholipase D enzyme. This reaction is reversible, the choline interconversion to phosphatidylcholine is catalyzed by the choline kinase enzyme. Furthermore, choline can be converted into betaine by two enzymes that catalyze the reaction sequentially namely choline dehydrogenase and betaine dehydrogenase[34].

1.6.6.2. Carnitine

L-Carnitine is an amino acid derivative synthesized in human body, mainly in liver and kidney, from methionine and lysine. It can also be introduced through the diet. Red meat (horse, sheep, lamb, and beef), and dairy products are the main foods that contain it. Low carnitine concentrations are found in vegetables, cereals, and fruit. In addition, the legumes consumption, rich in lysine, induces its endogenous

biosynthesis. L-carnitine is an important nutrient because it provides energy by transporting long-chain fatty acids from the cytosol to the cells mitochondria. About half of the exogenous L-carnitine is absorbed from the small intestine, the remaining carnitine arrives in the large intestine where it is degraded to TMA by the gut microbiota. Carnitine oxidoreductase is one of the enzymes responsible for transforming L-carnitine into TMA. In addition, carnitine TMA-lyase converts L-carnitine into TMA. This enzyme catalyzes the same reaction starting from other precursors such as choline, betaine and γ-butyrobetaine. These last two metabolites, which are TMA precursors, can be synthesized from carnitine, in reactions catalyzed by the enzymes L-carnitine dehydrogenase and γ-butyrobetainyl carnitine CoA transferase, respectively.

1.6.6.3. Betaine

Betaine is a natural substance extracted from sugar beets from which its name derives. The foods that contain it are cereals, spinach, whole meal flour and bread, barley flour, beetroot, wheat bran. It is also known as trimethyl glycine, being a well-known methylating agent because it is able to transfer methyl groups to various substances such as homocysteine. In the betaine homocysteine methyltransferase pathway, it is converted into methionine. Due to this biochemical function, it is used as a therapeutic approach in the conditions of hyperhomocysteinemia and homocystinuria. The TMA synthesis from choline occurs in the reaction catalyzed by the bacterial enzyme betaine reductase, where betaine acts as an oxidizing compound[11].

1.6.6.4. Ergothioneine

Ergothioneine is a biogenic amine derived from histidine. It was first extracted from the ergot fungus from which it takes its name. It is, mainly, found in porcini mushrooms, oysters, liver and kidneys, black and red beans, oat bran. Its biological properties are still little known. In vitro studies, not yet confirmed in vivo, have

demonstrated that ergothioneine could have antioxidant and cytoprotective properties. Furthermore, ergothioneasis is the bacterial enzyme that catalyzes the ergothioneine conversion to TMA.

1.6.6.5. Trimethylamine N-oxide

Trimethylamine N oxide (TMAO) is a colorless and odorless molecule with a molecular mass of 75.1 Dalton, belonging to the class of oxidized amines, soluble in water in the dihydrate form[35]. It is found in the marine organism tissues at 0.2 molar concentrations where it acts as an osmolyte protecting them from sudden changes in temperature, salinity, hydrostatic pressure, osmotic stress, and high urea concentrations[36]. TMAO is involved in the anaerobic respiration of both marine bacteria and most enterobacteria of human instinct, acting as an electron terminal acceptor. In humans, this molecule is introduced with the diet or is synthesized by the hepatic Flavin-Containing Monooxygenase-3 enzyme starting from the TMA precursor, produced by the gut microbiota in the intestine. TMAO is mostly contained in shellfish, saltwater fish, swordfish, salmon, and cod, tuna, mackerel, sardines, oily fish. However, the freshwater fish intake does not seem to affect the TMAO levels in the urine. Furthermore, another study suggests that the cooking fish method could also be responsible of TMAO levels. The fried fish consumption appears to be associated with an increase in TMAO values[37]. About half of the TMAO introduced with diet is not metabolized but is excreted in the urine, the remaining 50% is converted into TMA by the gut microbiota. TMAO reductase is the enzyme responsible for this reaction. Several studies have been done on the role that this molecule could have in the human body. Both positive and negative effects have been associated with increased TMAO concentrations. Regarding adverse effects, higher TMAO levels are associated with type 2 diabetes mellitus, cardiovascular disease (CVD) and atherosclerosis, colorectal cancer, and obesity. It is known that TMAO alters the cholesterol reverse transport[38], induces the CD36 and SR-A1 receptors expression in macrophages with consequent lipids

accumulation and foam cells formation in the arteries walls[34,39]. Furthermore, a study showed the TMAO role in the protein aggregates stabilization such as amyloid beta and subsequent plaque formation. High TMAO levels in rats were also associated with increased endothelial dysfunction and vascular inflammation caused by overexpression of tumor necrosis factor (TNF α), interleukin (IL6), and C-reactive protein. TMAO has been measured in human cerebrospinal fluid, however it is not yet clear whether it is directly synthesized in the brain, given that the FMO3 gene is also expressed in this organ, or whether TMAO crosses the blood-brain barrier (BBB). This could occur because of BBB increased permeability. TMAO appears to reduce the tight junction proteins expression such as claudin 5. One of the most discussed topics but which also arouses conflicting opinions concerns the association between fish consumption and the CVD onset. Fish contains high TMAO concentrations which is known to be linked to the CVD onset. On the other hand, people suffering from this pathology are advised to consume fish rather than meat. This incongruity can be explained also considering the other compounds contained in fish such as polyunsaturated fatty acids, eicosapentaenoic acid and docosahexanoic acid[34,37]. Although TMAO seems to be linked to various pathological conditions, several studies have also revealed beneficial effects for the body. In particular, in the renal cortex it counteracts the toxic effects of urea and other substances that accumulate when urine passes through the Henle loops in the renal nephrons inducing the microtubules polymerization[31]. TMAO could have a positive effect on prion diseases. In transmissible spongiform encephalopathy, the scrapie prion protein is converted to its pathogenic isoform. This conversion appears to be inhibited by TMAO. This protective role has also been documented in other pathologies such as Machado Joseph disease, spinocerebellar ataxia and amyotrophic lateral sclerosis (SLA). In addition, modulation of IDP (intrinsic conformation proteins) three-dimensional structure conformation such as synuclein is another positive role played by TMAO[34]. Finally, some studies have demonstrated the TMAO role against cellular stress caused by protein misfolding.

It is known that TMAO binds the luminal domain of protein kinase R-like endoplasmic reticulum kinase (PERK), activating the unfolded protein response and consequently reducing endoplasmic reticulum stress[40].

1.6.7. Bacteria Trimethylamine producer

Studies on the TMA precursors metabolism, especially for choline, were made in 1910, but since then the metabolic pathways involved in the TMA synthesis have remained unknown for more than 100 years. The interest in understanding these mechanisms has increased proportionally with the pathologies incidence growth such as cardiovascular disease (CVD), non-alcoholic fatty liver (NAFLD) associated with the TMAO levels increase[41]. It is known that the TMA levels production is different and depend on the metabolic pathways from which it derives. It is known that a higher concentration of TMA levels in urine is obtained starting from TMAO (about 80%) and choline (about 60%), followed by L-carnitine, γ-butyrobetaine and betaine. The betaine contribution to the TMA production is minimal. The study of such pathways was possible by the bioinformatics, molecular, genetics, biochemistry, and comparative omics analysis combination. To date, the metabolic pathways involved in the TMA production involve the following enzymes: choline TMA-lyase, carnitine monooxygenase, glycine-betaine reductase and TMAO reductase. These enzymes are involved in the choline, carnitine, betaine and TMAO metabolism, respectively. The enzyme choline TMA lyase is encoded by the Cut gene cluster which is currently the most studied. It is formed by 19 open reading frames (ORFs) which consist of: cut C, cut D, two predicted coenzyme A (CoA)-acylating aldehyde oxidoreductases (cut B and cut F), eight putative bacterial microcompartment shell proteins (cut AEGKLNQR), a putative chaperonin (cut I), a phosphotransacetylase (cut H), a ras-like GTPase (cut S), an alcohol dehydrogenase (cut O). The cut C/D cluster is involved in the choline anaerobic degradation. In detail cut C codes for choline TMA lyase, cut D instead codes for a cut C activating protein. The enzyme choline TMA lyase causes the cleavage of the

C-N bond in choline with the production of TMA and acetaldehyde. Cluster cut is present not only in many gut bacteria but also in some species of the urogenital tract, airways, and oral cavity[42]. The second metabolic pathway involved in the TMA synthesis is the carnitine degradation by the two component Rieske-type oxygenase/reductase enzyme, encoded by the cnt A/B gene, discovered in *Acinetobacter Calcoaceticus* and *Serratia Marcescens*. However, another two-step mechanism for the carnitine conversion to TMA exists. This mechanism uses another Rieske-type oxygenase/reductase enzyme, encoded by the YeaW/Y cluster, and transforms carnitine into TMA involving the intermediate γ-butyrobetaine (fig.6). This pathway is shown to be the main pathway for TMA production in the human gut[43]. For this reason, the carnitine metabolism is slower than that of choline[44]. Finally, a final metabolic pathway of TMA synthesis involves the enzyme TMAO reductase encoded by the Tor A gene which directly converts TMAO into TMA.

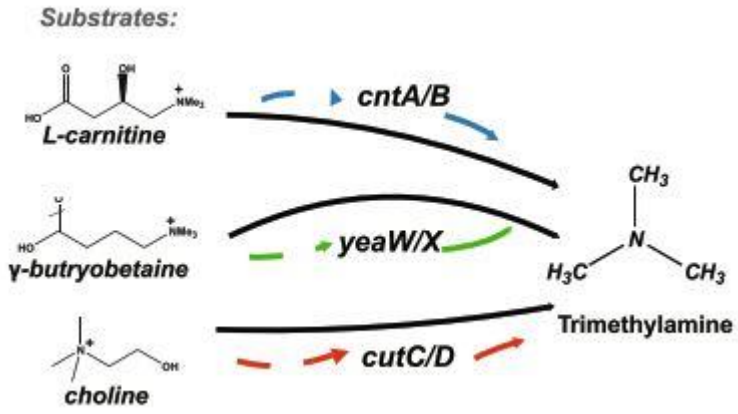

Figure 6. Microbial transformation pathways of TMA-lyases, cntA/B, yeaW/X, and cutC/D.

This mechanism is still poorly studied. It is known that it is mostly present in Proteobacteria (Escherichia and Klebsiella genera). Thanks to recent metagenomic analyses, it has been possible to associate the gene clusters discussed with the various bacterial genera of the gut microbiota. This study showed that the C/D cluster cut is present in 48 genera. Both cnt A/B and yeaW/Y clusters are found in

15 bacterial genera. Most of these bacterial genera belong to the following families: *Enterobacteriaceae*, *Coriobacteriaceae*, *Clostridiaceae*, *Lachnospiraceae*, *Enterococcaceae*, *Veilloneaceae*, and to philum *Firmicutes*, *Proteobacteria* and *Actinobacteria*. The main phyla and genera containing the clusters discussed are summarized in table 4.

Phylum	Genus	cntA	cntB	cutC	cutD	yeaW	yeaX
Actinobacteria	Atopobium			x	x		
	Collinsella			x	x		
	Egghertella				x		
	Olsenella			x	x		
Bacteroidetes	Bacteroides			x	x		
	Prevotella				x		
Firmicutes	Clostridium			x	x		
	Enterococcus			x	x		
	Faecalibacterium				x		
	Blautia			x	x		
	Lactobacillus			x	x		
	Roseburia				x		
	Ruminoclostridium			x	x		
	Veillonella			x	x		
	Lachnoclostridium			x	x		
Proteobacteria	Achromobacter	x	x			x	x
	Acinetobacter	x	x			x	x
	Citrobacter	x	x	x	x	x	x
	Desulfovibrio			x	x		
	Escherichia	x	x	x	x	x	x
	Klebiella	x	x	x	x	x	x
	Proteus			x	x		
	Pseudomonas	x	x			x	x
	Serratia	x	x			x	x
	Shigella	x	x			x	x

Table 4. cntA/B, cutC/D, yeaW/yeaX cluster distribution in several bacteria genus. The cross indicate that the genus contains the genes encoding the corresponding TMA-lyase.

Although most TMA is produced in the intestine, it can also be synthesized in the oral cavity and vaginal secretions. The oral microbiota strain *Streptococcus Sanguis* I can produce TMA from choline. In the vagina, however, the dominant strains are

Lactobacillus and *Atopobium*. In bacterial vaginosis conditions, very often, the Lactobacillus is replaced by the genera *Gardnerella*, *Pseudomonas*, *Mobiluncus*, *Bacteroides*, *Prevotella*, *Streptococcus* and *Phorphyromonas*. All these bacteria are able to produce TMA. This would explain the symptoms reported by many TMAU patients associated not only with the emanation of odor from sweat but also from breath and vaginal secretions. Furthermore, TMA is produced not only by commensal bacteria of the intestinal flora but also by some pathogens such as *Campylobacter*, *Salmonella*, *Aeromonas*, *Burkholderia*, *Shigella*, *Vibrio*[11].

1.6.8. Influence of diet on the gut microbiota variability

Diet has a fundamental role in the interindividual variability of the intestinal microbiota. A balanced diet is the first therapeutic approach recommended to the TMAU patients. Certain foods may favor the growth of some bacterial species over others. These alterations are more evident in subjects who consume mainly only animal or vegetable foods. The urine TMA and TMAO levels in vegetarian subjects was lower than in subjects who also consume meat[32,43]. Similarly, the cut and cnt clusters were less expressed in vegetarians. Thus, a vegetarian lifestyle could reduce the abundance of bacteria expressing these genes. The western diet, rich in proteins and animal fats and low in fibres, causes the body beneficial bacteria reduction such as *Bifidobacterium*, *Lactobacillus* and *Eubacteria*. On the contrary, the Mediterranean diet, characterized by cereals, fruit, vegetables and legumes, would induce their prevalence together with the *Prevotella* and *Bacteroides* species. In detail, it has been demonstrated that fruit consumption leads to an increase in *Bifidobacterium*. Red wine polyphenols taken for 4 weeks were associated with an increase in *Bacteroides*, *Prevotella*, *Enterococcus*, *Bifidobacterium*, *Blautia Coccoides* species. As far as proteins are concerned, the proteins vegetable consumption, such as those obtained from extract of peas leads to an increase in the Bifidobacterium species abundance and the *Ruminococcus*, *Alistipes*, *Bilophyla* species overexpression with consequent increase in the TMA concentration[11,45].

1.6.9. Trimethylaminuria secondary form: Diagnosis

TMAO/TMA ratio evaluation in urine is the first recommended approach not only for the TMAU primary form but also for the secondary one. Although in the TMAU secondary form the FMO3 enzyme is functional and most of the TMA produced by the gut microbiota is converted to TMAO, altered TMA levels result because of enzyme saturation. The microbiota test is recommended to patient to verify if the phenotype can be determined by the gut microbiota alteration. This is performed on faecal sample by sequencing bacterial 16s rRNA using second generation sequencing techniques. The analysis aims to characterize the quantitative and qualitative microbiota composition to evaluate microbial ecosystem alterations also defined as dysbiosis. This condition is known to be a major cause of TMAU2.

1.7. Transient Trimethylaminuria

A transient trimethylaminuria form exists. It can arise in women during menstruation because of the hormonal alteration that could determine the FMO3 enzyme down expression. Transient forms can also occur in newborns during the weaning period. The latter could manifest the TMAU phenotype because of both the increase in the TMA precursors levels introduced with the diet and the FMO3 enzyme down expression that is typical in this age group. Furthermore, intermittent forms can be due to intense physical activity, fever, and emotional stress[17].

1.8. Social impact

Although trimethylaminuria is not a physically disabling disease, affected patients very often show quite evident psychosocial disturbances that affect their daily activities. In most cases, patients realize to have TMAU by rejectionism and unkind jokes from family, friends, co-workers, boyfriends, and strangers. Their personal hygiene is questioned, and this causes a sense of guilt, embarrassment, shame, low self-esteem but also important behavioral disorders such as anxiety, depression, and in the most extreme cases even attempted suicide. They also show obsessive

compulsive behaviors with the aim of alleviating the unpleasant smell emanating. Frequent showers, the excessive use of perfume or hygiene products to mask the bad smell, are the strategies most used by these patients. Furthermore, the unpleasant odor has negative effects on the patient's social relationships, particularly career, personal life, love affairs, and education. Children suffer a lot from this condition because very often they are ridiculed and bullied by their peers, leading to aggressive or disruptive behavior and poor academic performance. Affected subjects are so much conditioned by their disorder that they organize their daily activities with the aim of limiting contact with other people to a minimum, such as planning spaces in the workplace. This led to social isolation, exclusion and consequentially depression.

1.9. Therapeutic approach

To date, unfortunately, there is no effective treatment for either TMAU1 or TMAU2, but only palliative measures exist that temporarily reduce symptoms in affected patients and can be classified into:

1.9.1. TMA precursors dietary restriction

The first therapeutic approach that is recommended to the TMAU patients is a balanced diet, avoiding all foods that contain TMAO or TMA precursors (choline, carnitine, lecithin, ergothioneine). Foods such as eggs, liver, legumes, peas, fish, peanuts, and others are not recommended. It is also preferable to avoid the tannins and Brussels sprouts consumption because, even if they are not TMA precursors, their prolonged administration could inhibit the FMO3 enzyme catalytic activity. Dietary regimens should be planned and monitored by a specialist to guarantee the minimum TMA precursors daily intake, especially choline. The latter is fundamental for the nerve and brain development in the fetus and in infants. For this reason, choline should not be limited in children, pregnant or lactating women[19]. In addition, it is very

important for the essential phospholipids and acetylcholine neurotransmitter biosynthesis. In healthy subjects, a choline-restricted diet for three weeks could cause liver dysfunction. Unfortunately, often patients do not rely on a specialist and go on a do-it-yourself diet causing the onset of other diseases. Furthermore, allicin, an organic sulfur compound obtained from garlic, appears to play a role in carnitine metabolism, it could act as a Rieske inhibitory protein by reducing TMA levels.

1.9.2. TMA protonation

Since trimethylamine is a tertiary amine, it is a basic compound. Frequent washing with acidic soaps neutralizes the TMA excreted in the odorless conjugate acid, thus decreasing body odor. Also, the use of strong-smelling substances could mask TMA odor such as E, E-2,4-Decadienal, an aromatic compound found in coriander leaves. Although it manages to mask the TMA smell at low levels (10 ppm), its use is not recommended because it has been found to be toxic in human fibroblasts at 25 mM.

1.9.3. Antibiotics treatment

The antibiotics administration is another therapeutic approach that is often recommended to the patient because TMA is produced by the fermentative metabolism of specific bacteria belonging to the gut microbiota. Though drugs treatment can easy the TMAU phenotype, their long-term use should be avoided if there is no medical emergency. Their excessive administration could determine the antibiotic resistance emergence and affect the bacterial infection. Furthermore, antibiotics treatment causes the gut microbiota alteration and consequentially, the intestinal barrier permeability increase leading to the other diseases onset. Metronidazole, Neomycin, and Rifaximin are the most used antibiotics.

- Metronidazole: inhibits the growth of TMA-producing gut microbiota species, especially anaerobic bacteria. Its administration for more than a week was effective in only some TMAU patients, reducing the urinary TMA levels. Other patients had no benefit. The long-term use is not recommended due to its high neurotoxicity and nephrotoxicity.
- Neomycin: it reduces the TMA urinary levels by altering the gut microbiota composition but since after the end of the treatment the latter quickly returns to baseline levels, its use is not recommended.
- Rifaximin: It has shown good efficacy and an action broad spectrum, inhibiting the growth of aerobic, anaerobic, gram negative and positive bacteria and consequently reducing urinary TMA levels. Compared to other systemically acting antibiotics, it exclusively inhibits the enteric bacteria proliferation, thus reducing the side effects risk.

1.9.4. Probiotics

The probiotics treatment has recently increased as an alternative therapeutic approach to antibiotics for Clostridium difficile infection. They have more beneficial effects and fewer side effects than antibiotics They are responsible of inhibitory substances production such as bacteriocins, nutrients competition and adhesion sites blocking for pathogenic bacteria, toxins degradation. A fecal microbial transplantation (FMT) has been performed in 2 TMAU patients after Metronidazole treatment. The fishy odor attenuation during the first 6 months after FMT resulted in only one patient. Nevertheless, the bad smell came back after a year suggesting that recurrent treatment would be necessary. One of the probiotics disadvantages is the difficulty in the gut microbiota composition obtaining important changes in the microbial community even if their administration occurs frequently. In addition, the probiotics low survival in the gastrointestinal tract represents another obstacle to overcome.

1.9.5. Synthetic compounds treatment

The 3,3 dimethyl 1 butanol compound (DMB) showed a lowering of urinary and plasma TMA levels in C57BL/6J mice. It inhibits different TMA Lyase enzyme including the choline TMA lyase. The latter is also inhibited by two other choline analogs compounds, iodomethylcholine (IMC) and fluoromethylcholine (FMC). Both compounds, administered as a single oral dose in C57BL/6J mice, almost reset the urinary TMA levels. The Meldonium anti-ischemic and antiatherosclerosis drug is another molecule that reduced urinary TMA levels in mice decreasing intestinal microbiota-dependent production of TMA/TMAO from L-carnitine, but not from choline.

1.9.6. TMA sequestering compounds

Another therapeutic approach recommended for TMAU patients consists in taking molecules with a TMA trapping action such as activated charcoal. The porous texture negatively charged of the carbon attracts positively charged molecules such as TMA. Administration of 750 mg activated charcoal 2 times a day for 10 days in TMAU patients decreases urinary TMA levels but after the end of the treatment they increased again. Another molecule used is copper chlorophyllin. It lowers the TMA levels because it complexes with it and unlike activated charcoal, the symptoms may reappear several weeks after the end of the treatment. The main disadvantage in using these compounds is that their action mechanism is not specific for TMA, which could lead to the other metabolites capture. Furthermore, osmotic laxatives such as the lactulose oligosaccharide also decrease the TMA concentration because they modify the gut microbiota by altering the intraluminal pH. However, their use is not recommended for long-term treatments because they have a dehydrating effect.

1.9.7. Modulatory compounds

Recent studies have demonstrated the modulatory effect of some compounds on the FMO3 enzyme catalytic activity. Riboflavin, in fact, acting as a FMO3 enzyme cofactor would increase its catalytic activity, consequently reducing the odor intensity. On the contrary, tannins and Brussels sprouts long-term consumption is not recommended because they have shown an inhibitory effect. Furthermore, the drugs intake, metabolized by FMO enzymes, such as Clozapine, Deprenyl, Ranitidine, should be avoided because competing for the active site with TMA could worsen the TMAU phenotype.

2. AIM OF THIS STUDY

Trimethylaminuria is a rare and complex metabolic syndrome. To date, many aspects of this disease, both for primary and secondary forms, are still unclear. For this reason, it is difficult to advise the correct therapeutic approach to the patient. TMAU1 diagnosis is based on *FMO3* screening. Only homozygous causative variants make the diagnostic test positive but patients showing only combined polymorphisms or heterozygous causative variants also manifest the TMAU phenotype. Furthermore, behavioral disorders such as anxiety, depression, and sense of marginalization are common. It is not yet known whether these disturbances are the consequence of the bad smell emitted or whether they may be linked to the gut microbiota alterations. The principal aim of this work is to evaluate the role that *FMO3* haplotypes could exert on the enzymatic folding and, consequently, on the FMO3 catalytic activity. Furthermore, the possible network between bacterial metabolites, TMA precursors and behavioral disturbances in TMAU2 patients was investigated[16].

3. MATERIALS AND METODS

A cohort of 38 patients presented to Molecular Genetics laboratories of University of Messina with a clinical diagnosis of suspected TMAU. The TMAO/TMA ratio dosage in urine and genetic screening of the *FMO3* gene was performed in all patients. A TMA/FMO3 docking prediction and an unbinding pathway study in patients who tested positive for one or more causative and non-causative variants within *FMO3* were performed using different platforms and software. Moreover, the microbiota analysis in patients who did not carry any *FMO3* variants was performed to evaluate whether the shown phenotype was due to a gut microbiota alteration. In addition, a bacterial metabolites biochemical pathways analysis was performed.

3.1 Patient's clinical features

The 38 patients included in this study (27 female and 11 male), belonging to different age groups (9-72 years) and coming from different regions of Italy, complained of an unpleasant one body odor noticed by themselves or by their family/friends. The patients' TMAU phenotype was suspected after a careful analysis of the odor emitted. In addition, a detailed anamnestic study was performed. Each subject was interviewed on specific personal data such as age, gender, ethnicity, age of onset, family history, drug intake, and liver disease to exclude any confounding factors. All subjects had given written informed consent prior to participation in the study. A detailed list of patients' clinical features is available in Table 5.

ID	AGE	SMELL DESCRIPTION	LIVER DISEASES	AGE OF ONSET	DRUGS
1	9	Rotten fish	/	6 months	/
2	42	Rotten fish	no	7/8 years	no
3	48	Genital fishy odor, body garbage odor and scalp acid/sulfur odor	no	10 years	Eutirox, Prisma 50
4	70	Rotten fish	/	/	/
5	36	Rotten fish	no	2/3 years	
6	71	Rotten fish	/	2/3 years	/
7	38	Rotten fish	/	37 years	Atazanavir, Abacavoir, Lamivudin
8	45	Rotten fish	/	38 years	Oral contraceptives
9	21	Rotten fish	no	6/7 years	no
10	73	Rotten fish	no	63 years	/
11	51	Fish	no	2/3 years	no
12	20	Rotten fish	no	6 months	no
13	28	Fish	no	After weaning	no
14	12	Rotten fish	/	5 years	/
15	31	Rotten fish, garbage, garlic	no	17 years	/
16	51	Rotten fish	/	44 years	Medicinal herbs
17	26	Rotten fish	no	14 years	Psychotropic drugs and tranquilizers
18	48	Rotten fish, Fecal odor	no	/	/
19	52	Rotten fish	no	6 years	/
20	24	Rotten fish	no	After weaning	no
21	38	Rotten fish	no	34 years	no
22	13	Rotten fish	no	10 years	no
23	28	Rotten fish	no	28 years	no
24	27	Rotten fish, Fecal odor, rot, sulfur	no	4 years	no
25	47	Rotten fish	/	39 years	/
26	71	Rotten fish	/	2/3 years	/
27	30	Rotten fish	no	17 years	no
28	40	Rotten fish	no	14 years	no
29	54	Rotten fish	no	6 years	no
30	45	Rotten fish, Fecal odor	no	7 years	Antibiotics
31	44	Rotten fish, sulfur	no	34 years	Antibiotics
32	36	Rotten fish, garlic	no	9 years	Antibiotics
33	25	Rotten fish, garbage	no	4 years	no
34	47	Rotten fish	no	8 years	no
35	26	Rotten fish	no	10 years	no
36	20	Rotten fish	no	16 years	no
37	72	Rotten fish	no	2 years	no
38	35	Rotten fish	no	35 years	no

Table 5. Clinical features of the 38 TMAU patients. Signs, symptoms, and pathological features listed are those most frequently observed in TMAU affected individuals.

3.2 TMA and TMAO levels determination in urine samples by ^{1}H-NMR spectroscopy

According to the guidelines, each patient was asked to eat a choline-based diet. The recommended foods were fish, cabbage, eggs, red meat, crustaceans at a concentration of around 300 g. After the urine collection (8h urine), the samples were immediately frozen at -20°C and thawed at room temperature only before the analysis. This was performed by tH-NMR spectroscopy, using the Bruker AVANCE III (Bruker Biospin) spectrometer with a ^{1}H nuclei resonance frequency of 500 MHz, set with a 5 mm gradient indirect detection probe and a probe temperature of 300 K. 600 μl of each urine sample was aliquoted into 5 mm diameter NMR tubes. 100 microliters of deuterium oxide 99.96% (Eurisotop) was added to each sample, as an internal field frequency lock. One-dimensional proton spectra were acquired in conditions that assured quantitative measurements using 64 scans, with a 90° pulse width and a relaxation delay of 2 s. Other parameters considered are a spectral width of 5000 Hz and 32 K complex points. The water signal suppression was realized with selective irradiation (or presaturation) using a continuous radiofrequency (RF) field. Resonances were assigned by reference to a spectral database of standard chemical shifts[46]. The Cr resonance at 3.05 ppm was used as an internal chemical shift reference. TMAO was detected at approximately 3.27 ± 0.03 ppm, depending on the urine's pH while TMA resonance was detected at 2.92 ± 0.02 ppm. The metabolite peaks for Cr, TMA, and TMAO were quantified by integration. Normalization of the total excreted TMA and TMAO levels against the excreted Cr amount was performed, with the purpose to evaluated quantity, considering the glomerular filtration. The values considered for healthy subjects were TMA/Cr < 10, TMAO/Cr ranging from 50 to 1000, and TMAO/ (TMA + TMAO) > 0.8[24].

3.3 *FMO3* genetic test

All patients under examination underwent peripheral blood sampling. The withdrawal was made at double rate. The DNA was purified with the QIAampDNA BloodMidi© kit (Qiagen, Hilden, Germany), following the protocol provided by the manufacturer. The quantification of the extracted nucleic acid, as well as the degree of purity, were evaluated in spectrophotometry using NanoDrop® (Thermo Fisher Scientific). *FMO3* coding exons (9 exons) were sequenced after amplification by polymerase chain reaction (PCR). The primer pairs, shown in Table 6, were drawn on the nucleotide sequences deposited in the GenBank database (accession numbers: NG_012690.2).

Exon	Forward Primer (5′→3′)	Reverse Primer (5′→3′)	Length (bp)
2	GTGAGCTACCATACTCA	CTGTGTGCACACAGTGT	353
3	GATGACTGTAATTACTTGG	TACTGGATTCTCATCTAC	348
4	TCCAGAAGATACTGGTTATG	GCACATTATTGTGACTGCAT	537
5	ACATTATTGTGACTGCATCTA	GTCTAAGAGTCATAACCTTCA	552
6	GTAATAGATCCATTCCTCA	CTTAATGTCCTGTAAGC	369
7	ATAACAACTTCTCTTACTTCC	GGACCTTGTAACTAGGATTAT	640
8	ACACCAATTAATGTAATTCA	TTGTAGTTGTCATTCCAAT	298
9	TCTGTTCTGTTTCTACAC	GTGTTGACCTAATCATC	409
10	GTGTTGACCTAATCATC	TTAGTCAGTAATACAGTG	427

Table 6. Summary table of primer pairs for each FMO3 exon.

Amplicons were obtained with 1,5 U MyTaq™ DNA Polymerase (Bioline, London, UK), using 0,8 ng of genomic DNA and 2 μL of each primer (10 μM) of each primer for a total volume of 50 μl for each reaction. After an initial denaturation step at 95° C for 1 min, the samples were subjected to 35 cycles of amplification consisting of 15 s of denaturation at 95°C and 10 s of annealing. The annealing temperature was optimized for each primer set. Following PCR, 5 μL of amplified product was examined by electrophoresis on a 1% agarose gel. Amplicons for sequencing were obtained with BigDye Terminator chemistry (BigDye™ Terminator v3.1 Cycle Sequencing Kit, Applied Biosystems®, Thermofisher Scientific), sequenced with the 3500 Genetic Analyzer (Applied Biosystems®, Thermofisher Scientific) and

analyzed using 3500 Dx Series Data Collection Software 3 (Applied Biosystems®, Thermofisher Scientific). The obtained nucleotide sequences were aligned with the reference sequences deposited in the GenBank database using the Basic Local Alignment Search Tool (BLAST, https://blast.ncbi.nlm.nih.gov/Blast.cgi).

3.4 Chemical-physical features prediction of fmo3 wild type and mutated forms by in silico proteomic analysis

An *in silico* proteomic analysis of both the FMO3 wild type and mutated forms detected in patients was performed. This study was performed to predict the possible variants and haplotypes role on the FMO3 enzyme catalytic activity. Different computational analysis tools such as ProtParam (https://web.expasy.org/protparam/), InterPro (https://www.ebi.ac.uk/interpro/), i-TASSER (https://zhanggroup.org/I-TASSER/), UCSF Chimera X (https://www.cgl.ucsf.edu/chimerax/) were used. ProtParam was used to determine and compare the different chemical-physical characteristics of both wild type and mutated FMO3 forms. The calculated parameters were molecular weight, theoretical pI, amino acid composition, atomic composition, instability index, aliphatic index, and grand average of hydropathicity (GRAVY). The INTERPRO tool was used to create a two-dimensional functional homology model of the FMO3 wild-type enzyme based on the primary amino acid structure. Moreover, binding sites for the FAD and $NADP^+$ co-factors were also predicted by sequence homology to other human proteins. In addition, the three-dimensional structure of both FMO3 forms (mutated and wild type) was computed using I-Tasser tool and, then, analyzed by the UCSF Chimera X tool to visualize conformational changes and variations in intramolecular contacts.

3.5 Molecular Dynamics Analyses of fmo3/TMA Complex

The use of an unbinding pathway analysis tool is fundamental for the dynamical study of ligand-protein interaction because the ligand binding might be simply

treated as a two-state process between the unbound and bound states that form the stable basins of attraction. While the relative free energy difference between the two states controls the binding affinity, the kinetics of the binding is theoretically determined by the height of the relevant free energy barrier. Thus, the binding affinity can be exclusively governed by the endpoint states, while the binding kinetics is influenced by the detailed pathway connecting the endpoints. In order to evaluate the possible docking between TMA and FMO3, together with the dynamical molecular modeling of their complex, the SAMSON-Connect platform (https://www.samson-connect.net) and its extensions AutoDock Vina Extended[48], FIRE state update[49], GROMACS Model Generator[50] and Ligand Path Finder[51] were exploited. Before using the extensions just described, each structural model was validated to find small free molecules and clashes (bound ligands which are superposed and covalently docked with each other and with the protein), check the bond length, check for alternate locations which must be removed. In details, the AutoDock Vina Extended permitted a high accurate docking between ligand and enzyme, reducing computation time with a multithreaded algorithm, and mixing a "physical" scoring with a machine learning one. The analyses were performed setting minimization to 5,000 steps and docking exhaustiveness to 8. The analyses calculated a total of 10 modes with affinity (kcal/mol), Ki (μmol), RMSD lower and upper bound (A). The Ligand Path Finder permitted to validate the predicted complexes from the previous docking analysis and allowed the prediction of kinetics properties such as binding affinity, binding/ unbinding rates and binding potency. Moreover, the tool helped to identify protein sites which hinder/facilitate the ligand entry/exit or whether certain entry/exit routes are more favorable. Mode 1 was chosen for each protein-ligand complex to find unbinding paths with Ligand Path Finder. Before applying Ligand Path Finder, each protein model was minimized without changing its backbone conformation and without changing the ligand's position. Next, another minimization was applied to refine the systems, using Universal Force Field (UFF) as the interaction model and FIRE as the state

updater. Geometry optimization is a fundamental step in many molecular modeling applications, used to produce stable, realistic structures which correspond to energy minima, so FIRE (Fast Inertial Relaxation Engine) is an efficient optimizer for molecular structures that implements the FIRE minimizer described by Bitzek et al[49]. The FIRE was set as follows: step size (the initial step size given to the algorithm) =1.00 fs, steps (frequency of the viewport update) =100 and fixed (forces the time step to be constant). After the minimization, the parameters were set in Ligand Path Finder, as follow: Use seed=1234, ARAP-modeling iterations=20, Initial temperature (T)=0.0010 K, Temperature factor=2.00, RRT extension step size=1.0000 A, Runs=2, Minimization iterations=10, Failures before T increases=1, Max. ligand displacement=40.00A. The sampling region was set according to the region of interest for the analysis. A single atom in the ligand was set as active atoms (Nitrogen) to control the movement of the ligand and extract it using the active atom from the receptor. The choice of fixed atoms may influence the resulting unbinding pathways and ensure that the protein does not drift along with the ligand, so a single atom in the center of the protein from one of its backbones away from the binding site was set as the fixed one (CA from SER 195 Backbone). The maximum time per run was set to 4 hours and 2 paths were found per model. The Pathlines extension was used to create a visual model that represent the trajectory of the center of mass of selected atoms along selected path and to understand the motion of atoms along a path.

3.6 Additional anamnestic data collection of patients carried no mutations in *FMO3* gene

Patients carried no mutations in *FMO3* gene underwent a second deeper interview to evaluate whether the phenotype shown could be determined by the TMAU secondary form. In this regard, it emerged that some of them had used antibiotics and probiotics. Moreover, some patients have reported suffering from behavioral disorders such as anxiety, depression, mood alterations. These behavioral disturbs

have been confirmed after clinical assessment of healthy mental state using the Mini-International Neuropsychiatric Interview[52]. A detailed list of patients' clinical features is available in Table 7.

Table 7. ***Subject metabolic and behavioral features***. TMAU patients with psychiatric symptomatology (27-33) and TMAU control patients without mental disturbs (34c–38c) were selected for retrospective comparison, mainly in relationship with relevant differences of behavioral phenotypes.

OTHER	/	/	/	Low levels of Folate, plasmatic Vitamin B2 and D, Cu2+, Zn2+; high levels of PTH, homocysteine, Ca2+	/	/	/	/	/	/	High ROS and arachidonic Acid, low vitamin D levels	Use of alcohol
KIND OF BEHAVIOR DISORDER	Anxiety, Fear, Suicidal instincts, Mood alteration	Excessive emotionality, anxiety	Migraine, sleep disorders, mood alteration, sense of marginalization, difficulties in social relations	Chronic and rapid mental fatigue, frequent headaches, dizziness, anxiety and	Obsessive-compulsive disorder, Sense of marginalization	Mood alteration, Sense of marginalization, Suicidal instincts	Depression, sense of persecution	NO	NO	NO	NO	NO
BEHAVIOR DISORDER	YES	YES	YES	YES	YES	YES	YES	NO	NO	NO	NO	NO
PROBIOTIC/FOOD SUPPLEMENTS	NO	NO	L-carnitine, bromelain	NO	L. acidophilus, Bifidobacterium lactis, L. rhamnosus, Streptococcus thermophilus and L. Paracasei	Zinc, selenium, folic acid, iron, inulin, magnesium, L. Helveticus, B. longum spp.longum, Vitamin B6, vitamin B1 and vitamin D	NO	NO	Bifidobacterium lactis, L. acidophilus, L. plantarum, L. paracasei; Streptococcus salivarius subsp. thermophilus, Bifidobacterium brevis, Lactobacillus delbrueckii subsp. bulgaricus, Enterococcus faecium.	L. acidophilus, Bifidobacterium lactis, L. rhamnosus,Streptococcus thermophilus and L. Paracasei	NO	NO
ANTIBIOTIC USE	NO	NO	NO	YES	YES	YES	NO	NO	NO	NO	NO	NO
ID	27	28	29	30	31	32	33	34c	35c	36c	37c	38c

3.7 Fecal microbiota analysis

The qualitative and quantitative composition analysis of each patient's microbiota was performed in collaboration with the Wellmicro technology services (Bologna, Italy). Each patient collected the fecal sample using the appropriate kit provided by the same company. Samples were, then, processed for total bacterial DNA extraction using the QIAExpert (Qiagen, Hilden, Germany) following the manufacturer's instructions. The quantification of the extracted DNA was evaluated in spectrophotometry using QIAExpert (Qiagen, Hilden, Germany) at an absorbance of 260 nm. The DNA quality was verified by electrophoretic run on the QIAdvanced (Qiagen, Hilden, Germany). The 16S rRNA gene sequences of the bacterial genome were then amplified by Polymerase Chain Reaction (PCR) using primer pairs SD-Bact-0341-bS17/SD-Bact-0785-aA-21, that target the V3 and V4 regions of the 16S rRNA gene[53]. Each PCR reaction was carried out in 25 μl of final volume of PCR mix consisting of 2x PCRBIO Taq Mix (PCR biosystem, London, UK) and 2.5 μL of DNA (5 ng/μL). The thermal protocol foresaw an initial denaturation at 95°C for 3 minutes, followed by 25 denaturation cycles of 30 seconds at 95°C, annealing at 55 °C for 30 s, extension to 72°C for 30 s, and a final step extension at 72°C for 5 min. The obtained products following the V3 and V4 regions amplification of the 16S gene rRNAs underwent magnetic purification using a magnetic bead system (Agencourt AMPure XP; Beckman Coulter, Brea, CA, United States) to remove primer dimers. The amplicons were diluted to a concentration of 4 nM, denatured and 5 μL of each diluted amplicon solution was used to prepare the final library with Nextera V2 kit (Illumina, San Diego, CA, United States). The sequencing was performed using MiSeq sequencer (Illumina, San Diego, CA, USA). The obtained raw data in FASTQ format were processed using a pipeline made of PANDAseq[54] and QIIME[55] tools. The high-quality reads were grouped into Operational Taxonomic Units (OTUs) using UCLUST[81] defined by a sequence

homology value of 97%. Taxonomy was assigned using the Greengenes database (May 2019). All experiments were performed at least in triplicate.

3.8 Statistical analysis

Statistical analyses were performed with IBM QSPSS software (https://www.ibm.com/analytics/us/en/technology/spss/). P-values ≤ 0.05 were considered statistically significant. QIIME was used to calculate alpha diversity by pairwise non-parametric t-test with 999 permutations. Significant differences in beta diversity were computed with QIIME by PERMANOVA, and permDISP permitted us to check for significant differences in dispersion[57,58]. Analysis of microbiomes composition (ANCOM), based on compositional log-ratios, was used for comparing the composition of microbiomes, detecting differences in microbial mean taxa abundance[59]. Canonical Correspondence Analysis (CCA)[60] was implemented with the R package "vegan", and its significance (consisting of the variables sex, age and TMAU affected or not) was tested with ANOVA and stepwise analysis and corrected by Bonferroni post-hoc method.

3.9 Analysis of metabolic pathways involved in neurotransmission

The relative abundances of the bacterial families resulted altered in each patient's microbiome were, finally, studied. In details, a metabolic pathway analysis was performed, firstly by literature review and then by the Metabolic Pathways Database for Microbial Taxonomic Groups (MACADAM)[61], focusing on nodes related to neural alterations. After each complete genome has been retrieved from NCBI refseq, a pathway genome database (PGDB) was created by MACADAM exploiting integrated tools and databases such as MetaCyc which contains pathways involved in both primary and secondary metabolism, as well as associated metabolites, reactions, enzymes, and genes. To guarantee the highest quality of the genome functional annotation data, MACADAM also includes Functional Annotation of Prokaryotic Taxa (FAPROTAX), a manually curated

functional annotation database, MicroCyc, a manually curated collection of PGDBs, and the IJSEM phenotypic database.

4 RESULTS

4.1 ^{1}H-NMR spectrometry evidenced high TMA urinary levels in most of suspected TMAU patients

In 17 of the 38 H-NMR spectra obtained from the spectrometry analyses, the urine TMA level was within the normal range reported for the control subjects. 21 ^{1}H-NMR spectra showed higher TMA levels than TMAO. The most significant spectra are shown in the Figure 8. The TMA peak was much more intense in patients 1 (figure 7a), 2 (figure 7b), 3 (figure 7c), 4 (figure 7d), 5 (figure 7e), 9 (figure 7f), 11 (figure 7g), 12 (figure 7h), 13 (figure 7i).

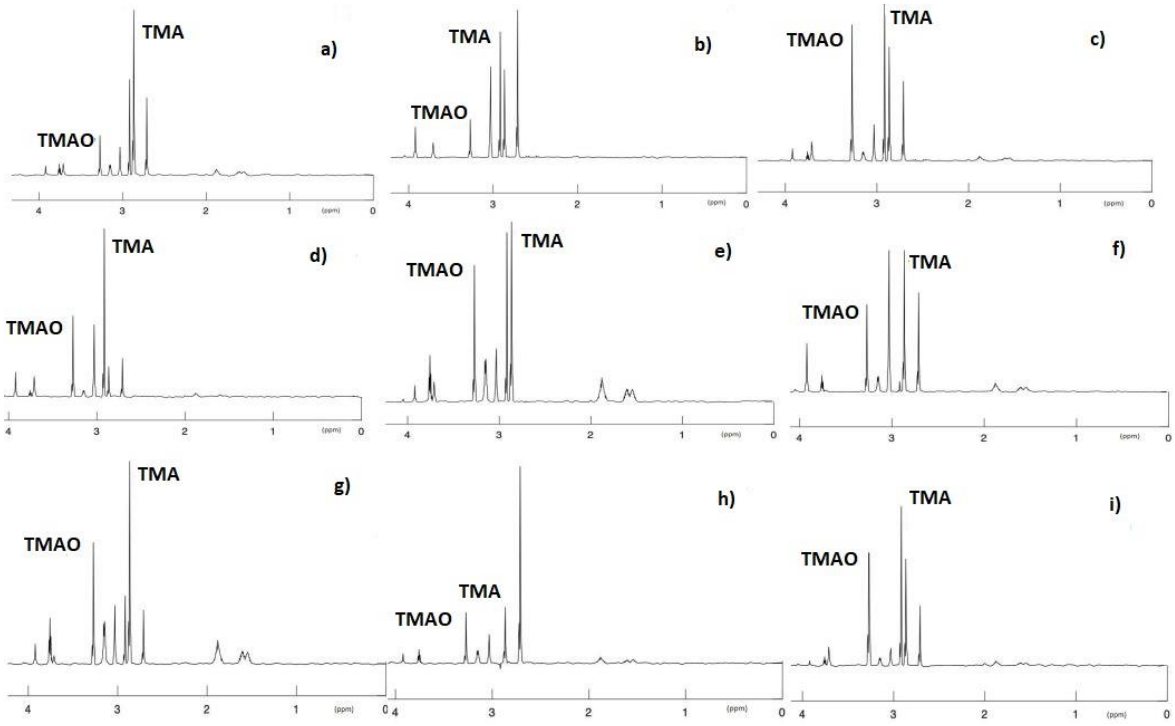

Figure 7. 500 MHz ^{1}HNMR spectra resulting from ^{1}HNMR spectroscopy of the urine collected from patients. A healthy subject should present no peak for TMA and an intermediate peak for TMAO (not shown). (a) patient 1, (b) patient 2, (c) patient 3, (d) patient 4, (e) patient 5, (f) patient 9, (g) patient 11, (h) patient 12, (i) patient 13.

4.2 The genetic analysis of TMAU1 suspected patients highlighted the possibly role of haplotype in the disease etiopathogenesis

The research of genetic variants within TMAU1 suspected patients, together with in silico prediction studies, evidenced the potential role of variant combination in the onset and progression of pathology phenotype.

4.2.1 Sanger sequencing permitted the identification of 26 haplotypes probably related to TMAU phenotype

From the *FMO3* genetic analysis conducted on the 38 patients, no variants were found in 12 patients only, while 26 carried one or more causative and/or non-causative TMAU variants. In details, 17 variants distributed in 26 haplotypes were found. Only 6 causative variants, in heterozygous condition, were found in 7 patients, including a stop variant (Y331stop) in patient 1, and five missense variants (c. 1474C > T p.R492W, p. 713G > A p. R238Q, G475D, c. 713G > C p. R238P, c. 458C > T p. P153L) uniquely distributed in patients 2, 5, 9, 10, 11 and 13. All these missense variants were associated with the E158K variant (in heterozygous condition). In addition, a heterozygous stop variant (P380Fs), still not recognized as TMAU causative, was found in association with the E158K/P153L and E308G variants in patients 2 and 4, respectively. Four patients (12, 17, 20, and 21) showed homozygous variants, with a missense common to three patients (c. G472A p.E158K) and an intronic one common to two (c. 627 + 10 C > G). The most complex haplotypes were exhibited by patients 5 and 8, which carried four common variants (c. G472A p.E158K, c. 485-22G > A, c. 1184-32_1184-31insT, and c. 923A > G p.E308G) and, respectively, c. 458C > T (p.P153L) and c. 441C > T (p. S147=). Finally, the most frequent variants resulted the c. G472A (p.E158K), carried by 18 TMAU patients. Further details are available in Table 8.

ID	*FMO3* VARIANTS																	
	c. G472A (p.E158K) (DFP)	c.627+10 C>G (DM?)	c.485-22G>A	c.1184-32_1184-31insT	c.923A>G (p.E308G) (DFP)	c.769G>A (p.V257M) (FP)	c.458C>T (p.P153L) (DM)	c.441C>T (p. S147=) (DP)	c.993_994delTA (p. Tyr331Stop) (DM)	c.1474C>Tp.R492W (DM)	c.1139_1140del (p.Pro380fs)	c.713G>A (p.R238Q) (DM)	c.1424G>A (G475D) (DM)	c.713G>C (p.R238P) (DM)	c.855C>T (Asn285=)	c.422A>T (Asp141Val)	c.539G>T (Gly180Val)
1									X									
2	X						X				X							
3											X							
4					X						X							
5	X		X	X			X											
6	X	X																
7		X	X			X												
8	X		X	X	X			X										
9	X		X							X								
10	X											X		X				
11	X												X					
12								O							O	O	O	
13													X	X				
14	X	X			X													
15	X	X				X												
16	X				X													
17	O	O	O															
18	X	X				X												
19	X	X																
20	O	O																
21	O	X						X										
22	X		X		X													
23						X												
24						X												
25	X		X															
26	X	X	X	X														

Table 7. FMO3 detected variants genotyping and distribution through the cohort of patients. Of 38 genotyped patients, 26 of them showed variants. DM = disease mutation (HGMD). DM? = disease mutation without certain evidence (HGMD). DFP = disease-associated polymorphism with additional supporting functional evidence (HGMD). DP = disease-associated polymorphism (HGMD). FP = in vitro/laboratory or in vivo functional polymorphism (HGMD). Variants without HGMD acronym are not yet fully evaluated. X= heterozygous variant, O = homozygous variant.

4.2.2 Physico-chemical features in silico analyses of mutated fmo3 predicted possible alterations of protein stability

Results obtained from ProtParam analysis showed an alteration of some physico-chemical characteristics in the FMO3 mutated forms compared to the wild type one, especially in patients 1 (Y331Stop), 2 (E158K_P153L_P380fs), 3 (P380fs), 4 (E308G_ P380fs). In detail, the molecular weight, which in the wild-type protein was 60.033 g/mol, in the one carrying haplotypes consisting of missense variants was slightly altered but, in the truncated proteins, this value decreased sharply (36.917 g/mol for Y331stop). The theoretical pI represents the pH at which a particular molecule or surface carries no net electrical charge, and it could help to understand the protein charge stability[62]. Its value ranged from 6.26 of Y331Stop to 8.47 of E158K_E308G. The GRAVY value for a peptide or protein is calculated as the sum of hydropathy values of all the amino acids, divided by the sequence length[37]. This parameter indicates the hydrophilicity (negative values) and hydrophobicity (positive values) degree of the protein based on the amino acids that make it up. This information might be useful for localizing these proteins. The mutated FMO3 proteins presented GRAVY indexes ranging from -0.06 of D141V_G180V to -0.21 of Y331Stop compared to the wild type of value of -0.08. Aliphatic index (AI), defined as the relative volume of a protein occupied by its aliphatic side chains (alanine, valine, isoleucine, and leucine), plays role in protein thermal stability. With a high Aliphatic index proteins are more thermally stable. In almost all the FMO3 mutated forms this value was almost like that of the wild-type form (82.07) except for the truncated protein (Y331stop) which was lower (73.21). In addition, few changes in the index value were detected in all FMO3 mutated forms that it is resulted <40. A protein whose instability index is <40 is predicted as stable; thus, all computed proteins are stable. Further details on biochemical properties of wild-type and mutated FMO3 proteins are available in table 9.

	WILD	P153L_E158K	V257M	E158K	E158K_E308G	E158K_R492W	E158K_R238Q	E158K_G475D	D141V_G180V	Y331Stop	R238P_G475D	P380fs_P153L_E158K	P380fs	P380fs_E308G
Residues	532	532	532	532	532	532	532	532	532	330	532	381	381	381
MW (g/mol)	60,033	60,048	60,065	60,032	59,96	60,062	60,004	60,09	60,059	36,917	60,032	42,556	42,541	42,469
1µg to pmol	16,66	16,65	16,65	16,66	16,68	16,65	16,67	16,64	16,65	27,09	16,66	23,5	23,51	23,55
Net charge (pH=7)	2,17	4,17	2,17	4,17	5,17	3,17	3,17	3,17	3,17	-2,74	0,17	-0,65	-2,65	-1,65
pI	7,9	8,33	7,9	8,33	8,47	8,15	8,15	8,15	8,16	6,26	7,09	6,76	6,33	6,52
Avg. hydropathy (GRAVY)	-0,08	-0,07	-0,08	-0,08	-0,07	-0,07	-0,08	-0,09	-0,06	-0,21	-0,08	-0,1	-0,11	-0,1
Aliphatic index	82,07	82,8	81,52	82,07	82,07	82,07	82,07	82,07	83,16	73,21	82,07	80,05	79,03	79,03
Instability index	34,24	33,64	35,12	33,87	33,19	33,19	33,59	33,75	34,37	33,02	34,48	33,48	34,31	33,36
1 mg/mL to A_{280}	1,46	1,46	1,46	1,46	1,46	1,55	1,46	1,46	1,46	1,23	1,46	1,14	1,14	1,14
ε_{280} ($M^{-1}cm^{-1}$)	87,485	87,485	87,485	87,485	87,485	92,985	87,485	87,485	87,485	45,42	87,485	48,4	48,4	48,4
1 A_{280} to mg/mL	0,69	0,69	0,69	0,69	0,69	0,65	0,69	0,69	0,69	0,81	0,69	0,88	0,88	0,88
1 mg/mL to A_{280} (red.)	1,45	1,45	1,45	1,45	1,45	1,54	1,45	1,45	1,45	1,22	1,45	1,13	1,13	1,13
ε_{280} ($M^{-1}cm^{-1}$) (red.)	86,86	86,86	86,86	86,86	86,86	92,36	86,86	86,86	86,86	44,92	86,86	47,9	47,9	47,9
1 A_{280} to mg/mL (red.)	0,69	0,69	0,69	0,69	0,69	0,65	0,69	0,69	0,69	0,82	0,69	0,89	0,89	0,89
Features	NAP, FAD, WP5, OXY, ADP, IND, NA, 23 helices, 22 strands	NAP, FAD, WP5, OXY, ADP, IND, NA, 46 helices, 44 strands	NAP, FAD, WP5, OXY, ADP, IND, NA, 46 helices, 44 strands	NAP, FAD, WP5, OXY, ADP, IND, 46 helices, 44 strands	NAP, FAD, WP5, OXY, ADP, IND, NA, 46 helices, 44 strands	NAP, FAD, WP5, OXY, ADP, IND, NA, 46 helices, 44 strands	NAP, FAD, WP5, OXY, ADP, IND, NA, 46 helices, 44 strands	NAP, FAD, WP5, OXY, ADP, IND, NA, 46 helices, 44 strands	NAP, FAD, WP5, OXY, ADP, IND, NA, 46 helices, 44 strands	NAP, FAD, OXY, MG, IND, MMZ, CYH, 11 helices, 20 strands	NAP, FAD, WP5, OXY, ADP, IND, NA, 46 helices, 44 strands	NAP, FAD, WP5, OXY, ADP, IND, NA, 28 helices, 52 strands	NAP, FAD, OXY, IND, MMZ, CYH, 14 helices, 26 strands	NAP, FAD, WP5, OXY, ADP, IND, NA, 28 helices, 52 strands

Table 8. Biochemical and physical changes prediction between wild-type and mutated FMO3.

The output data obtained by Interpro database showed the probable cofactors FAD and NADP binding sites in the wild type fmo3 enzyme. These sites are located approximately in the 1-230 and 310-470 aminoacidic region as shown in figure 8.

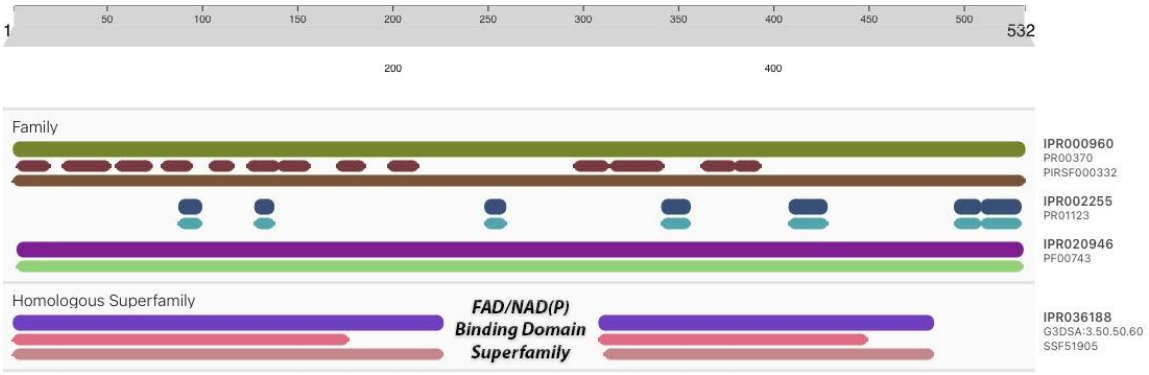

Figure 8. Aminoacidic region where cofactors FAD and NADP binding sites are located.

4.2.3 Tertiary structure 3D analysis of mutated fmo3 proteins predicted possible alterations within FAD/NADP binding domains

Due to the FMO3 3D structure unavailability in the PDB Molecule Database, the i-TASSER servers were used to predict and model multiple domains of wild-type and mutated proteins with high confidence based on the high scoring template. Prediction by i-TASSER resulted the most confident, showing a normalized Z-score of 8.91 for wild-type structure and a mean value of 8.77 for the mutated ones. Chimera X tool was used to analyze the tertiary structure of the FMO3 mutated proteins. The output data revealed that in the haplotypes consisting of missense variants, the mutated amino acids were distributed along the enzyme external domains (fig.9).

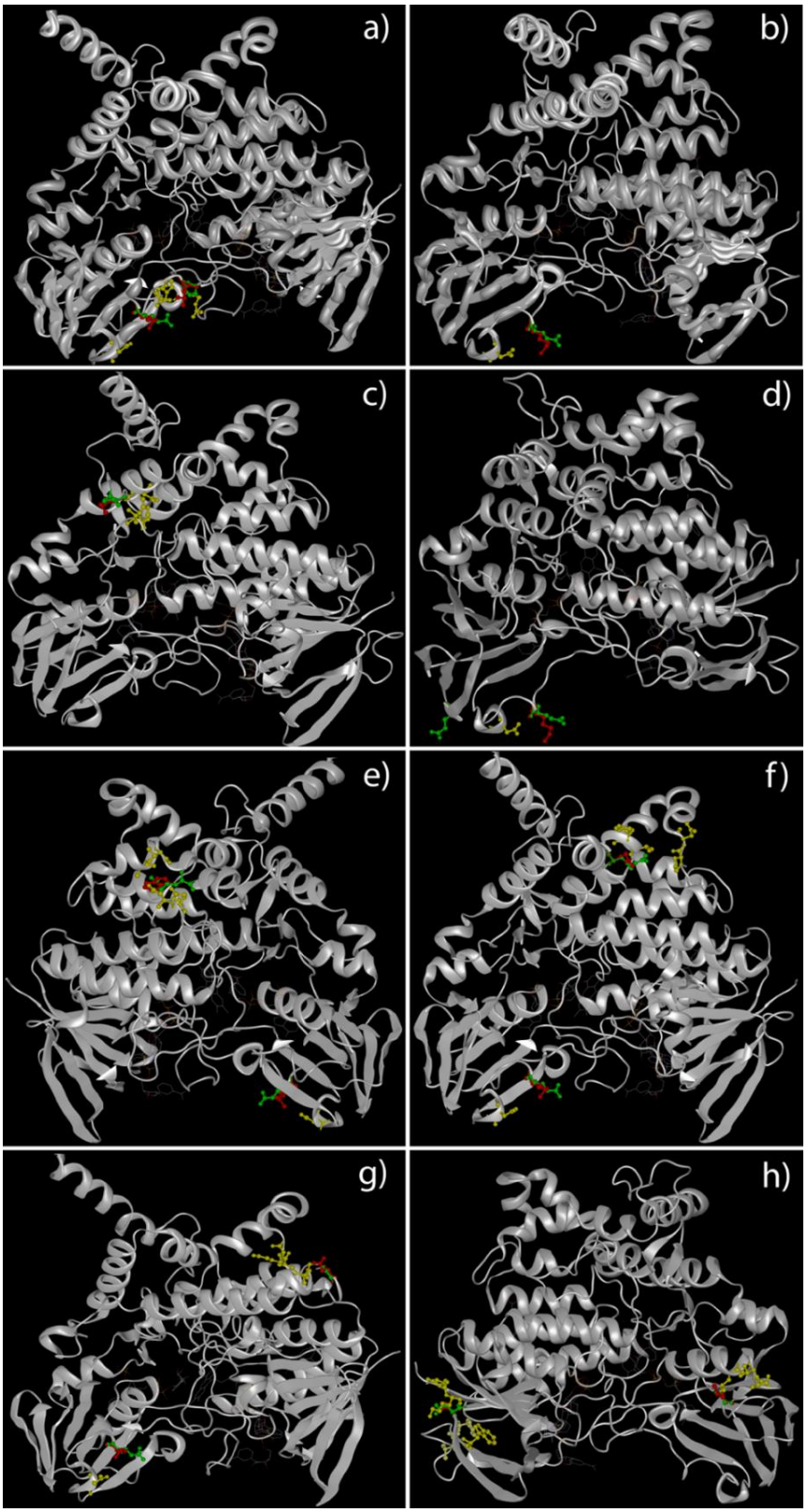

Figure 9. 3D structural models of FMO3 proteins in patients carrying missense variants. This panel highlights the predicted tertiary structure of FMO3 in patients 5 (P153L and E158K) (a), 6 (E158K) (b), 7 (V257M) (c), 8 (E158K and E308G) (d), 9 (E158K and R492W (e), 10 (E158K and R238Q) (f), 11 (E158K and G475D) (g) and 12 (D141V and G180V) (h). Green ball-and-stick aa = wild-type aa. Red ball-and-stick aa = mutated aa. Yellow ball-and-stick aa = aa nearest to aa involved in variant.

A possible binding sites alteration for the FAD and NADP cofactors appears to occur in truncated proteins caused by nonsense variants. Only one FAD and two NADP binding sites were computed from i-Tasser in wild-type FMO3. In detail, in FMO3 wild-type form, the FAD binding site was roughly computed in the 310-470 aminoacidic region. These amino acid residues are absent in all truncated *FMO3* forms investigated (Tyr331stop, P153L_E158K_Pro380fs, E308G_Pro380fs, Pro380fs). The two NADP binding sites were, instead, approximately computed in the 1-230 and 310-470 aminoacidic regions. In all FMO3 truncated forms, only the NADP binding site between the 1 -210 amino acid position was retained. In addition, a second NADP binding site was found near the latter, almost overlapping. The binding site between the 310 - 470 amino acid position was lost. Furthermore, observing the three-dimensional structure of wild-type FMO3, the folding of enzymatic pocket seemed to resemble that of a "cage". This conformation resulted absent in all protein truncated forms (figure 10).

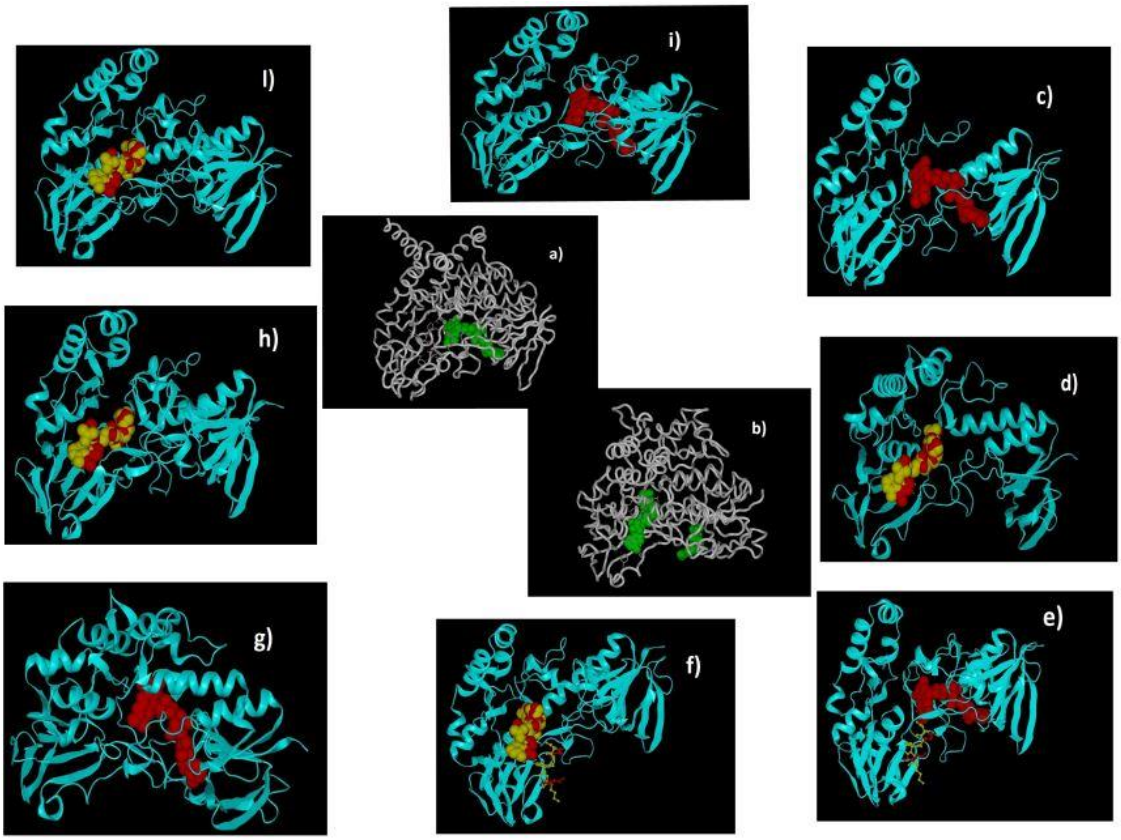

Figure 10. 3D structural models of FMO3 proteins in patients carrying nonsense variants. This panel highlights the predicted tertiary structure of FMO3 in wild type (a and b), patient 1 (Y331stop) (c and d), 2 (E158K, P153L and P380fs) (e and f), 3 (P380fs) (g and h), 4 (P380fs and E308G) (I and l). The green spheres represent the cofactor FAD (a) and NADP (b) while the red spheres the FAD in truncated enzymes (c, e, g, i). The red and yellow spheres represent two NADP molecules (d,f,h,l)

Furthermore, the distance between the amino acid changed due to missense variants and the surrounding ones was calculated. Comparing these data with those obtained from the FMO3 wild-type form, significant changes emerged in at least 5 patients. Two altered forms of FMO3 (E158K_P153L and E158K_G475D) showed a global reduction in distance between mutated amino acid and its nearest ones, while other two (E158K_R492W and E158K _R238Q) evidenced a wider distance between the same considered amino acids. The haplotype (R238P_G475D) showed a global reduction in distance between Proline (P) mutated amino acid and its nearest ones. Conversely, an increase in distance resulted between the aspartic acid (D) mutated amino acid and the surrounding ones. More details of the distances are given in the table 10.

ID	Variant	Wt	Nearest a.a.	a.a. distance (Å)	Mut	Nearest a.a.	a.a. distance (Å)
2	P153L	Pro153 (CG)	Arg174 (NE)	4.33	Leu153 (CD1)	Arg174 (NE)	5.20
		Pro153 (C)	Leu155 (N)	3.20	Leu153 (CD2)	Leu155 (CD2)	1.71
		Pro153 (CB)	His172 (CE1)	3.32	Leu153 (CB)	His172 (CG)	4.00
	E158K	Glu158(N)	Asn164 (OD1)	5.94	Lys158 (CA)	Asn164 (ND2)	5.71
4	E308G	Glu308	/	/	Gly308	/	/
5	P153L	Pro153 (CG)	Arg174 (NE)	4.33	Leu153 (CD1)	Arg174 (NE)	5.20
		Pro153 (C)	Leu155 (N)	3.20	Leu153 (CD2)	Leu155 (CD2)	1.71
		Pro153 (CB)	His172 (CE1)	3.32	Leu153 (CB)	His172 (CG)	4.00
	E158K	Glu158(N)	Asn164 (OD1)	5.94	Lys158 (CA)	Asn164 (ND2)	5.71
6	E158K	Glu158(N)	Asn164 (OD1)	5.94	Lys158 (CA)	Asn164 (ND2)	5.71
7	V257M	Val257 (N)	Tyr256 (C)	1.35	Met257 (N)	Tyr256 (C)	1.2
			Asp253 (O)	2.97		Asp253 (O)	3.13
		Val257 (CG2)	Val277 (N)	4.03	Met257 (CE)	Val277 (N)	4.09
8	E158K	Glu158(N)	Asn164 (OD1)	5.94	Lys158 (CA)	Asn164 (ND2)	5.71
	E308G	Glu308	/	/	Gly308	/	/
9	E158K	Glu158(N)	Asn164 (OD1)	5.94	Lys158 (CA)	Asn164 (ND2)	5.71
	R492W	Arg492 (CD)	Asp76 (OD2)	3.07	Tyr492 (NE1)	ASp76 (OD2)	2,53
		Arg492 (NH2)	Thr488 (OG1)	2,76	Trp492 (CH2)	Thr488 (O)	3,11
		Arg492 (NH1)	Ala485 (O)	2,72	Trp492 (N)	Ala485 (CB)	4,3
		Arg492 (NE)	Glu65 (OE2)	2,68	Trp492 (CE3)	Glu65 (OE2)	2,92
10	E158K	Glu158(N)	Asn164 (OD1)	5.94	Lys158 (CA)	Asn164 (ND2)	5.71
	R238Q	Arg238 (NH2)	Pro445 (O)	4.95	Gln238 (OE1)	Pro445 (O)	7.59
			Asn446 (N)	7.15		Asn446 (N)	9.81
		Arg238 (CG)	Val261 (O)	3.12	Gln238 (CB)	Val461 (O)	3.59
		Arg238 (CB)	Tyr462 (O)	3.06		Tyr462 (O)	2.59
11	E158K	Glu158(N)	Asn164 (OD1)	5.94	Lys158 (CA)	Asn164 (ND2)	5.7
	G475D	Gly475 (N)	Pro445 (N)	7.07	Asp475 (OD2)	Pro445 (N)	5.90
			Lys444 (N)	6.18		Lys444 (N)	3.83
		Gly475 (CA)	Ala443 (CA)	4.30		Ala443 (CA)	3.02
			Gly442 (O)	4.52		Gly442 (O)	1.41
12	D141V	D141 (N)	Lys4 (O)	2.87	Val141 (N)	Lys4 (O)	3.02
			Val139 (C)	4.52		Val139 (C)	4.50
			Phe140 (C)	1.34		Phe140 (C)	1.25
		D141 (OD1)	Lys3 (CA)	3.52	Val141 (CG1)	Lys3 (CG)	3.88
		D141 (C)	Trp125 (CD1)	4.59	Val141 (C)	Trp125 (CD1)	4.44
	G180V	Gly180 (N)	Leu203 (CD2)	6.28	Val180 (N)	Leu203 (CD2)	6.22
			Ala207 (N)	8.42		Ala207 (N)	8.28
			Thr206 (OG1)	5.63		Thr206 (OG1)	5.49
13	R238P	Arg238 (NH1)	Ile447 (CD)	3.62	Pro238(CB)	Ile447(CD)	6.78
		Arg238 (NH2)	Pro445 (O)	4.95	Pro238(CG)	Pro445 (O)	9.01

	Arg238 (N)	Gly464(O)	3.44	Pro238(CD)	Gly464(O)	2.74
	Arg238 (N)	Cys466(N)	4.56	Pro238(CD)	Cys466(N)	3.65
G475D	Gly475 (N)	Pro445 (N)	7.07	Asp475 (OD2)	Pro445 (N)	5.90
		Lys444 (N)	6.18		Lys444 (N)	3.83
	Gly475 (CA)	Ala443 (CA)	4.30		Ala443 (CA)	3.02
		Gly442 (O)	4.52		Gly442 (O)	1.41

Table 9. FMO3 missense variants highlighting the highest distance differences between changed amino acid and nearest ones. The wild-type alleles compared to mutated ones showed possible interactions with difference nearest amino acids, also involving different atoms or functional groups (between brackets). Side chains functional groups are reported following the IUPAC-IUB Commission on Biochemical Nomenclature. Wt = wild-type amino acid and atom/functional group involved in a possible interaction with the nearest aa. Mut = mutated amino acid and atom/functional group involved in a possible interaction with the nearest aa.

4.2.4 Docking analysis of wild-type and mutated fmo3 evidenced relevant differences within enzyme active site

The AutoDock Vina Extended permitted a high accurate docking between TMA and FMO3 enzyme, unveiling the most likely TMA binding sites of and how considered variants could impair this binding. The docking analyses calculated a total of 10 modes with affinity (kcal/mol), Ki (mol), and RMSD lower and upper bound (A) for each protein. The mode presenting the lowest values for such variables, considered the most significant, was chosen for next steps (Table 11).

Protein	Affinity (kcal/mol)	Ki (µmol)	Lower bound of the RMSD from this ligand's best mode (A)	Upper bound of the RMSD from this ligand's best mode (A)
WILD-TYPE	-2,103	28756.2	0	0
D141V_G180V	-2,16	26096.6	0	0
E158K_E308G	-2,242	22732.4	0	0
E158K_G475D	-2,239	22844.0	0	0
E158K_R238Q	-2,24	22789.5	0	0
E158K_R492W	-2,242	22739.5	0	0
E158K	-2,24	22791.2	0	0
P153L_E158K	-2,24	22807.7	0	0
P380fs	-2,079	29951.3	0	0
P380fs_P153L_E158K	-2,082	29760.4	0	0
P380fs_E308G	-2,082	29789.6	0	0
R238P_G475D	-2,242	22736.2	0	0
V257M	-2,242	22749.4	0	0
Y331Stop	-2,033	32327.0	0	0

Table 10. Best significant modes of TMA/FMO3 docking models. AutoDock Vina permitted to compute 10 different modes for docking analysis between TMA and FMO3. This table shows the most reliable models, based on energetic variables. Ki = inhibition constant. RMSD values are calculated relative to the best mode (the first model) and use only movable heavy atoms (i.e., only ligand atoms, not hydrogen). RMSD upper bound matches each atom in one conformation with itself in the other conformation, ignoring any symmetry. RMSD lower bound matches each atom in one conformation with the closest atom of the same element type in the other conformation.

In wild-type FMO3 the amino acids predicted to constitute the TMA active site resulted Ser216, Gly217, Ser218, Trp219, Pro273, Asn275, Gly276, Leu278, Arg279, Lys280, Glu 281, Pro282. This computed TMA active site remained the same only in the FMO3 mutated form (V257M). All other mutated forms showed very relevant differences in amino acids active site compared to the wild-type form. Arg 279 was the only amino acid active site shared with the wild-type protein except for the mutated form determined by haplotypes (Asp141Val_Gly180Val, E308G_Pro380fs, E158K_P153L). The latter did not share any amino acids active site with FMO3 wildtype. Furthermore, by comparing the active site amino acids of the mutated proteins, it was evident that some of them were in common. In detail, the mutated

form P153L_E158K, R238Q_E158K, G475D_E158K, G475D_R238P shared the same active site as well as E308G_E158K, R492W_E158K and P153L_E158K_P380Fs, P380Fs_E308G. Finally, the Y331Stop and D141V_G180V FMO3 forms were the only ones which presented unique aa in their active sites. More details about aa of mutated FMO3 active sites are available in Table 12 and Figure 11.

	FMO3 haplotypes													
Active site a.a. residues	**Wild-type**	**Y331Stop**	**P153L + E158K + P380Fs**	**P380Fs**	**P380Fs+E308G**	**P153L + E158K**	**E158K**	**V257M**	**E308G + E158K**	**R492W + E158K**	**R238Q + E158K**	**G475D + E158K**	**D141V + G180V**	**R238P + G475D**
Gly 9			x	x	x									
Ala 10			x	x	x									
Gly 11			x	x	x									
Val 12			x	x	x									
Ser 13			x	x	x									
Gly 14			x	x	x									
Glu 32			x	x	x									
Gly 38			x		x									
Gly 39			x	x	x									
Leu 40			x	x	x									
Ala 52			x	x	x									
Cys 146			x	x	x									
Ser 147			x	x	x									
Gly 148			x	x	x									
Hys 149			x	x	x									
Val 151			x		x									
Ser 216	x							x						
Gly 217	x							x						
Ser 218	x							x						
Trp 219	x							x						
Gly 240		x												
Leu 243		x												
Lys 244		x												
Leu 247		x												
Ile 251		x												
Ser 252		x												
Asp 253		x												

Leu 255		X													
Tyr 256		X													
Gln 259		X													
Pro 273	X							X							
Asn 275	X							X							
Gly 276	X							X							
Leu 278	X							X							
Arg 279	X	X	X				X	X	X	X	X	X	X		X
Lys 280	X							X							
Glu 281	X							X							
Pro 282	X							X							
Leu 352														X	
Phe 353														X	
Lys 354														X	
Gly 355														X	
Phe 371														X	
Val 372														X	
Ser 381			x	X	X										
Lys 412						X	X		X	X	X	X	X	X	
Met 413														X	
Lys 415						X	X		X	X	X	X			X
Lys 416						X	X		X	X	X	X	X	X	
Arg 417						X			X	X	X	X			X
Trp 419						X	X		X	X	X	X			X
Phe 420						X	X		X	X	X	X			X
Lys 422						X	X				X	X			X
Thr 425						X	X		X	X	X	X			X
Ile 426														X	
Gln 427						X	X		X	X	X	X			X
Thr 428						X	X		X	X	X	X	X	X	
Asp 429						X	X		X	X	X	X			X
Tyr 433														x	

Table 11. Mutated FMO3 showed different amino acids predicted for the TMA binding sites. The "X" indicates that the specific aa in the related row is an integral part of the FMO3 active site when the variant/s reported in the columns is/are carried by the FMO3 gene.

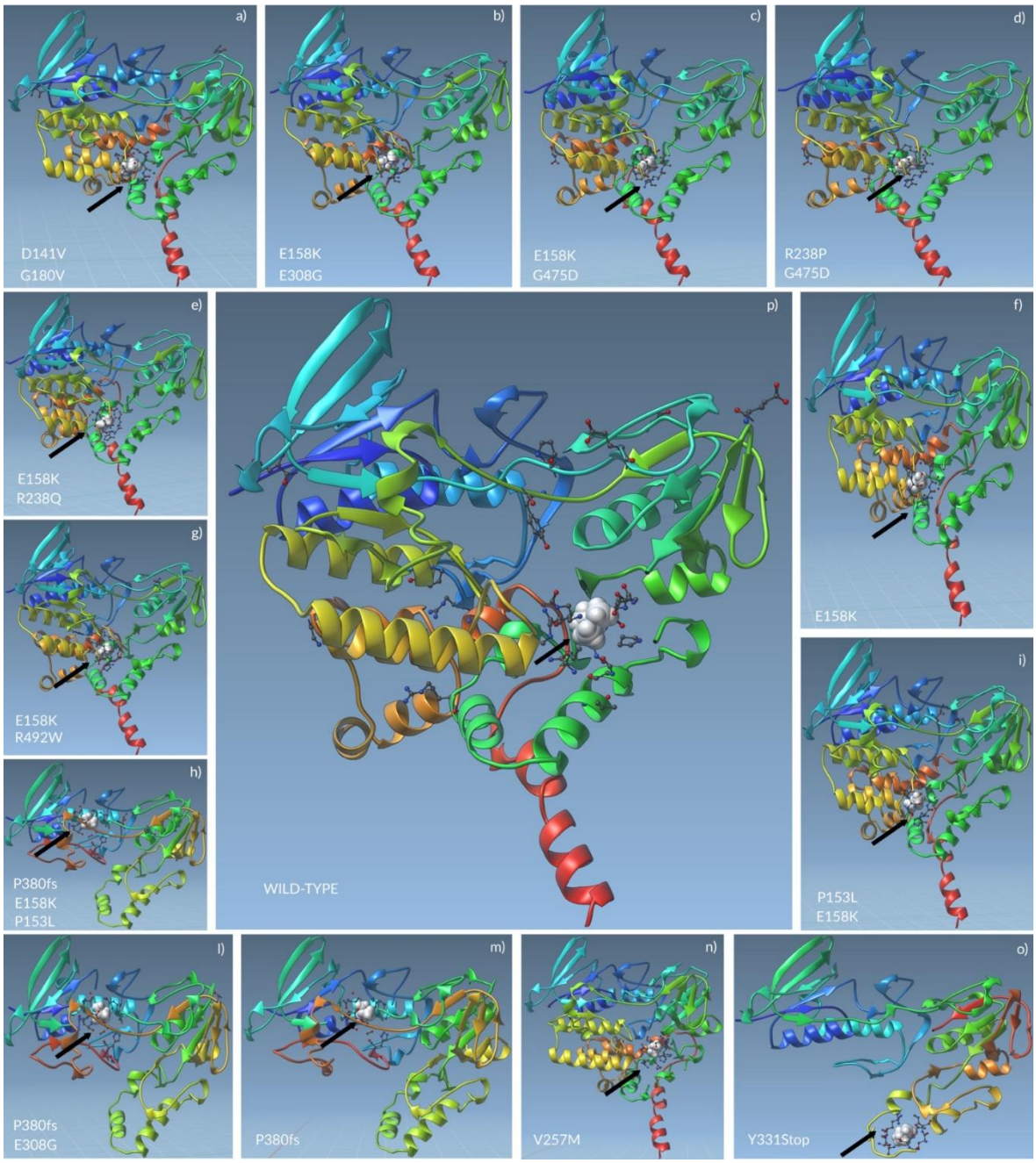

Figure 11. TMA docking to FMO3 could involve different amino acids in mutated enzymes. The non-sense and missense variants carried by mutated FMO3 (a–o) might shift the TMA binding sites far from the wild-type active site of the enzyme (p). The black arrows indicate the TMA (white spheres) bonded to the active site of FMO3, whose aa are represented as ball-and-stick. The other aa, represented as ball-and-stick, separated from the ones in the catalytic site, are the aa involved in mutations.

4.2.5 TMA unbinding pathway analysis in both wild-type and mutated FMO3 showed a possible alteration of enzyme kinetics.

The possible TMA pathway through wild-type and mutated FMO3 proteins was determined by the ligand PathFinder tool. The interactive simulations allowed to detect the TMA trajectory and direction. Furthermore, the probable interactions between TMA and FMO3 amino acid residues encountered along the TMA path were also disclosed. In the wild-type FMO3, the TMA mainly interacted with the aa Ser 216, Trp 219, Leu 278, and Lys 280. It went through the entire protein, also interacting with the Pro 282 and the Glu 281, passing along the area containing the FAD and $NADP^+$ binding sites. Only in patient 7 (carrying V257M), the TMA path resembled the wild-type FMO3 one, interacting with Lys 280, Pro 273, Asn 275 and, at the end, with Ser 216. During its exit path, the TMA seemed to be able to interact with NADP+. Even if such an exit way was opposite if compared to the wild-type, the TMA seemed to bind several aa of wild-type FMO3 active site. The TMA path was very similar in the mutated forms E158K, E308G_E158K, R238Q_E158K, G475D_E158K, as well as in R492W_E158K and R238P_G475D, but compared to the wild-type it was the exact opposite. Here, the TMA firstly interacted with the Trp 419 (near to the FAD binding site), then bounced on the Arg 279, the Asn 245, and the Asn 246. A similar path was shown for mutated form R492W_E158K, with the difference represented by the interaction with the Leu 278 after Trp 419. An interesting case was determined by the P153L_E158K haplotype, wherein the TMA interacted with Trp419 first, then with the Leu 278 and the Arg 279. After these interactions, due to the FMO3 folding, Lys 280 and Glu 281 changed their conformation. All the FMO3 truncated forms showed the FAD and NADP binding sites alteration. The Y331stop nonsense variant would seem to determine a significant enzyme folding change. The TMA interacted only with Leu 235 before exiting in a way like the wild type (from bottom to top). In mutated form P380fs, the TMA interacted with Ala377, Ala378, Ile379, Glu9, Ala10, Gly11, and, finally, with

Glu281. The same path was determined by the P380fs_E308G haplotype, with the only difference being that in the latter TMA interacts with Glu281 before Lys280. In both mutated forms, the exit path was in the opposite direction compared to the wild-type form. Finally, in the mutated form P153L_E158K_P380Fs the TMA interacted with Ile87, Glu39, Gly38, Gly11, Ser85, and Asn84, tracing a path, completely away from the enzyme active site. A graphical representation of unbinding pathways for wild-type and all mutated FMO3 enzymes is shown in Figure 12.

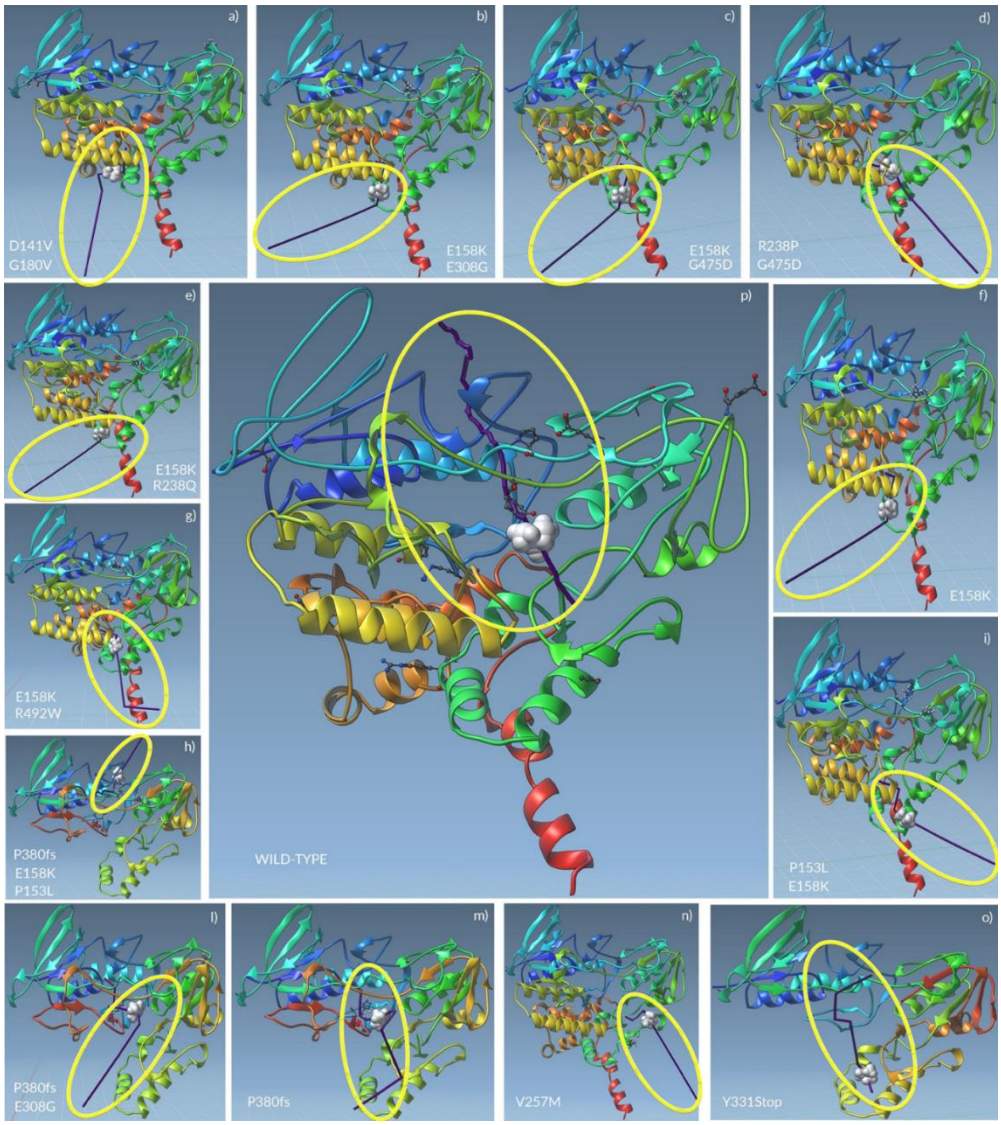

Figure 12. The TMA unbinding pathways through the whole FMO3 mutated proteins (a–o). The yellow circles indicate the unbinding pathway produced by pathlines (purple line) of TMA (white spheres) through the FMO3.

4.3 The origins of TMAU2 suspected patients could be found in gut microbiota dysbiosis related to alterations of several bacterial families

The secondary form of TMAU, on the basis of gut microbiota NGS analyses, suggested us that alterations of different bacterial families could determine the TMAU phenotype in FMO3 negative patients, also inducing psychiatric manifestations.

4.3.1 Differences of gut microbiota composition in healthy and illness

All 12 patients who underwent microbiota testing were positive for TMAU2. TMAU2 patients with neurological disorders were defined “cases”, and mentally healthy patients as "controls." Microbiota comparative analysis of TMAU cases versus controls highlighted very interesting differences in composition, bacterial family heterogeneity, and relative abundance (Figure 13).

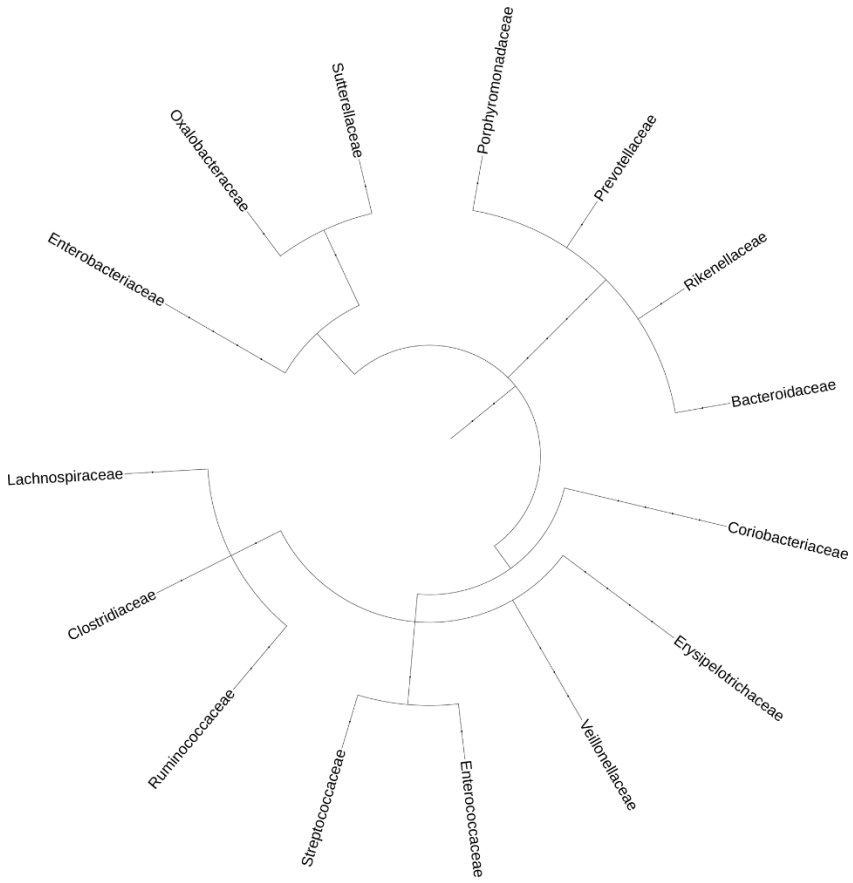

Figure 13. Cladogram of most altered bacterial families in TMAU behavioral disordered cases.

The cases showed the global overexpression of 10 altered bacterial families. Among these, the *Clostridiaceae* and *Enterococcaceae* families showed the highest relative abundance values in 4 cases and 3 cases, respectively. Among controls, on the other hand, the altered bacterial families distribution was more homogeneous and balanced. In the 34c and 35c controls the *Roseburia* and *Lachnospiraceae* families overexpression was mainly compensated by the *Enterobacteriaceae* and *Ruminococcaceae* families down-expression. The same situation occurred in control 38c. Here the more highly expressed *Roseburia* and *Prevotellaceae* families were compensated by the Enterobacteriaceae and *Streptococcaceae* down-expression. Unlike them, the 36c control showed a global down-expression of 4 bacterial families. In contrast, overexpression of 6 bacterial families occurred in the 37c control. By performing a comparative analysis between cases and controls, it emerged that the bacterial families found to be altered only in the cases were *Clostridiaceae*, *Bacteroidaceae*, *Enterococcaceae*. The *Bifidobacteriaceae*, *Sutterellaceae*, *Porphyromonodaceae*, and *Enterococcaceae* families were altered exclusively in controls. Bacterial families with relative abundances above the normal range in both cases and controls were *Roseburia* (in patient 33 and controls 34c, 35c, 37c, 38c), *Rikenellaceae* (in patient 32 and control 37c), *Erysipelotrichaceae* (in patient 32 and control 37c), *Oxalobacteriaceae* (in patient 28 and control 37c). Among cases, the n° 6 highlighted the highest number of bacterial families with altered expression (*Enterococcaceae* = 0.68%; *Erysipelotrichaceae* = 3.9%; *Rikenellaceae* = 6.95%; *Streptococcaceae*= 2.62%; *Lachnospiraceae* = 3.78%; *Coriobacteriaceae* = 6.5%), while the control showing the most differentially expressed bacterial family was the 4c (*Enterobacteriaceae* = 2.8%; *Oxalobacteraceae* = 0.08%; *Erysipelotrichaceae* = 3.8%; *Rikenellaceae* = 6.78%; *Veilloneaceae* = 0.48%; *Roseburia* = 1%). The *Streptococcaceae* bacterial family was overexpressed in the cases, vice versa down-expressed in the controls. The most altered family both in cases and controls was the just cited

Lachnospiraceae which, however, showed an opposite trend, reaching the highest relative abundance in controls (about 72%), and the lowest in cases (from 1.86% to 3.78%). Detailed list of differentially represented bacterial families and genera in case and controls is available in Table 13.

ID	27	28	29	30	31	32	33	34c	35c	36c	37c	38c
Enterobacteriaceae [0.1–1.1]	0.85	1.08	0.45	0.1	0.74	0.15	0.00	0.02	0.01	0.1	2.8	0.05
Oxalobacteraceae [0.0–0.0]	0	0.05	0	0	0	0	0	0	0	0	0.08	0
Enterococcaceae [0.0–0.0]	0.02	0	0.02	0	0	0.68	0	0	0	0	0	0
Erysipelotrichaceae [0.1–2.9]	2.8	0.4	0.78	0.1	0.38	3.9	2.7	0.15	0.21	0.1	3.8	2.62
Rikenellaceae [0.2–5.3]	0.48	5.22	1.25	0.2	2.2	6.95	0.2	0.2	0.2	0.2	6.78	0.48
Veilloneaceae [0.8–7.7]	6.35	3.15	1.58	0.8	2.8	5.35	3.35	0.8	0.8	0.8	0.48	1.85
Roseburia [0.0–0.9]	0	0.15	0.25	0.85	0	0.04	1.03	3.09	4.4	0	1	1.53
Streptococcaceae [0.1–1.8]	0.28	0.22	3.48	0.01	0.15	2.62	0.15	0.1	0.1	0.03	0.32	0.08
Clostridiaceae [0.1–1.4]	0.28	1.45	1.25	28.8	134.1	0.28	0.01	0.1	0.1	0..23	0.32	0.18
Lachnospiraceae [12.8–37.26]	20.52	9.98	24.78	1.86	15.8	3.78	23.22	72.24	44.65	0.04	18.58	23.25
Prevotellaceae [0.1–13.66]	0.12	2.3	16.68	0.1	0.7	3.85	14.0	0.02	0.1	0.1	0.13	26.65
Coriobacteriaceae [0.3–5.9]	0.15	1.08	2.12	0.01	0.7	6.5	0.82	0.3	0.3	0.04	0.52	1.7
Bacteroidaceae [3.2–35.36]	55.62	17.5	9.98	3.2	9.2	25.38	1.4	3.2	3.2	3.2	14.58	9.45
Ruminococcaceae [13.7–34.7]	2.42	24.4	23.38	13.7	18.7	24.35	16.23	0.27	1.43	0.13	24.25	19.8
Faecalibacterium [2.5–15.56]	0	3.05	9.35	5.2	5.5	0.58	8.43	6.4	23.97	10.33	8.25	7.2
Porphiromonodaceae [0.2–3.2]	1.25	0.2	0.98	0.22	0.52	1.5	0.55	0.12	0.2	0.2	1.22	0.28
Sutterellaceae [0.1–3.5]	0.1	0.1	0.1	0.1	0.1	0.1	0.1	0.01	0.61	0.1	0.1	0.1
Bifidobacteriaceae [0.1–7.96]	4.38	1.82	0.38	0.39	3.55	3.88	0.1	0.1	0.003	0.11	0.1	1.05

Table 12. Differentially represented bacterial families/genera in TMAU psychiatric cases and controls. The normal range of % relative abundance is indicated between squared brackets.

4.3.2 Altered bacterial families in TMAU2 patients determined an unbalanced pattern of produced metabolites

A very important feature of the analysed bacterial families was the production of different metabolites. The latter are able of modulating human metabolic pathways important for inflammation, immune and neurotransmission function. This is carried out by serotonin, dopamine, gamma aminobutyric acid, norepinephrine produced directly or indirectly by the gut microbiota. Such neurotransmitters are produced directly by the *Enterobacteriaceae* family. Serotonin is also produced by *Enterococcaceae* and *Streptococcaceae* and gamma aminobutyric acid by *Bifidobacterium* and *Bacteroidaceae*. Short-chain fatty acids such as acetate, butyrate and propionate are produced by most bacteria, especially *Roseburia*, *Clostridiaceae* and *Lachnospiraceae*. A complete list of all metabolites produced by considered bacteria, involved in nervous physiology, is available in Table 14.

BACTERIA/ METABOLITES	Lactate	Dopamine	Norepinephrine	Acetate	Serotonin	Succinate	Butyrate	Glycolate	Propionate	Pyruvate	alfa-ketoglutarate	LPS	Malate	Tryptophan	GABA
Enterobacteriaceae	X	X	X	X	X	X									X
Oxalobacteraceae	X						X	X		X	X		X		
Enterococcaceae	X				X							X			
Erysipelotrichaceae	X			X											
Bifidobacteriaceae	X			X											X
Rikenellaceae				X		X			X						
Sutterellaceae												X		X	
Veillonaceae	X			X		X			X						
Roseburia	X			X			X		X						
Ruminococcaceae	X			X		X									
Streptococcaceae	X			X	X										
Clostridiaceae	X			X			X		X						
Lachnospiraceae	X			X		X	X								
Prevotellaceae				X		X			X						
Coriobacteriaceae	X			X											
Bacteroidaceae				X		X	X		X						X
Faecalibacteriaceae							X								
Porphiromonodaceae				X		X			X						

Table 13. Metabolites produced by altered microbiotas related to neural metabolism.

An intriguingly scenario emerged by linking the alterations of microbiota bacterial families to each produced metabolite. The short-chain fatty acids (SCFAs) resulted the most altered molecules in both case and controls, even if with different trends, with the propionate more differentially produced in cases. Tryptophan and GABA, instead, showed different levels only in controls, in which resulted down-represented (Table) 15.

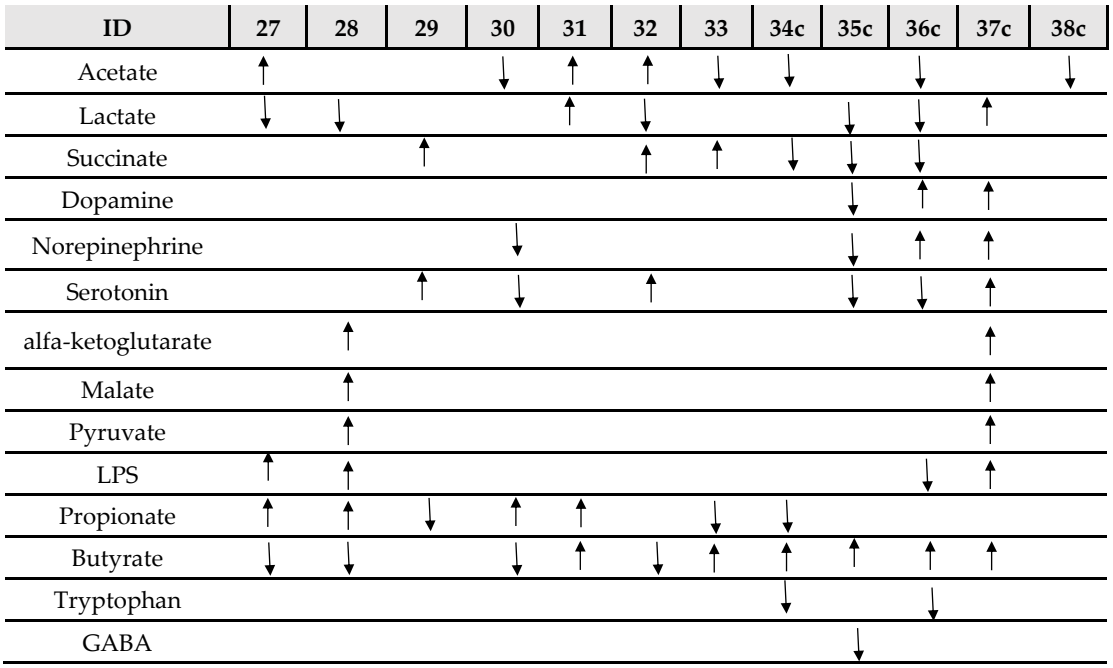

Table 14. Correspondence between altered microbiota families/genera and nervous-related metabolite levels. Considered metabolites only refer to microbiota biosynthesis, and they are retrieved from MACADAM database and literature. ↑=over-production.↓= down-production. "[empty space]" = no expression differences.

4.3.3 A suggestive hypothesis: biochemical crosstalk between SCFA, neurotransmitters, TMA synthesis, and brain disorders in TMAU2 patients

Once obtained the bacterial families relative abundances of all patients, the study continued by analyzing the single bacterial metabolites produced. Both the MACADAM tool and an in-depth literature analysis showed a very interesting and complex network. The latter would explain the connection between the bacterial

metabolites production, the TMA synthesis, and the behavioral disorders onset. By analyzing the gut microbiota qualitative composition, it emerged that most of the altered bacterial families (*Clostridiaceae*, *Streptococcaceae*, *Roseburia*, *Bacteroidaceae*, *Enterobacteriaceae*) is TMA producer. This is not only produced directly by the microbiota, but also indirectly as an intermediate product of human metabolic pathways. The same situation occurs with some neurotransmitters (serotonin, GABA, dopamine, norepinephrine). These are produced both directly by some bacterial families but could also be synthesized from bacterial metabolites which then enter human metabolic pathways. In detail, short-chain fatty acids (acetate, propionate, butyrate, also resulted from mixed acid fermentation, figure 14), together with lactate and alpha-ketoglutarate, play a fundamental role into biogenesis of glutamate and GABA. In this process, might be involved the BGT1 member of solute transporter family 6 (the neurotransmitter, sodium symporter transporter family), which mediates cellular uptake of betaine and GABA in a sodium- and chloride-dependent process. GABA altered levels could interfere with the betaine transport, resulting in a possible TMA accumulation[63,64] (Figure 15).

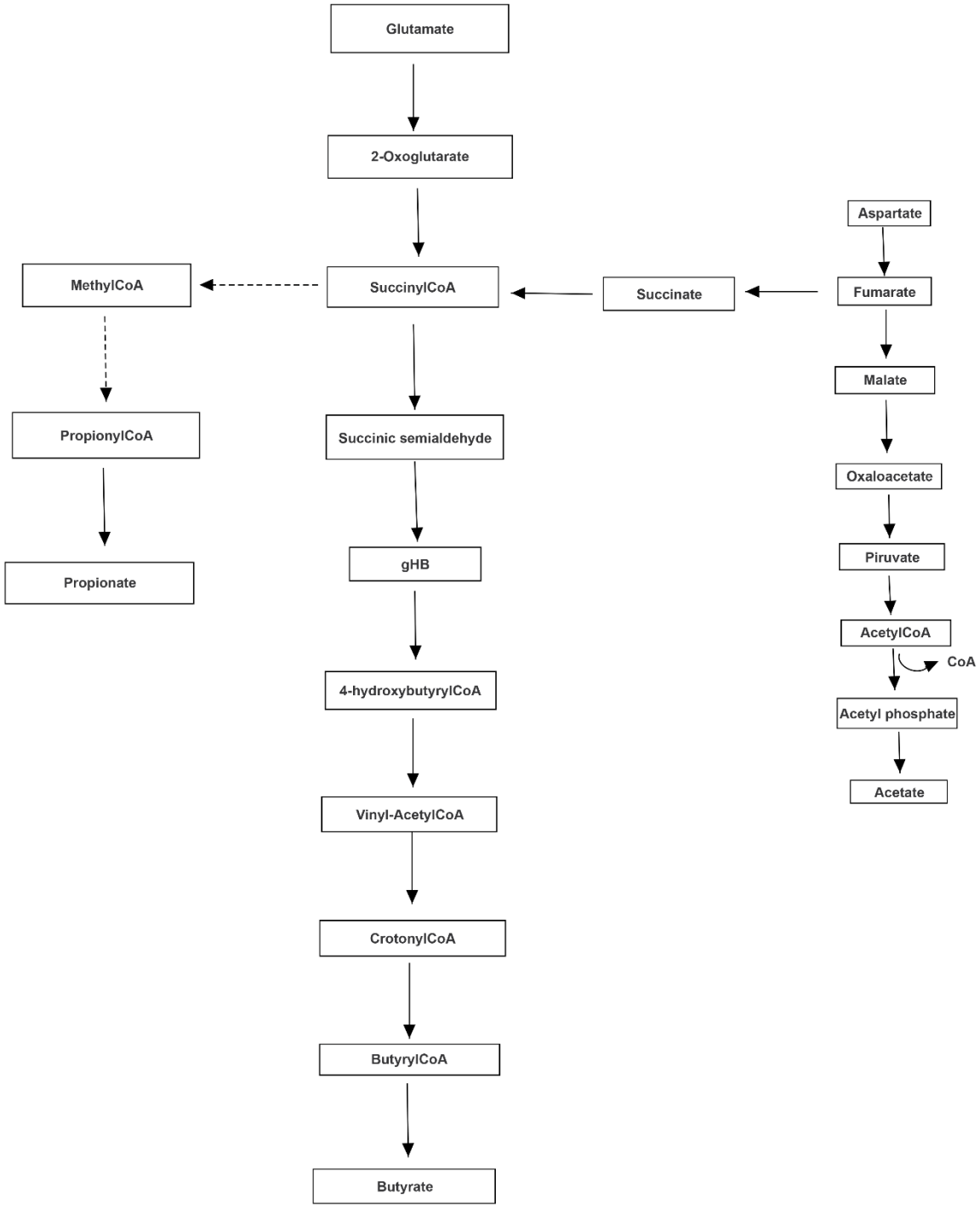

Figure 14. Mixed acid fermentation involving microbiota bacteria.

Fig. 15. Metabolism of glutamate and GABA linked to ACh. The complex pathway, also showing the involvement of lactate, could play a relevant role in regulation of betaine, a precursor of TMA.

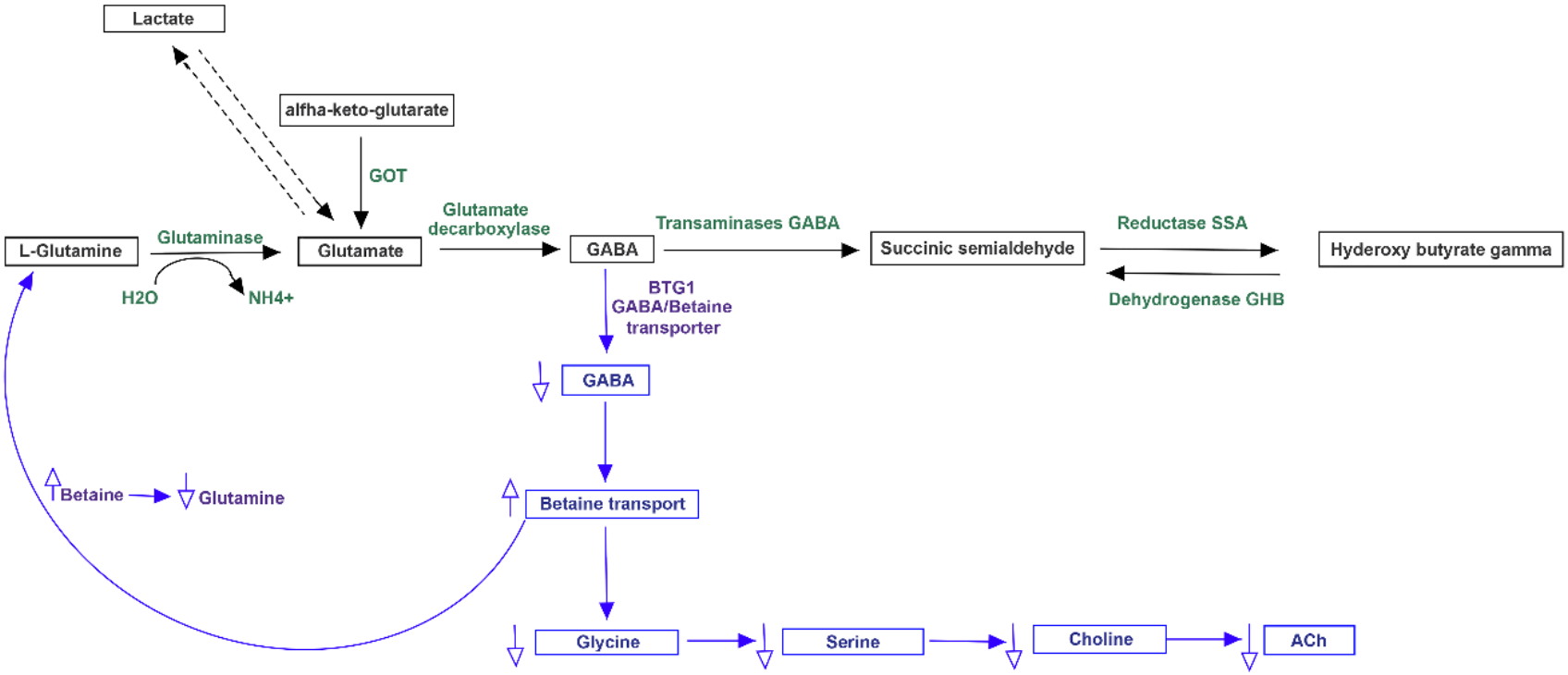

The TMA accumulation could also result from catecholamine metabolism. The norepinephrine concentration, synthetized by dopamine, could regulate the Phosphatidylethanolamine N-methyltransferase (PEMT) enzyme activity, which is also able to metabolize the phosphatidylethanolamine into phosphatidylcholine[65], then converted to choline, with final increase of TMA levels (Figure 16).

Fig. 16. Metabolism of catecholamine and link to serotonin. The scheme also shows that tyramine, produced from tyrosine, is a substrate of FMO3.

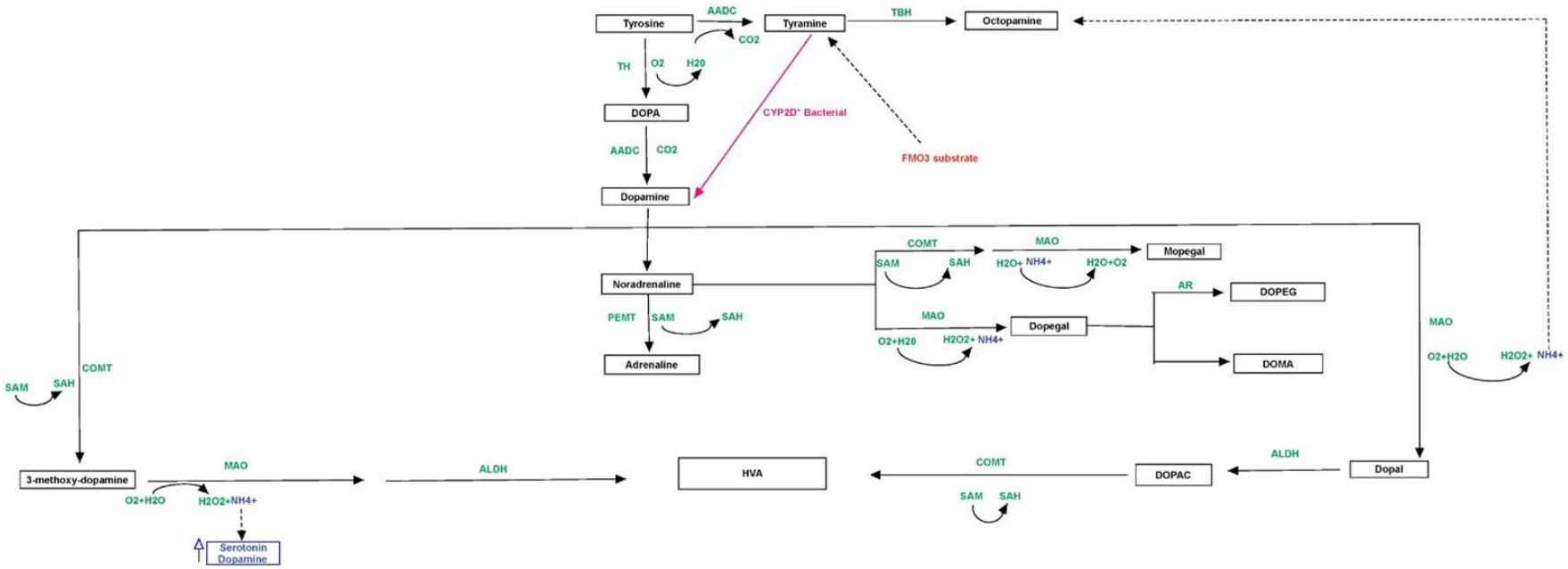

Furthermore, the indirect TMA production could occur from carnitine as a consequence of the increased acetylcholine levels Fig 17.

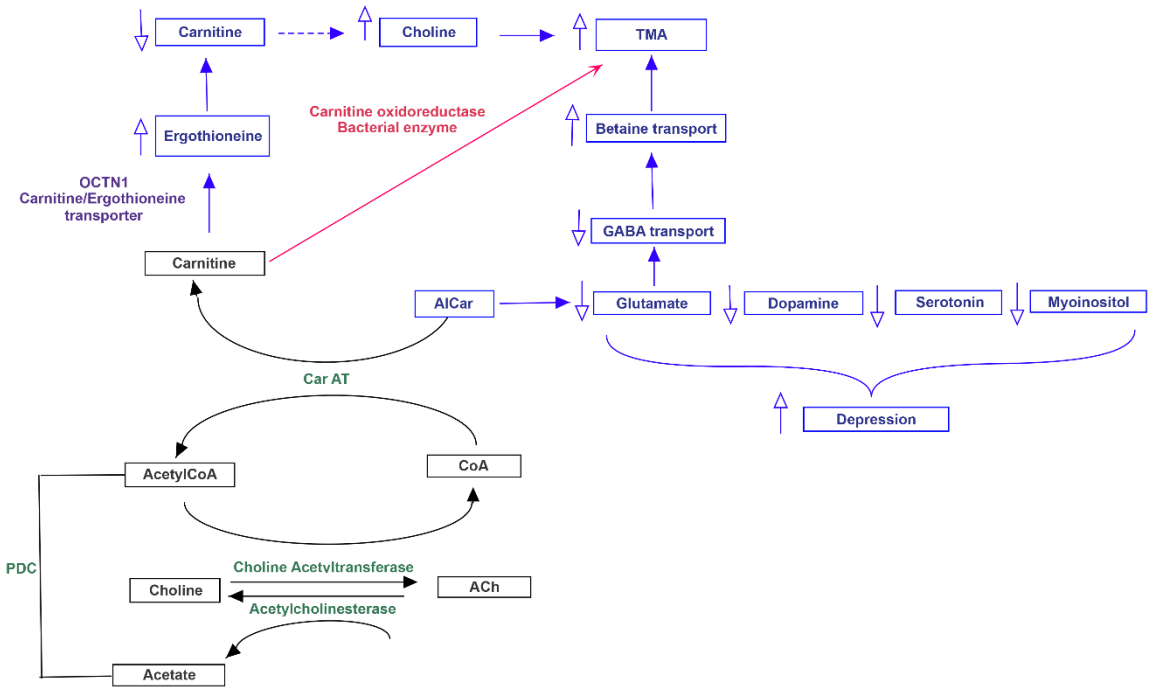

Fig. 17. Acetylcholine and carnitine metabolism could influence TMA accumulation and behavioral phenotype. Both carnitine and acetylcholine could alter choline and acetyl-carnitine biosynthesis, determining an accumulation of TMA. At the same time, the acetyl-carnitine could influence the release of main neurotransmitters, determining important behavioral alterations.

In addition, lactate appears to play an important role in the serotonin synthesis, inducing the amino acid tryptophan synthesis from which it derives[66]. Furthermore, the serotonin biosynthesis is strictly connected to melatonin one, whose involvement in circadian rhythms such as sleep-wake cycle is well known. Interestingly, in condition of elevated oxidative stress and inflammation, the tryptophan could shift from serotonin biosynthesis to quinolinic acid one, a neurotoxic byproduct able to induce depression (Figure 18).

Figure 18. Serotonin metabolism and its "shunt" following oxidative stress and inflammation. Serotonin, produced from tryptophan, could be converted in melatonin. In condition of oxidative stress and inflammation, the amino acid shifts to kynurenine and quinolinic acid pathway, exerting neurotoxic effects.

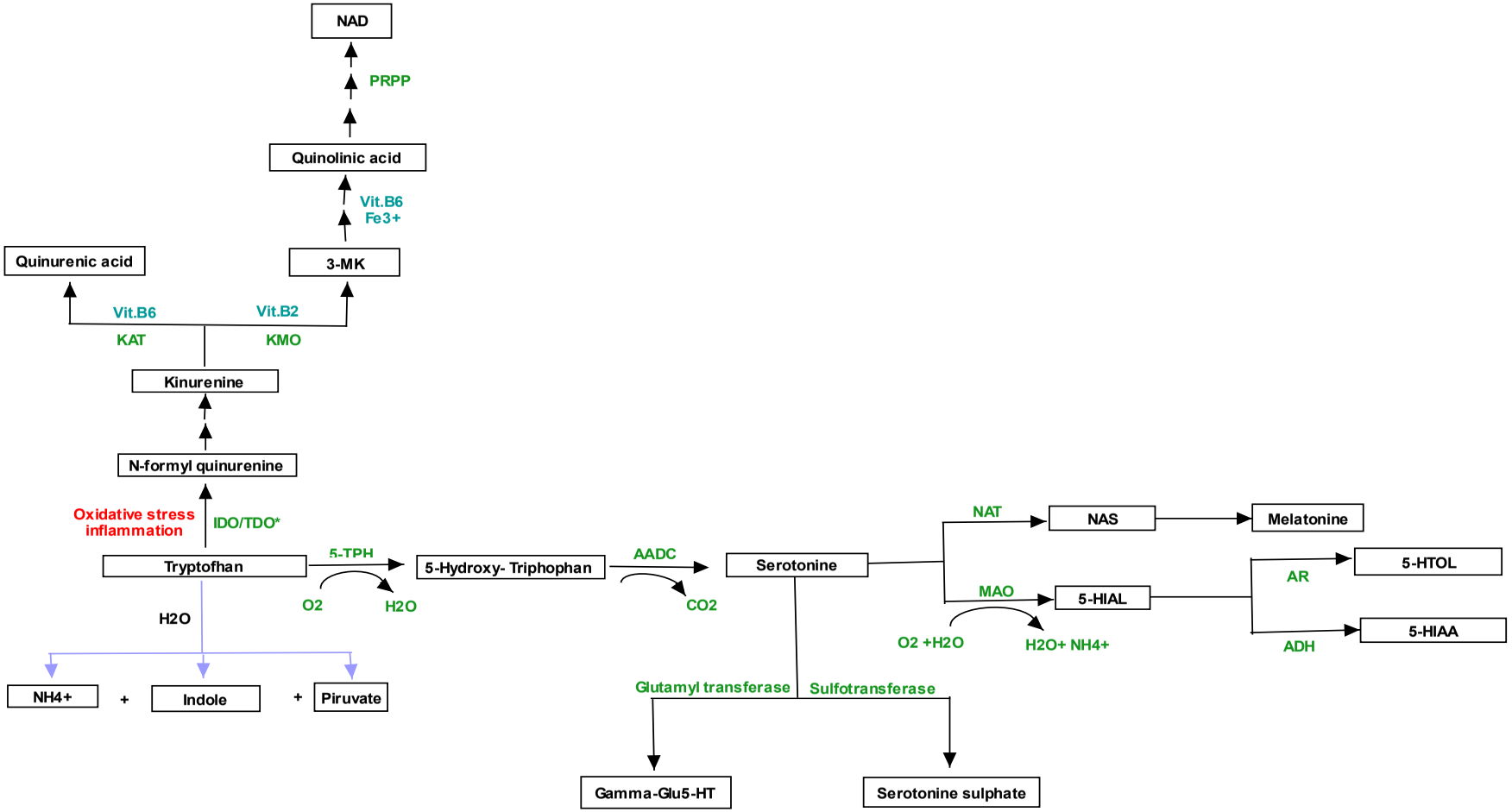

Fluctuation of described neurotransmitters could lead to vagus activation/deactivation and limbic deregulation, with behavioral and mood disturbs, like one evidenced by cases in exam. A detailed scheme of all evaluated biochemical pathways linking neurotransmitter and TMA metabolisms is represented in Figure 19.

Figure 19. Detailed diagram of biochemical pathways linking neurotransmitter and TMA metabolisms. The figure represents how neurotransmitter and TMA pathways might be correlated. Dashed lines represent indirect and candidate relationships. Empty arrows indicate over- or -down-expression of adjacent metabolite[67].

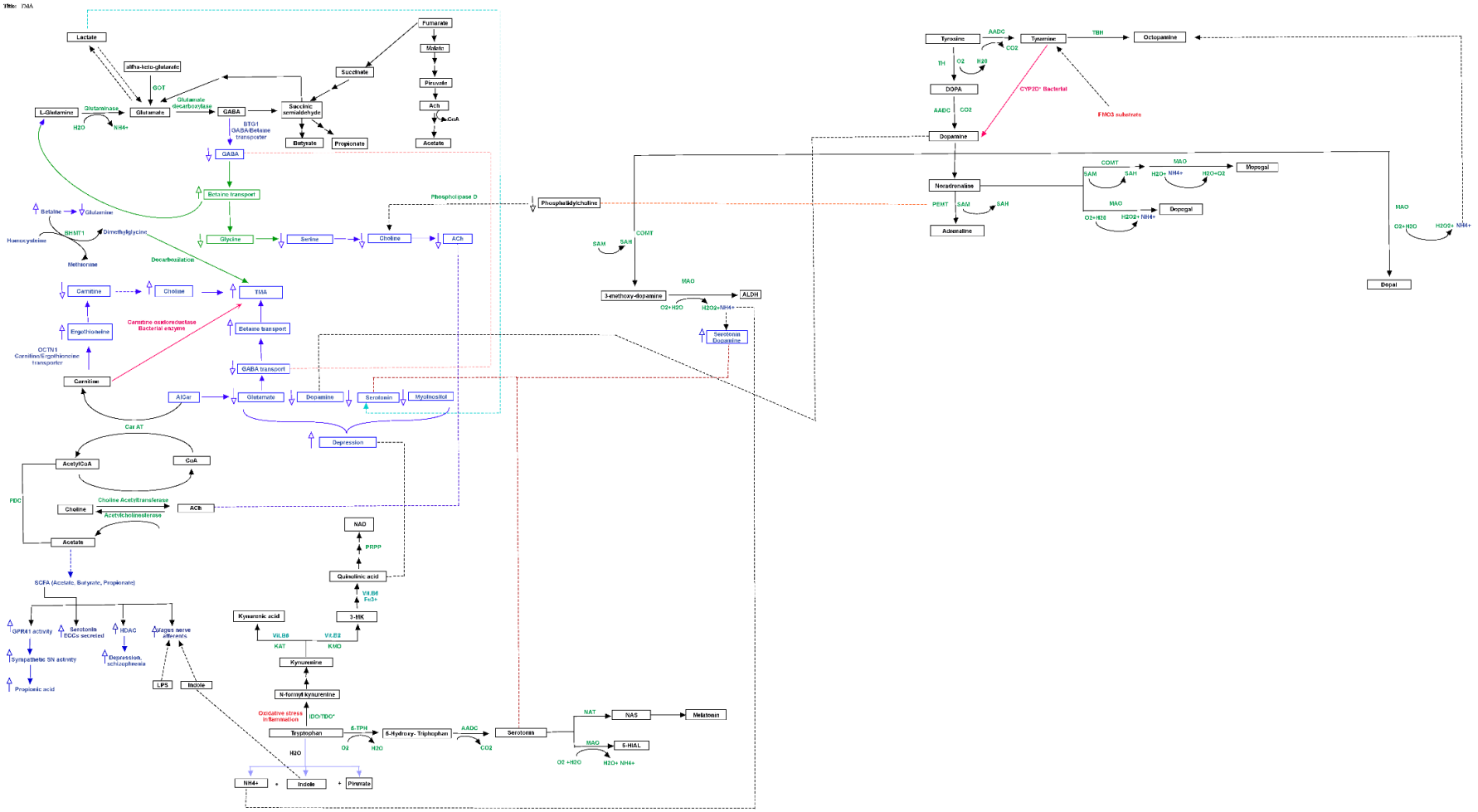

5 DISCUSSION

Trimethylaminuria is a very rare but also quite complex metabolic syndrome. To date, unfortunately, many aspects of this pathology are poorly understood, so it is very difficult to advise the patient on the correct therapeutic approach to follow. Both main forms of this syndrome, primary and secondary, cause TMA accumulation, even if in different ways. The primary form is determined by the FMO3 enzyme malfunction, while the secondary form is mainly driven by gut microbiota alterations[68,69]. For TMAU1 the diagnosis consists in the TMAO/TMA+TMAO ratio urine dosage and in the *FMO3* genetic screening. The genetic test is considered positive only when causative variants are present and in homozygous condition. This is supported by functional evidence, e.g. TMA urine dosage, but the exact molecular genetic mechanisms that cause the FMO3 enzyme impairment are not yet full known. This is due to the complex structural features of this enzyme. Unlike bacterial FMOs and yeast, all mammalian FMOs have a strong membrane association and are insoluble. This scenario prevented to solve the FMO3 three-dimensional structure in an easy way, due to difficulties in the x-ray liver microsomes crystallography[70]. For TMAU2 diagnosis, instead, in addition to the urinary TMA and TMAO levels evaluation, the gut microbiota analysis should be performed. This is important to confirm or not a dysbiosis condition. In recent years, the interest in the gut microbiota influence on the several diseases onset (obesity, cardiovascular disease CVD, atherosclerosis, colon cancer) has increased, but its role on TMAU onset remains unclear[71,72,73]. It is now known that TMAO is considered a marker for other diseases diagnosis, such as atherosclerosis and CVD[74]. Thus, the only useful information is obtained indirectly from the study of these pathologies. Moreover, it is also known that some bacterial families produce directly TMA. Among these, the most studied are the bacterial families that convert choline into TMA (cluster C/D), which is considered the main route of

production. This does not exclude that other bacteria, whose metabolic pathways are still unknown, may perform this function.

Furthermore, the metabolites role on both the indirect TMA production, aggravating its phenotype, and in neurotransmission, causing the behavioral disorders onset, has not yet been investigated.

The present study was performed on 38 suspected TMAU patients with the aim of clarifying some of these aspects. The first diagnostic approach was the TMAO/TMAO+TMA ratio dosage in urine by mass spectrometry after a suitable choline-loaded diet. 21 of the 38 examined patients showed a low TMAO/TMAO+TMA ratio; however, in 17 patients this ratio was within the normal range reported for control subjects. Although some of these tests resulted negative, the *FMO3* genetic screening was performed in all recruited patients. This choice was made on experimental basis to exclude patient's intrinsic physiological factors that could have compromised the dosage result. TMA is a volatile amine and its urine concentration could depend on the quantity and speed with which it is expelled through sweat. Furthermore, defects in the renal filtration process could cause a TMA reabsorption and, consequently, its lower level in the urine. *FMO3* genetic testing was performed by Sanger sequencing. Stop and missense variants, some of which were causative, were found in 26 patients. All the causative variants were identified in heterozygous condition and constituted 26 different haplotypes. Therefore, the next step was to evaluate these haplotypes role on protein folding and, consequently, on the enzyme catalytic activity. Furthermore, in the 12 patients without any *FMO3* variant, a further anamnestic investigation was conducted to evaluate if the shown phenotype could be determined by the TMAU secondary form. From this analysis, 7 patients showed behavioral disorders, also confirmed after the clinical assessment of healthy mental state. Then, gut microbiota 16s rRNA sequencing of all 12 patients was performed to verify a possible dysbiosis condition. All the examined patients showed alteration of the main bacterial families currently

known as TMA producer. After confirming the TMAU2 diagnosis, the study continued on the metabolic pathways analysis including TMA and its precursors, together with the neurotransmitters involved in the limbic system activity. The purpose of the latter investigation was the clarification of another aspect, very often underestimated, which distinguishes many TMAU patients, namely the social discomfort and behavioral disorders that derive from it. Very often some patients complain of behavioral disorders such as anxiety, depression. To date it is not clear whether this disturbance is a consequence of the strong social discomfort caused by the bad smell emitted or whether it could be linked to the gut dysbiosis from which the patients are affected.

5.1 Could FMO3 haplotypes impair the FMO3 enzyme catalytic activity and affect the TMAU phenotype?

As already widely discussed, the TMAU1 diagnosis consists in the *FMO3* screening for homozygous causative mutations. However, despite this, some patients (ID 1-2-3-4-5-9-11-12-13), presenting high TMA urinary levels, showed haplotypes made of causative and not causative missense variants, and/or stop variants combination. All these variants were in heterozygous condition except for the haplotype found in patient 12 (S147=, Asn285=, Asp141Val, Gly180Val), consisting of homozygous non causative variants. One hypothesis developed to explain such phenomenon relies on the possibility that other genes could be involved in TMAU etiopathogenesis. In the meantime, the role of many polymorphic variants able to impact on FMO3 folding and activity is still unexplored, as well as the involvement of haplotypes in the onset and progression of trimethylaminuria[75]. It has been widely acknowledged that haplotype analysis in association studies can provide much more useful information than the information derived from single polymorphisms analysis[76]. The primary reason for considering the haplotype organization of variation resides in the fact that the folding kinetics, stability, and other physical features of a protein may depend on interactions between pairs or

higher-order combination of aminoacidic sites; if such interactions are relevant, then haplotypes are of direct biological importance. To study these haplotypes impact on the enzyme activity it is necessary to know the physicochemical properties of the enzyme, its active site, and the NADP and FAD cofactors binding site position. All this information is currently not known. Thus, in order to try and unveil these aspects, several bioinformatics tools have been exploited. Thanks to AutoDock Vina it was possible to determine the FMO3 active site aminoacidic residues, so far unknown. Today, indeed, only isolated domains were homologically modelled on the basis of the bacterial FMO3[77]. The unbinding pathway analysis showed that TMA mainly interacts with Ser216, Gly217, Ser218, Trp219, Val220, Pro273, Asn 275, Gly 276, Leu278, Lys280, Glu281, and Pro282 FMO3 amino acids, suggesting that these aa might play an important role in the TMA oxidation process. The single variant and haplotypic analyses on the mutated FMO3 revealed that V257M was the only one that does not appear to cause a change within the enzyme active site. The folding also looked very similar to the wild-type. Furthermore, from the ligand pathfinder analyses, it emerged that the TMA, during its path, seems to interact with most of the active site amino acids. The situation resulted completely different for the haplotypes P153L_E158K, E158K_R492W, E158K_G475D, R238P_G475D, D141V_G180V. These showed different active site amino acids than the wild-type form, the proteins folding, especially in the mutated form (D141V_G180V) is also quite different. Probably the combination of several variants could favour or reduce chemical interactions between different amino acids, influencing protein folding and causing a lower TMA-active site binding stability. This hypothesis was also confirmed by the interactive simulation obtained with the Ligand Path Finder tool. Both trajectory and direction are different. Therefore, the described haplotypes might cause an enzymatic pocket narrowing, altering the TMA transit through the FMO3. Furthermore, such impairments could determine not only a different route for the TMA, but also a reduced interaction time of the ammine with the catalytic site of the enzyme. The final result of this altered enzymatic kinetics might be the

reduced levels of TMAO and an accumulation of TMA, leading to the characteristic TMAU phenotype, whose different expression levels could depend on a specific haplotype. Regarding the Y331stop, P380fs variants and the P153L_E158K_P380fs and P380fs_E308G haplotypes (found in 1, 3, 2, 4 patients, respectively), the molecular genetic mechanism that could cause the FMO3 enzyme malfunction appears to be different. Thanks to the Interpro tool, the FAD and NADP cofactors binding sites were predicted, then also confirmed by the i-Tasser tool. Both cofactors are essential for the TMA N-oxidation process. The FAD binding site was computed approximately in the 310-470 aminoacidic region. This region was altered in all 4 mutated forms. Both Y331stop and P380fs stop variants could cause the loss of several amino acids within FAD binding sites. Furthermore, observing the three-dimensional structure, it emerged that the enzymatic pocket conformation is different from wild-type. In this case, therefore, the enzyme malfunction could be mainly due to the cofactors binding sites alteration, especially for the FAD.

5.2 Importance of the gut-brain axis in behavioral disorders affecting TMAU2 patients

In recent years, there has been growing recognition of the involvement of the gut microbiota in the modulation of multiple neurochemical pathways through the highly interconnected gut-brain axis. This link is possible through neurotransmitters, produced directly by the gut microbiota, which can influence the microglia activation and many other brain functions. Short-chain fatty acids may also play a key role in brain pathophysiology. Once produced, these are absorbed by the colonocytes, mainly via H^+-dependent or sodium-dependent monocarboxylate transporters (MCTs and SMCTs, respectively) expressed in several tissue. The abundant expression of MCTs in endothelial cells could facilitate the BBB crossing and reaching CNS areas such as amygdala and hippocampus, thus modulating crosstalk gut-brain[63]. Furthermore, the same metabolites can directly act on the autonomous nervous system, regulating synapses of vagus nerve in

enteric nervous system (ENS)[29]. Although several studies have hypothesized the gut microbiota and behavioral disorders connection, little is known whether these may also be linked to metabolic disorders such as TMAU. Anxiety, depression, manic behaviors, mood disorders are characteristic in TMAU patients. These psychological comorbidities, strictly linked to limbic system, represent the most controversial aspects of this pathology, because it is still unknown whether these disturbs are the consequences of social reactions to malodor or could depend on bacterial metabolites-induced biochemical alterations of nervous system. To shed new light on this aspect, the microbiota of each patient was examined. All the possible metabolic pathways involving neurotransmitters, SCFA and TMA, produced by the altered bacterial families, were investigated. In the networks analysis, additional information provided by patients, such as antibiotic or probiotics intake, were also considered. Making a brief description of the cases, the patient 31 (fig. 20) showed a high relative abundance of the *Clostridiaceae* bacterial family, known to produce SCFA (propionate, butyrate, acetate) and lactate[27]. Elevated levels of SCFA may increase the afferent component stimulation of the vagus nerve resulting in serotonin syndrome, especially obsessive-compulsive disorder. The latter, of which the patient is affected, is aggravated by the high lactate levels, by the antibiotics and probiotics intake such as *L. acidophilus*, *Bifidobacterium*, *L. rhamnosus*, *Streptococcus* and *L. paracasei*. These are known to produce serotonin, GABA, lactate, acetate resulting in the TMA accumulation at the same time.

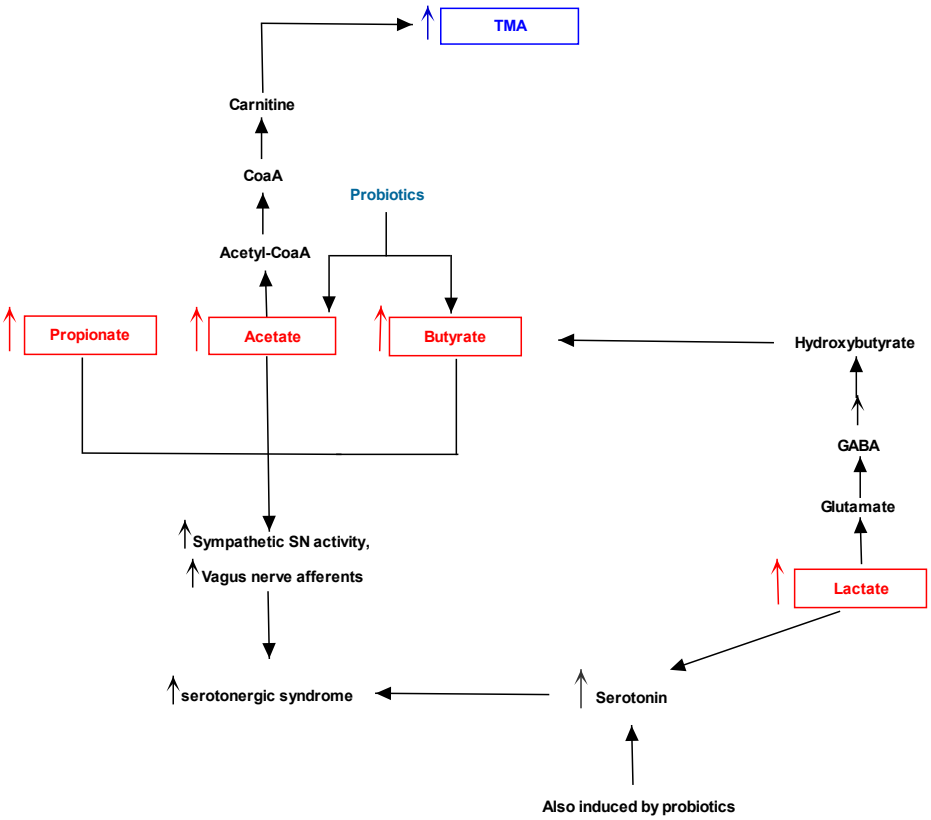

Figure 20. Biochemical pictures of TMAU patient 31. The panel represents how metabolites produced directly or indirectly by patient's microbiota could influence the biosynthesis/release of neurotransmitters (in particular serotonin) and the production/accumulation of TMA.

Patients 27 (Figure 21) and 32 (Figure 22) showed an analogue serotoninergic syndrome like symptomatology. Patient 27 showed an overabundance of the *Enterococcaceae* and *Bacteroidaceae* bacterial families, on the contrary the *Coriobacteriaceae* and *Ruminococcaceae* bacterial families were under-expressed. Patient 32 instead showed the highest number of altered bacterial families. It showed increased levels of gut *Enterococcaceae*, *Erysipelotrichaceae*, *Rikenellaceae*, *Streptococcaceae* and *Coriobacteriaceae*, and low levels of the only *Lachnospiraceae*. This bacterial alteration induces in both patients an increase in the acetate, propionate and LPS levels and a decrease in butyrate and lactate. As already explained, an increase in acetate levels can induce the carnitine biosynthesis, a known TMA precursor, causing its accumulation. The known excitatory effects of lactate on

neural metabolism can determinate an increase of both serotonin and glutamate, while provokes neurotoxicity in neural physiological environment[78]. Thus, low levels of lactate could reduce serotonin and glutamate, whose reduction might decrease GABA biosynthesis in central nervous system, mainly in hippocampus (https://www.proteinatlas.org/ENSG00000145692-BHMT/brain). This portion of limbic system expresses the betaine/GABA transporter BTG-1[79] which, due to plasma low GABA concentration, might trigger the neuronal internalization of betaine. Betaine can be converted to TMA by betainehomocysteine-S methyltransferase (BHMT1) and a following decarboxylation. Furthermore, regarding serotonin, despite the lactate and butyrate low levels, its concentration could increase thanks to the afferent component stimulation of the vagus nerve by acetate, propionate and LPS. This induces what is generally called "gut instincts" or visceral sensations consisting in the emotional responses elaboration by the brain such as fear, anxiety, peculiar to the patient 1. In patient 6 instead, the *L. helveticus* and *B. longum* probiotics intake, known to increase the serotonin and norepinephrine levels in the hippocampus[80], could induce the increased release of serotonin from enterochromaffin cells (ECC) and the hyperactivation of the vagus nerve.

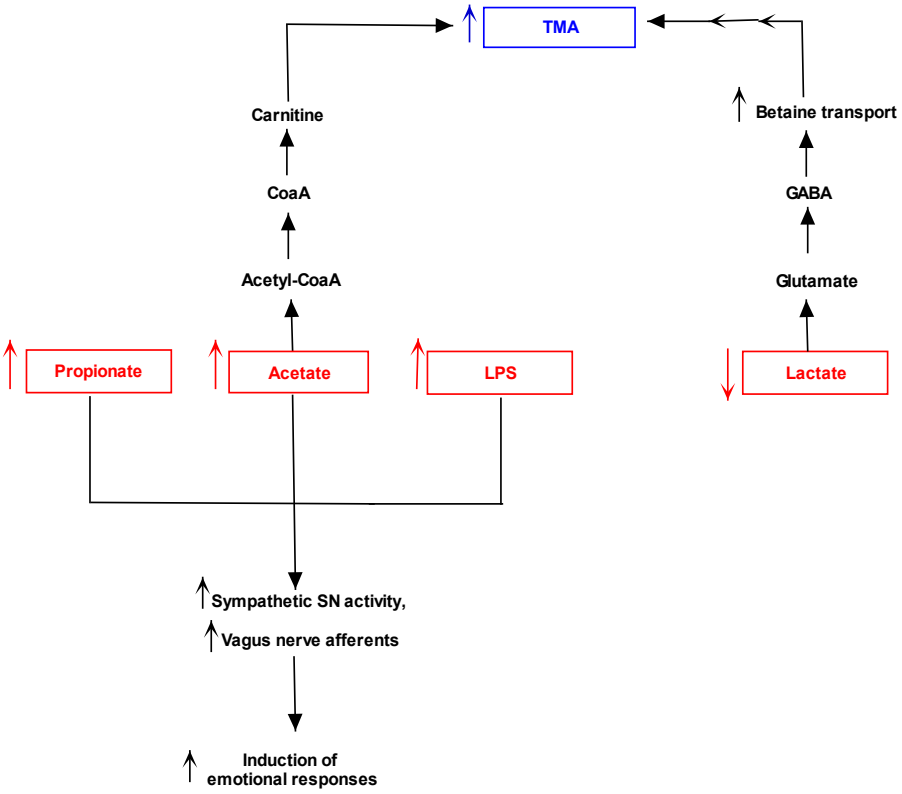

Figure 21. Biochemical pictures of TMAU patients 27.

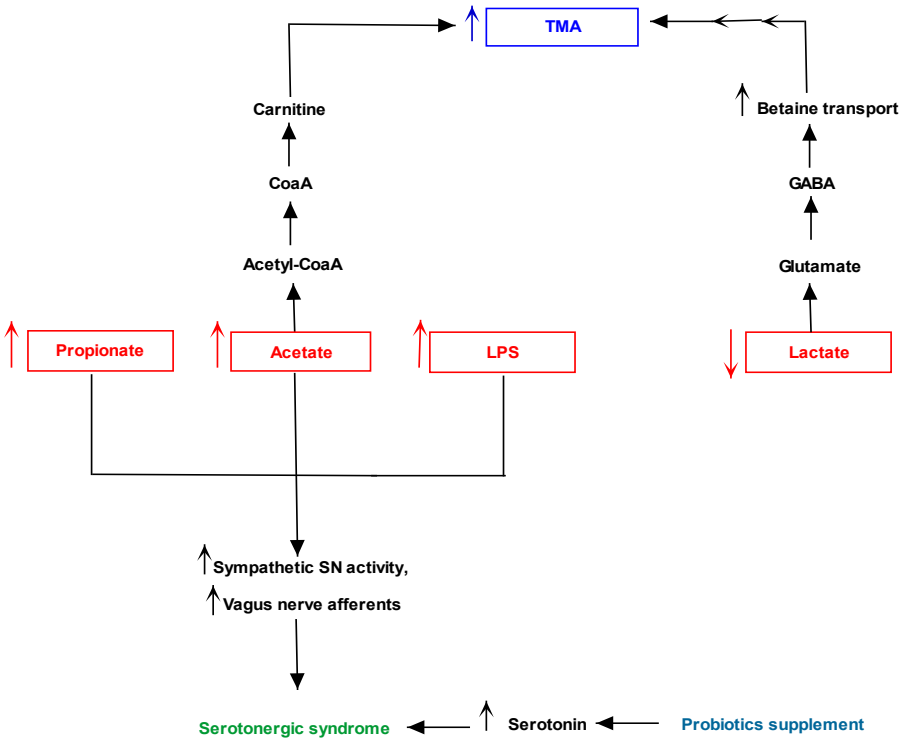

Figure 22. Biochemical pictures of TMAU patients 32.

A different situation occurred in patient 29 (Fig. 23). Microbiota testing showed an overabundance of the bacterial families *Enterococcaceae*, *Streptococcoceae* and *Prevotellaceae*, known to produce mainly serotonin and succinate. The latter through mixed acid fermentation is transformed into succinyl CoA, which follows the biochemical pathway starting from succinic semialdehyde determining the butyrate synthesis. Its overproduction could induce enterochromaffin cells to produce serotonin that, together with serotonin secreted by altered gut bacteria, can determine the serotoninergic syndrome typical phenotype. Furthermore, the TMA accumulation could be determined by the L-carnitine administration, reported by the patient. L-carnitine is converted directly to TMA by bacterial carnitine oxidoreductase. This condition reflects the major nervous-related symptoms shown by the patient (migraine, mood alteration, sense of marginalization and social phobia)[81]. Furthermore, the serotonin excess can increase levels of melatonin, explaining alteration of sleep-wake cycle of patient 29.

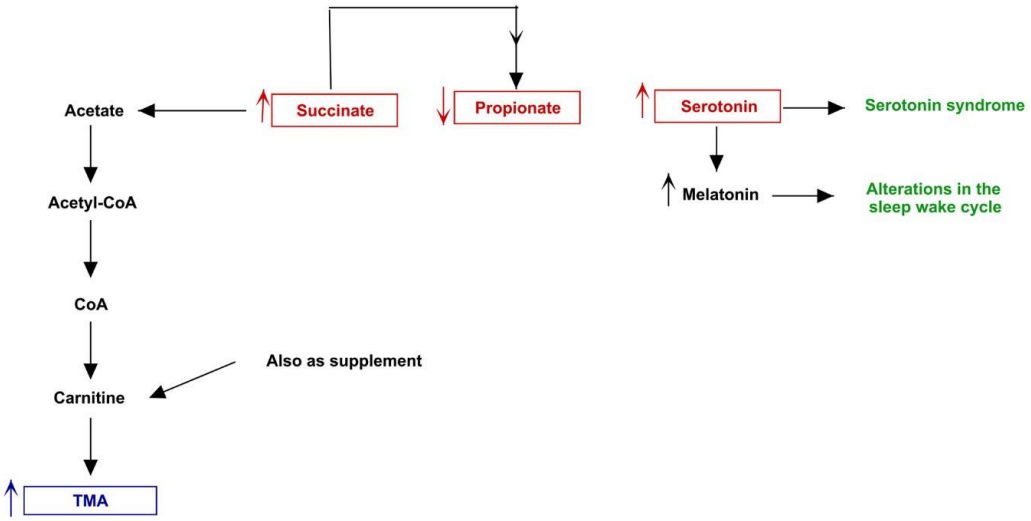

Figure 23. Biochemical pictures of TMAU patient 29.

A unique condition was evidenced in patient 30 (fig. 24). Additional blood tests provided by the patient revealed a reduction in B2 and D vitamins, and folate levels vice versa an increase in homocysteine. The latter could be converted into

methionine by the homocysteine methyl transferase enzyme which transfers a methyl group from betaine. Together with methionine, dimethylglycine (DMG) is also formed which is converted to TMA by decarboxylation. Furthermore, the high TMA concentration could be also determined by the low folate levels that could impair the norepinephrine biosynthesis[82]. This event could shift the catalytic activity of PEMT from epinephrine biosynthesis towards phosphatidylcholine production, which could increase TMA levels via choline pathway. In addition, the patient showed a *Lachnospiraceae*, *Coriobacteriaceae* and *Streptococcaceae* reduction and an increase of *Clostridiaceae*. This is reflected in the low acetate and butyrate production but in the propionate higher synthesis. As already explained, SCFAs are involved in the vagus nerve stimulation. In this case, its hypoactivation could occur which would lead to a decrease in the serotonin release. The most interesting metabolic pathway related to mood disorders was represented by low levels of plasmatic vitamin B2, which could be accumulated in nervous tissue following increased blood brain barrier (BBB) permeability. This permeability, indeed, is known to be caused by microbiota dysbiosis[83]. Moreover, this inflammatory scenario determined by altered microbiota could trigger the shifting of the tryptophan from serotonin pathway to degradation, producing kynurenine, which cross the BBB and, inside the nervous tissue, is converted into quinolinic acid[84]. This molecule is an antagonist of NMDA receptors and a non-competitive inhibitor of acetylcholine receptors, able to produce oxidative stress and neurotoxic effects, also inducing anxiety and depression, two behavioral alterations of patient 30.

Figure 24. Biochemical pictures of TMAU patient 30.

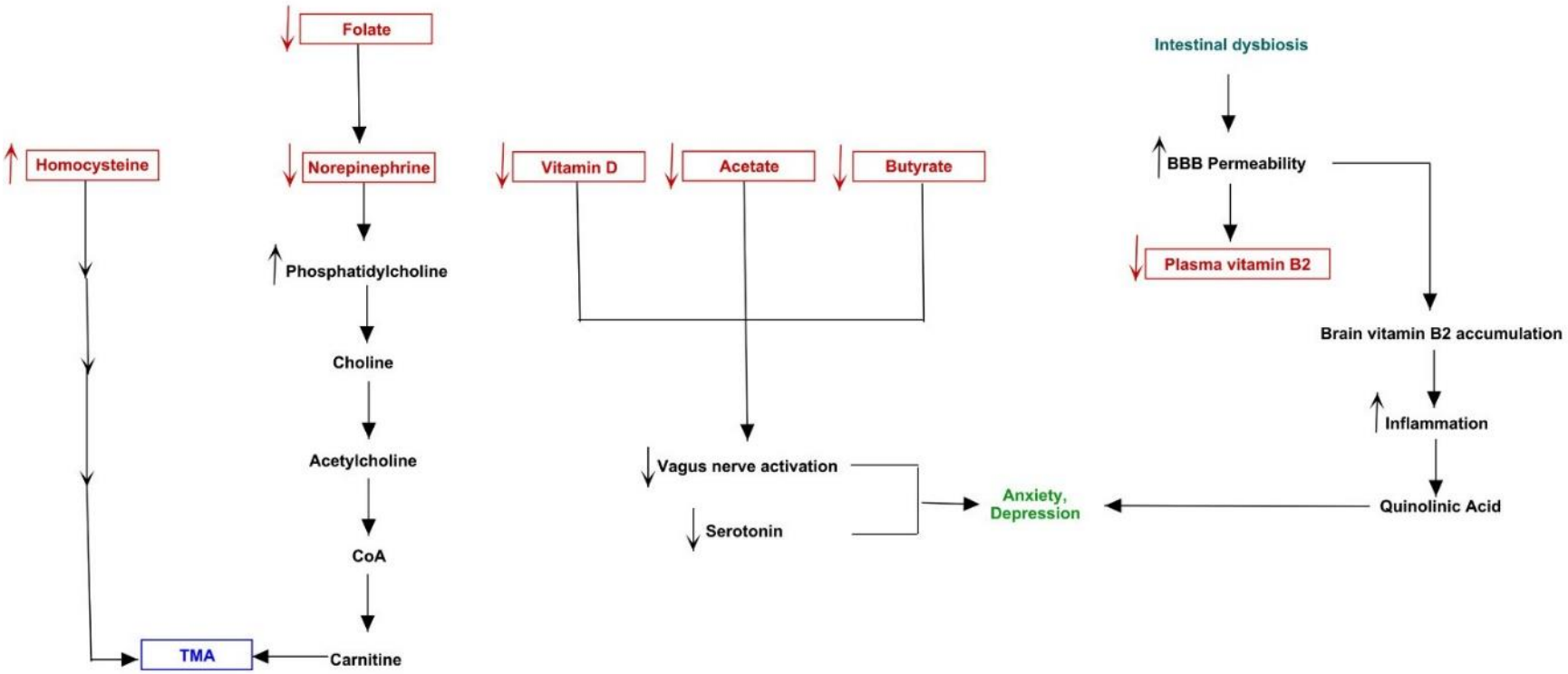

Patient 28 (fig. 25) showed increased relative abundance of *Clostridiaceae* and *Oxalobacteriaceae*[85], the latter being related to higher alpha-ketoglutarate, propionate, and malate levels. This through the mixed acid fermentation pathway could be converted into pyruvate and then into acetyl CoA and butyrate as the final product. The coenzyme A produced by this reaction could contribute to the carnitine biosynthesis and therefore to the TMA accumulation. Additionally, the high levels of alpha-ketoglutarate, could increase the succinic semi-aldehyde via GABA, determining the butyrate production through the already cited fermentation. Thus, the overall increase of main SCFAs, also including the elevated propionate levels produced by altered microbiota, could favor the ECC endogenous serotonin release and the activation of the vagus nerve, along with LPS. Such scenario could explain the excess of anxiety and the uncontrolled emotional status.

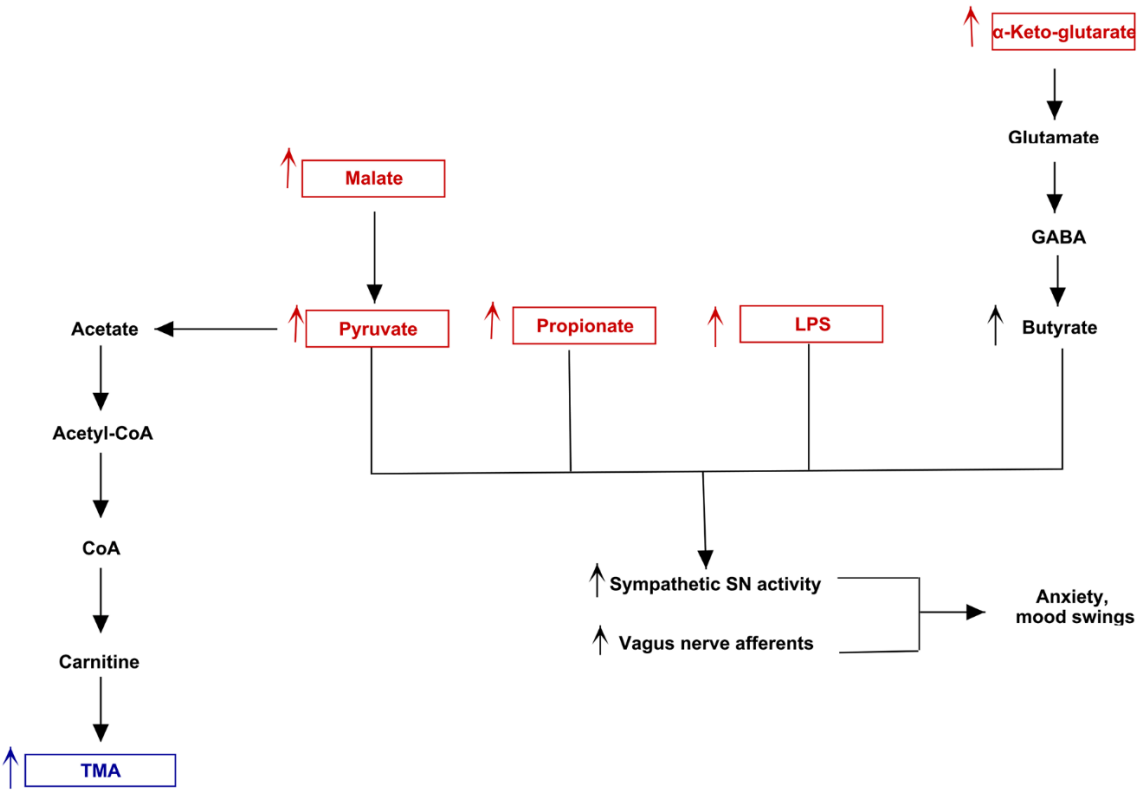

Figure 25. Biochemical pictures of TMAU patient 28.

The depressive phenotype shown by patient 33 (fig. 26) can be explained by considering the gut dysbiosis from which he is affected. This is characterized by the low relative abundances of the *Enterobacteriaceae*, *Clostridiaceae*, *Bacteroidaceae* families. Therefore, a global reduction in acetate and propionate levels could occur resulting in the vagus nerve hypoactivation and down-regulation of serotonin release. This scenario could lead to the depressive phenotype onset, typical of this patient, by nerve activation. In the meantime, the low acetate levels could reduce the acetyl-CoA production, arresting the reaction which converts choline to acetylcholine. So, the accumulation of choline could augment TMA levels, leading to TMAU phenotype.

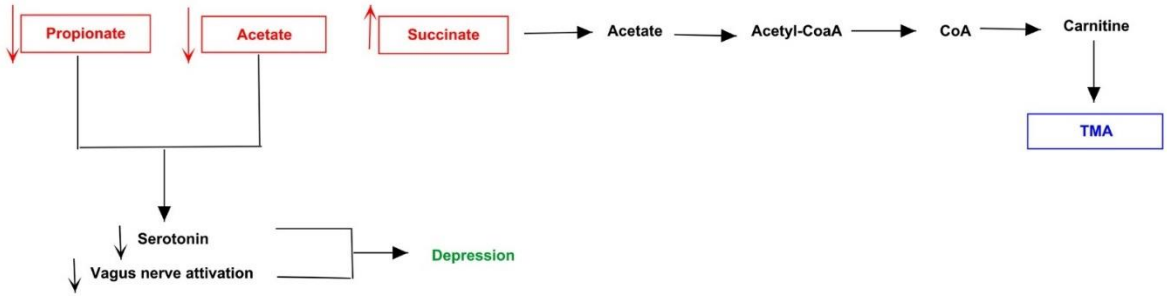

Figure 26. Biochemical pictures of TMAU patient 33.

While all analyzed cases showed relevant changes in production of behavioral disorder-related metabolites, considering both microbiota and human biochemical pathways, evaluated controls highlighted different alterations in the same pathways. However, the probiotic supplements intake could balance the pathological phenotype. The latter is the scenario that characterizes controls 35c and 36c, which showed alteration of the main neurotransmitters. Their global concentration could be normalized by the probiotics intake, as well as dopamine levels from *Enterococcus faecium* supplemented in subject 35c[86]. Patient 34c showed a global reduction of the tryptophan and main SCFAs because of the bacterial families alteration that produce them. This results in a reduced serotonin production which, however, could be balanced by the high butyrate levels inducing its biosynthesis. An opposite situation occurred in patient 37c. Increased serotonin

production, because of high SCFA levels, was found. It could be balanced by vitamin D reduction, which could decrease the neurotransmitter concentration. Moreover, the microbiota synthesis of dopamine might not exert positive effects on neurotransmission, because it could be converted to 6-hydroxydopamine (6-OHDA) in condition of high oxidative stress, further increasing the already elevated levels of ROS detected in this patient. Interestingly, the biochemical picture of control 38c highlighted how the increase of only *Prevotellaceae* and *Roseburia* might not be sufficient to determine a psychiatric phenotype. Probably the metabolites produced by both these bacteria are qualitative and quantitative not enough to exert a cytotoxic effect on nervous system. Thus, the integrity of psychic activities might be maintained or very little impaired. All controls, considering the already discussed biochemical pathways analyzed in relation to cases, showed an TMA accumulation.

3 CONCLUSIONS

In this work, the use of different computational analysis tools supported genetic analyses, allowing us to unveil the *FMO3* haplotypes role on the enzyme catalytic activity. Different physico-chemical features of both wild-type FMO3 and mutated forms were detected through *in silico* proteomic analyses. The enzyme active site, the binding site for the FAD and NADP cofactors were predicted. The obtained results showed that haplotypes consisting of missense variants might impair the FMO3 enzymatic kinetics with different severities, probably reducing the interaction time between the protein catalytic site and TMA. In haplotypes consisting of nonsense variants, on the other hand, the binding site for the FAD and NADP cofactors might be altered, compromising the TMA N-oxidation process. This evidence was also confirmed with the molecular dynamics analysis of the FMO3/TMA complex. However, it cannot be asserted with certainty that the same effect, *in vivo*, is limited to their presence, as there will be other factors involved into FMO3 catalysis alterations. Despite this, considering the possible role of *FMO3* variants with still uncertain effects, might be a relevant step towards the detection of novel scenarios in TMAU etiopathogenesis. Furthermore, by analyzing the gut microbiota of TMAU2 patients it was possible to clarify the possible network between altered bacterial metabolites and psychiatric disorders. The hypothesis developed is that the gut-brain axis plays a key role. The mental disturbs affecting TMAU patients are probably not only related to social consequence of their metabolic disease but also to a physiopathological effect determined by TMA accumulation. Further experiments on a higher statistical number of patients should be performed to strengthen this hypothesis. Several physiological essays to ensure the role of each metabolite in each considered pathway will be needed.

7. BIBLIOGRAPHY

1. Hoyles L, Pontifex MG, Rodriguez-Ramiro I, et al. Regulation of blood-brain barrier integrity by microbiome-associated methylamines and cognition by trimethylamine N-oxide. *Microbiome*. **2021**. doi: 10.1186/s40168-021-01181-z.
2. Rehman HU. Fish odor syndrome. *Postgrad Med J*. **1999.** doi: 10.1136/pgmj.75.886.451.
3. Mitchell, S. C. The Fish-Odor Syndrome. *Perspectives in Biology and Medicine*, **1996**, doi:10.1353/pbm.1996.0003.
4. Shephard EA, Treacy EP, Phillips IR. Clinical utility gene card for: Trimethylaminuria - update 2014. *Eur J Hum Genet*. **2015**. doi: 10.1038/ejhg.2014.226.
5. Kim JH, Cho SM, Chae JH. A compound heterozygous mutation in the *FMO3* gene: the first pediatric case causes fish odor syndrome in Korea. *Korean J Pediatr*. **2017**. doi: 10.3345/kjp.2017.60.3.94.
6. D'Angelo R, Esposito T, Calabrò M, Rinaldi C, Robledo R, Varriale B, Sidoti A. FMO3 allelic variants in Sicilian and Sardinian populations: trimethylaminuria and absence of fish-like body odor. *Gene*. **2013**. doi: 10.1016/j.gene.2012.12.047.
7. Phillips IR, Shephard EA. Drug metabolism by flavin-containing monooxygenases of human and mouse. *Expert Opin Drug Metab Toxicol*. **2017**. doi: 10.1080/17425255.2017.1239718.
8. Shephard EA, Chandan P, Stevanovic-Walker M, et al. Alternative promoters and repetitive DNA elements define the species-dependent tissue-specific expression of the FMO1 genes of human and mouse. *Biochem J*. **2007**. doi: 10.1042/BJ20070523.
9. Başaran R, Can Eke B. Flavin Containing Monooxygenases and Metabolism of Xenobiotics. *Turk J Pharm Sci*. **2017**. doi: 10.4274/tjps.30592.
10. Phillips IR, Shephard EA. Drug metabolism by flavin-containing monooxygenases of human and mouse. *Expert Opin Drug Metab Toxicol*. **2017**. doi: 10.1080/17425255.2017.1239718.
11. Fennema D, Phillips IR, Shephard EA. Trimethylamine and Trimethylamine N-Oxide, a Flavin-Containing Monooxygenase 3 (FMO3)-Mediated Host-Microbiome Metabolic Axis Implicated in Health and Disease. *Drug Metab Dispos*. doi: 10.1124/dmd.116.070615.
12. Krueger SK, Williams DE. Mammalian flavin-containing monooxygenases: structure/function, genetic polymorphisms and role in drug metabolism. *Pharmacol Ther*. **2005**. doi: 10.1016/j.pharmthera.2005.01.001.
13. Alfieri A, Malito E, Orru R, Fraaije MW, Mattevi A. Revealing the moonlighting role of NADP in the structure of a flavin-containing monooxygenase. *Proc Natl Acad Sci U S A*. **2008**. doi: 10.1073/pnas.0800859105.

14. Eswaramoorthy S, Bonanno JB, Burley SK, Swaminathan S. Mechanism of action of a flavin-containing monooxygenase. *Proc Natl Acad Sci U S A*. **2006**. doi: 10.1073/pnas.0602398103.
15. Nicoll CR, Bailleul G, Fiorentini F, Mascotti ML, Fraaije MW, Mattevi A. Ancestral-sequence reconstruction unveils the structural basis of function in mammalian FMOs. *Nat Struct Mol Biol*. **2020**. doi: 10.1038/s41594-019-0347-2.
16. Schmidt AC, Leroux JC. Treatments of trimethylaminuria: where we are and where we might be heading. *Drug Discov Today*. **2020**. doi: 10.1016/j.drudis.2020.06.026.
17. Mackay RJ, McEntyre CJ, Henderson C, Lever M, George PM. Trimethylaminuria: causes and diagnosis of a socially distressing condition. *Clin Biochem Rev*. **2011**. PMID: 21451776.
18. Phillips IR, Shephard EA. Flavin-containing monooxygenase 3 (FMO3): genetic variants and their consequences for drug metabolism and disease. *Xenobiotica*. **2020**. doi: 10.1080/00498254.2019.1643515.
19. Phillips IR, Shephard EA. Primary Trimethylaminuria. *GeneReviews®* **2020.** PMID: 20301282.
20. Cruciani G, Baroni M, Benedetti P, Goracci L, Fortuna CG. Exposition and reactivity optimization to predict sites of metabolism in chemicals. *Drug Discov Today Technol*. **2013**. doi: 10.1016/j.ddtec.2012.11.001.
21. Cruciani G, Valeri A, Goracci L, Pellegrino RM, Buonerba F, Baroni M. Flavin monooxygenase metabolism: why medicinal chemists should matter. *J Med Chem.* **2014**. doi: 10.1021/jm5007098.
22. Xu M, Bhatt DK, Yeung CK, Claw KG, Chaudhry AS, et al. Genetic and Nongenetic Factors Associated with Protein Abundance of Flavin-Containing Monooxygenase 3 in Human Liver. *J Pharmacol Exp Ther*. **2017**. doi: 10.1124/jpet.117.243113.
23. Guo Y, Hwang LD, Li J, Eades J, Yu CW, Mansfield C, Burdick-Will A, et al. Genetic analysis of impaired trimethylamine metabolism using whole exome sequencing. *BMC Med Genet*. **2017**. doi: 10.1186/s12881-017-0369-8.
24. Bouchemal N, Ouss L, Brassier A, Barbier V, et al. Diagnosis and phenotypic assessment of trimethylaminuria, and its treatment with riboflavin: ^{1}H NMR spectroscopy and genetic testing. *Orphanet J Rare Dis*. **2019**. doi: 10.1186/s13023-019-1174-6.
25. Sekirov I., shannon L., russell, L., Caetano M. Gut Microbiota in Health and Disease. *Physiol Rev.* **2010.** doi:10.1152/physrev.00045.2009.
26. Korpela K. Diet, Microbiota, and Metabolic Health: Trade-Off Between Saccharolytic and Proteolytic Fermentation. *Annu Rev Food Sci Technol*. **2018**. doi: 10.1146/annurev-food-030117-012830.

27. Oliphant K, Allen-Vercoe E. Macronutrient metabolism by the human gut microbiome: major fermentation by-products and their impact on host health. *Microbiome.* **2019**. doi: 10.1186/s40168-019-0704-8.
28. Parker A, Fonseca S, Carding SR. Gut microbes and metabolites as modulators of blood-brain barrier integrity and brain health. *Gut Microbes*. **2020**. doi: 10.1080/19490976.2019.1638722.
29. Carabotti M, Scirocco A, Maselli MA, Severi C. The gut-brain axis: interactions between enteric microbiota, central and enteric nervous systems. *Ann Gastroenterol*. **2015**. PMID: 25830558.
30. Jacobson A, Yang D, Vella M, Chiu IM. The intestinal neuro-immune axis: crosstalk between neurons, immune cells, and microbes. *Mucosal Immunol*. **2021**. doi: 10.1038/s41385-020-00368-1.
31. Loo RL, Chan Q, Nicholson JK, Holmes E. Balancing the Equation: A Natural History of Trimethylamine and Trimethylamine-*N*-oxide. *J Proteome Res*. **2022**. doi: 10.1021/acs.jproteome.1c00851.
32. Fadhlaoui K, Arnal ME, Martineau M, Camponova P, et al. Archaea, specific genetic traits, and development of improved bacterial live biotherapeutic products: another face of next-generation probiotics. *Appl Microbiol Biotechnol*. **2020**. doi: 10.1007/s00253-020-10599-8.
33. Corbin KD, Zeisel SH. Choline metabolism provides novel insights into nonalcoholic fatty liver disease and its progression. *Curr Opin Gastroenterol*. **2012**. doi: 10.1097/MOG.0b013e32834e7b4b.
34. Janeiro MH, Ramírez MJ, Milagro FI, Martínez JA, Solas M. Implication of Trimethylamine N-Oxide (TMAO) in Disease: Potential Biomarker or New Therapeutic Target. *Nutrients*. **2018**. doi: 10.3390/nu10101398.
35. Liu Y, Dai M. Trimethylamine N-Oxide Generated by the Gut Microbiota Is Associated with Vascular Inflammation: New Insights into Atherosclerosis. *Mediators Inflamm*. **2020**. doi: 10.1155/2020/4634172.
36. Velasquez MT, Ramezani A, Manal A, Raj DS. Trimethylamine N-Oxide: The Good, the Bad and the Unknown. *Toxins (Basel)*. **2016**. doi: 10.3390/toxins8110326.
37. Lombardo M, Aulisa G, Marcon D, Rizzo G, et al. Association of Urinary and Plasma Levels of Trimethylamine N-Oxide (TMAO) with Foods. *Nutrients*. **2021**. doi: 10.3390/nu13051426.
38. Krueger ES, Lloyd TS, Tessem JS. The Accumulation and Molecular Effects of Trimethylamine N-Oxide on Metabolic Tissues: It's Not All Bad. *Nutrients*. **2021**. doi: 10.3390/nu13082873.
39. Dalla Via A, Gargari G, Taverniti V, Rondini G, et al. Urinary TMAO Levels Are Associated with the Taxonomic Composition of the Gut Microbiota and with the Choline TMA-Lyase Gene (*cutC*) Harbored by Enterobacteriaceae. *Nutrients*. **2019**. doi: 10.3390/nu12010062.

40. Chen S, Henderson A, Petriello MC, Romano KA, Gearing M, et al. Trimethylamine N-Oxide Binds and Activates PERK to Promote Metabolic Dysfunction. *Cell Metab*. **2019** doi: 10.1016/j.cmet.2019.08.021.
41. Falony G, Vieira-Silva S, Raes J. Microbiology Meets Big Data: The Case of Gut Microbiota-Derived Trimethylamine. *Annu Rev Microbiol*. **2015.** doi: 10.1146/annurev-micro-091014-104422.
42. Ramireddy L, Tsen HY, Chiang YC, Hung CY, Chen FC, Yen HT. The gene expression and bioinformatic analysis of choline trimethylamine-lyase *(CutC*) and its activating enzyme (*CutD*) for gut microbes and comparison with their TMA production levels. *Curr Res Microb Sci*. **2021**. doi: 10.1016/j.crmicr.2021.100043.
43. Rath S, Rud T, Pieper DH, Vital M. Potential TMA-Producing Bacteria Are Ubiquitously Found in Mammalia. *Front Microbiol*. **2020**. doi: 10.3389/fmicb.2019.02966.
44. Day-Walsh P, Shehata E, Saha S, Savva GM, et al. The use of an in-vitro batch fermentation (human colon) model for investigating mechanisms of TMA production from choline, L-carnitine and related precursors by the human gut microbiota. *Eur J Nutr*. **2021**. doi: 10.1007/s00394-021-02572-6.
45. Guy Van den. The Human Gut Microbiota. Eede Joint Research Centre (JRC). **2018**. doi:10.2760/17381.
46. Acconcia C, Paladino A, Valle MD, Farina B, Del Gatto A, et al. High-Resolution Conformational Analysis of RGDechi-Derived Peptides Based on a Combination of NMR Spectroscopy and MD Simulations. *Int J Mol Sci*. **2022**. doi: 10.3390/ijms231911039.
47. Hibar DP, Stein JL, Ryles AB, Kohannim O, Jahanshad N, et al. Alzheimer's Disease Neuroimaging Initiative. Genome-wide association identifies genetic variants associated with lentiform nucleus volume in N = 1345 young and elderly subjects. *Brain Imaging Behav*. **2013**. doi: 10.1007/s11682-012-9199-7.
48. Trott O, Olson AJ. AutoDock Vina: improving the speed and accuracy of docking with a new scoring function, efficient optimization, and multithreading. *J Comput Chem*. **2010**. doi: 10.1002/jcc.21334.
49. Bitzek E, Koskinen P, Gähler F, Moseler M, Gumbsch P. Structural relaxation made simple. *Phys Rev Lett*. **2006**. doi: 10.1103/PhysRevLett.97.170201.
50. Van Der Spoel D, Lindahl E, Hess B, Groenhof G, Mark AE, Berendsen HJ. GROMACS: fast, flexible, and free. *J Comput Chem*. **2005**. doi: 10.1002/jcc.20291.

51. Nguyen MK, Jaillet L, Redon S. ART-RRT: As-Rigid-As-Possible search for protein conformational transition paths. *J Comput Aided Mol Des*. **2019.** doi: 10.1007/s10822-019-00216-w.
52. Reas DL, Pedersen G, Karterud S, Rø Ø. Self-harm and suicidal behavior in borderline personality disorder with and without bulimia nervosa. *J Consult Clin Psychol*. **2015**. doi: 10.1037/ccp0000014.
53. Klindworth A, Pruesse E, Schweer T, Peplies J, Quast C, Horn M, Glöckner FO. Evaluation of general 16S ribosomal RNA gene PCR primers for classical and next-generation sequencing-based diversity studies. *Nucleic Acids Res*. **2013**. doi: 10.1093/nar/gks808.
54. Masella AP, Bartram AK, Truszkowski JM, Brown DG, Neufeld JD. PANDAseq: paired-end assembler for illumina sequences. *BMC Bioinformatics.* **2012**. doi: 10.1186/1471-2105-13-31.
55. Caporaso JG, Kuczynski J, Stombaugh J, Bittinger K, Bushman FD, et al. QIIME allows analysis of high-throughput community sequencing data. *Nat Methods*. **2010**. doi: 10.1038/nmeth.f.303.
56. Golob JL, Margolis E, Hoffman NG, Fredricks DN. Evaluating the accuracy of amplicon-based microbiome computational pipelines on simulated human gut microbial communities. *BMC Bioinformatics*. **2017**. doi: 10.1186/s12859-017-1690-0.
57. Leong LEX, Taylor SL, Shivasami A, Goldwater PN, Rogers GB. Intestinal Microbiota Composition in Sudden Infant Death Syndrome and Age-Matched Controls. *J Pediatr*. **2017**. doi: 10.1016/j.jpeds.2017.08.070.
58. Wandro S, Osborne S, Enriquez C, Bixby C, Arrieta A, Whiteson K. The Microbiome and Metabolome of Preterm Infant Stool Are Personalized and Not Driven by Health Outcomes, Including Necrotizing Enterocolitis and Late-Onset Sepsis. *mSphere*. **2018**. doi: 10.1128/mSphere.00104-18.
59. Niu J, Xu L, Qian Y, Sun Z, Yu D, Huang J, Zhou X, Wang Y, Zhang T, Ren R, Li Z, Yu J, Gao X. Evolution of the Gut Microbiome in Early Childhood: A Cross-Sectional Study of Chinese Children. *Front Microbiol*. **2020**. doi: 10.3389/fmicb.2020.00439.
60. McNeill TW, Sinkora G, Leavitt F. Psychologic classification of low-back pain patients: a prognostic tool. *Spine*. **1986** Nov;11(9):955-9. doi: 10.1097/00007632-198611000-00018.
61. Le Boulch M, Déhais P, Combes S, Pascal G. The MACADAM database: a MetAboliC pAthways DAtabase for Microbial taxonomic groups for mining potential metabolic capacities of archaeal and bacterial taxonomic groups. *Database (Oxford)*. **2019**. doi: 10.1093/database/baz049.

62. Razmazma H, Ebrahimi A. The effects of cation-π and anion-π interactions on halogen bonds in the $[N\cdots X\cdots N]^+$ complexes: A comprehensive theoretical study. *J Mol Graph Model*. **2018**. doi: 10.1016/j.jmgm.2018.06.006.
63. Dalile B, Van Oudenhove L, Vervliet B, Verbeke K. The role of short-chain fatty acids in microbiota-gut-brain communication. *Nat Rev Gastroenterol Hepatol*. **2019**. doi: 10.1038/s41575-019-0157-3.
64. Tsiaoussis J, Antoniou MN, Koliarakis I, Mesnage R, et al. Effects of single and combined toxic exposures on the gut microbiome: Current knowledge and future directions. *Toxicol Lett*. **2019**. doi: 10.1016/j.toxlet.2019.04.014.
65. Murphy MM, Guéant JL. B vitamins and one carbon metabolism micronutrients in health and disease. *Biochimie.* **2020**. doi: 10.1016/j.biochi.2020.04.018.
66. Jenkins TA, Nguyen JC, Polglaze KE, Bertrand PP. Influence of Tryptophan and Serotonin on Mood and Cognition with a Possible Role of the Gut-Brain Axis. *Nutrients*. **2016**. doi: 10.3390/nu8010056.
67. Kutmon M, van Iersel MP, Bohler A, Kelder T, Nunes N, Pico AR, Evelo CT. PathVisio 3: an extendable pathway analysis toolbox. *PLoS Comput Biol*. **2015**. doi: 10.1371/journal.pcbi.1004085.
68. Yamazaki H, Shimizu M. Survey of variants of human flavin-containing monooxygenase 3 (FMO3) and their drug oxidation activities. *Biochem Pharmacol.* **2013**. doi: 10.1016/j.bcp.2013.03.020.
69. Shimizu M, Yoda H, Nakakuki K, Saso A, Saito I, et al. Genetic variants of flavin-containing monooxygenase 3 (FMO3) derived from Japanese subjects with the trimethylaminuria phenotype and whole-genome sequence data from a large Japanese database. *Drug Metab Pharmacokinet*. **2019**. doi: 10.1016/j.dmpk.2019.06.001.
70. Catucci G, Gilardi G, Jeuken L, Sadeghi SJ. In vitro drug metabolism by C-terminally truncated human flavin-containing monooxygenase 3. *Biochem Pharmacol*. **2012**. doi: 10.1016/j.bcp.2011.11.029.
71. Caspani G, Kennedy S, Foster JA, Swann J. Gut microbial metabolites in depression: understanding the biochemical mechanisms. *Microb Cell*. **2019**. doi: 10.15698/mic2019.10.693.
72. Ting Liu, K. Anton Feenstra, Jaap Heringa et al. Influence of Gut Microbiota on Mental Health via Neurotransmitters: A Review. *Journal of Artificial Intelligence for Medical Sciences.* **2020.** 10.2991/jaims.d.200420.001
73. Liu L, Huh JR, Shah K. Microbiota and the gut-brain-axis: Implications for new therapeutic design in the CNS. *EBioMedicine*. **2022**. doi: 10.1016/j.ebiom.2022.103908.

74. Shi C, Pei M, Wang Y, Chen Q, Cao P, Zhang L, Guo J, Deng W, Wang L, Li X, Gong Z. Changes of flavin-containing monooxygenases and trimethylamine-N-oxide may be involved in the promotion of non-alcoholic fatty liver disease by intestinal microbiota metabolite trimethylamine. *Biochem Biophys Res Commun*. **2022**. doi: 10.1016/j.bbrc.2022.01.060.
75. Lambert DM, Mamer OA, Akerman BR, Choinière L, Gaudet D, Hamet P, Treacy EP. In vivo variability of TMA oxidation is partially mediated by polymorphisms of the FMO3 gene. *Mol Genet Metab*. **2001**. doi: 10.1006/mgme.2001.3189.
76. Donato L, Scimone C, Nicocia G, Denaro L, Robledo R, Sidoti A, D'Angelo R. GLO1 gene polymorphisms and their association with retinitis pigmentosa: a case-control study in a Sicilian population. *Mol Biol Rep*. **2018**. doi: 10.1007/s11033-018-4295-4.
77. Chen Y, Patel NA, Crombie A, Scrivens JH, Murrell JC. Bacterial flavin-containing monooxygenase is trimethylamine monooxygenase. *Proc Natl Acad Sci U S A.* **2011**. doi: 10.1073/pnas.1112928108.
78. Newington JT, Harris RA, Cumming RC. Reevaluating Metabolism in Alzheimer's Disease from the Perspective of the Astrocyte-Neuron Lactate Shuttle Model. *J Neurodegener Dis*. **2013.** doi: 10.1155/2013/234572
79. Jin XT, Galvan A, Wichmann T, Smith Y. Localization and Function of GABA Transporters GAT-1 and GAT-3 in the Basal Ganglia. *Front Syst Neurosci*. **2011**. doi: 10.3389/fnsys.2011.00063.
80. Cheng LH, Liu YW, Wu CC, Wang S, Tsai YC. Psychobiotics in mental health, neurodegenerative and neurodevelopmental disorders. *J Food Drug Anal*. **2019**. doi: 10.1016/j.jfda.2019.01.002.
81. Frick A, Åhs F, Engman J, Jonasson M, Alaie I, Björkstrand J, et al. Serotonin Synthesis and Reuptake in Social Anxiety Disorder: A Positron Emission Tomography Study. *JAMA Psychiatry*. **2015**. doi: 10.1001/jamapsychiatry.2015.0125.
82. Fava M, Mischoulon D. Folate in depression: efficacy, safety, differences in formulations, and clinical issues. *J Clin Psychiatry*. **2009**. doi: 10.4088/JCP.8157su1c.03.
83. Spector R, Johanson CE. Vitamin transport and homeostasis in mammalian brain: focus on Vitamins B and E. *J Neurochem*. **2007**. doi: 10.1111/j.1471-4159.2007.04773.x.
84. Kennedy PJ, Cryan JF, Dinan TG, Clarke G. Kynurenine pathway metabolism and the microbiota-gut-brain axis. *Neuropharmacology*. **2017**. doi: 10.1016/j.neuropharm.2016.07.002.
85. Baldani, J.I., Rouws, L., Cruz, L.M., Olivares, F.L., Schmid, M., Hartmann, A. The Family *Oxalobacteraceae*. *The Prokaryotes. Springer*. **2014.** https://doi.org/10.1007/978-3-642-30197-1_291.

86. Yano JM, Yu K, Donaldson GP, Shastri GG, Ann P, et al. Indigenous bacteria from the gut microbiota regulate host serotonin biosynthesis. *Cell*. **2015**. doi: 10.1016/j.cell.2015.02.047.